Graduate School ETD Form 9
(Revised 12/07)

PURDUE UNIVERSITY
GRADUATE SCHOOL
Thesis/Dissertation Acceptance

This is to certify that the thesis/dissertation prepared

By Ankita Saha

Entitled
Potential role of histone deactylases in the development of the chick and murine retina.

For the degree of Master of Science

Is approved by the final examining committee:

Dr. Teri Belecky-Adams
Chair

Dr. David Stocum

Dr. Jason Meyer

To the best of my knowledge and as understood by the student in the *Research Integrity and Copyright Disclaimer (Graduate School Form 20)*, this thesis/dissertation adheres to the provisions of Purdue University's "Policy on Integrity in Research" and the use of copyrighted material.

Approved by Major Professor(s): Dr. Teri Belecky-Adams

Approved by: Dr. Simon Atkinson 06/28/2013
Head of the Graduate Program Date

POTENTIAL ROLE OF HISTONE DEACTYLASES IN THE DEVELOPMENT OF THE CHICK AND MURINE RETINA

A Thesis

Submitted to the Faculty

of

Purdue University

by

Ankita Saha

In Partial Fulfillment of the

Requirements for the Degree

of

Master of Science

August 2013

Purdue University

Indianapolis, Indiana

ACKNOWLEDGEMENTS

I would like to express my deepest gratitude towards the principal investigator of this study and my mentor, Dr. Teri Belecky-Adams. It is with her constant encouragement, guidance and unrelenting support that I have made it this far in my journey as a researcher. The chinchillas, chipmunks, cakes and brownies have played a role of prime importance during this time. I would also like to thank my committee members, Dr. David Stocum and Dr. Jason Meyer for their guidance over this duration.

I especially thank my parents, who have been pillars of support through all the ups and downs that research had to offer. Their constant encouragement and blessings have made me the researcher I am today. A special vote of thanks to my friends, Rajula Elango, Sreejith Ramakrishnan and Shashank Nambiar for being available whenever I needed them. Last, but not the least, I thank all my lab members for the great camaraderie, brain storming sessions, etc. that I was able to enjoy.

TABLE OF CONTENTS

Page

Page

Page

Page

LIST OF FIGURES

Figure Page

Figure Page

LIST OF TABLES

LIST OF ABBREVIATIONS

Histone acetyl transferases ..... HAT
Histone deacetylases ..... HDAC
Paired box 6 ..... PAX6
Retinal homeobox 1 ..... RX1
Semilobar sine oculis homeobox homolog3 ..... SIX3
LIM homeobox protein 2 ..... LHX2
Fibroblast Growth Factor ..... FGF
Sonic Hedgehog ..... SHH
Basic helix-loop-helix ..... bHLH
Mammalian achaete-scute 1 ..... Mash1
Mammalian atonal 5 ..... Math5
Hairy and enhancer of split ..... Hes
Neurogenic differentiation 1 ..... NEUROD1
Cone-rod homeobox ..... CRX
Structural maintenance of chromosomes ..... SMC
Histone ..... H
CREB Binding protein ..... CBP
Histone methyl transferases ..... HMT
Suppressor of variegation 39h1 ..... Suv39h1
DNA methyl transferases ..... DNMT
Small Ubiquitin- related modifier ..... SUMO
Myocyte enhancing factor 2 ..... MEF2
Chromosome region maintenance CRM1
Signal transducer and activator of transcription ..... STAT
Deoxy- ribonucleic acid ..... DNA
Optimal Cutting temperature ..... OCT
Biological Oxygen demand ..... BOD
Phosphate Buffer saline ..... PBS
Quantitative Real time polymerase chain reaction ..... RT-qPCR
Ribonucleic Acid ..... RNA
Immunohistochemistry ..... IHC
Calcium Magnesium Free ..... CMF
Hank's balanced salt solution ..... HBSS

ABSTRACT

Saha, Ankita A. M.S., Purdue University, August 2013. Potential role of histone deacetylases in the development of the chick and murine retina. Major Professor: Teri Belecky-Adams.

The epigenetic state of any cell is, in part, regulated by the interaction of DNA with nuclear histones. Histone tails can be modified in a number of ways that impact on the availability of DNA to interact with transcriptional complexes, including methylation, acetylation, phosphorylation, ubiquituination, and sumoylation. Histones are acetylated by a large family of enzymes, histone acetyl transferases (HATs), and deacetylated by the histone deacetylases (HDACs). Acetylated histones are generally considered markers of genomic regions that are actively being transcribed, whereas deacetylated and methylated histones are generally markers of regions that are inactive.

The goal of the present study was to 1) study the epigenetic state with regard to the presence of euchromatin and heterochromatin in the developing chick and murine retina, 2) study and compare the localization patterns of the classical HDACs in the developing chick and murine retina with respect retinal progenitors and early differentiated cell types 3) to test the hypothesis that overall HDAC activity is required for dividing retinal progenitors to leave the cell cycle and

differentiate. Our results showed that the classical HDACs were ubiquitously expressed in the developing chick and murine retinas. Species specific differences as well as stage dependent variations were observed in the localization of the HDACs in the cell types that were studied in the chick and murine retina. Our preliminary results also showed that HDAC inhibition may lead to the inability of the cell types to leave the cell cycle and a subsequent increase in the number of progenitor cells present in the developing chick retina.

CHAPTER 1 INTRODUCTION

1.1 Development of the eye

The development of the eye begins with the induction of the neural plate by a variety of factors including, noggin, chordin and follistatin (Figure 1a). During neurulation, the neural plate starts folding upwards and inwards to give rise to the neural tube. In the rostral region of the neural plate, a region known as the eye field expresses molecules that are associated with early eye development, such as PAX6, RX1, SIX3 and LHX2. During this period, the eye field bisects to give rise to two depressions called the optic grooves which eventually enlarge and give rise to the optic vesicles. These optic vesicles induce the formation of the lens placode when they come in close opposition to the surface ectoderm (Figure 1d). The optic vesicle then invaginates to form a double-layered optic cup and the lens placode differentiates to form the lens. The inner layer is referred to as the presumptive neural retina and the outer layer will eventually give rise to the retinal pigmented epithelium (RPE). The neural retina develops into a multilayered neuronal tissue composed of the outer nuclear layer containingthe rod and cone photoreceptors, the inner nuclear layer, which contains the cell bodies of horizontal, bipolar, amacrine and Müller glial cells, and finally the ganglion cell layer that contains ganglion cells and retinal astrocytes. The

developing ganglion cells send out axons across the inner retinal surface towards the ventral region of the eye where the developing optic stalk lies. As development proceeds, the ganglion cell axons project out of the eye, using signals released by the optic stalk, the mesenchyme surrounding the optic stalk and the retinal neurons to guide them. Eventually the optic stalk cells become type I astrocytes that inhabit the mature optic nerve. Precursor cells that migrate from the base of the diencephalon migrate into the optic nerve give rise to oligodendrocytes that make up the myelin sheath surrounding the ganglion cell axons (Harada et al., 2007). These cells can also potentially give rise to other astrocytes (Lamb et al., 2007), (Chow & Lang, 2001). Together the ganglion cell axons, astrocytes and oligodendrocytes comprise the mature optic nerve.

Thus, the optic nerve serves as the physiological link between the eye and the brain by transmitting the electrical impulses generated by in the neural retina in response to external stimuli. The different cell types that make up this multi-neuronal tissue follow a distinct pattern of development which is discussed in the next section.

1.2 Development of the retina

A number of investigators have shown that retinal progenitor cells are multipotent and can give rise to more than one of the seven different retinal cell types in a specific but overlapping order (Morrow et al., 2008, Doh et al., 2010). The progenitor cells present in the neuroepithelium of the developing optic vesicle

undergo a well characterized pattern of replication. The soma of the cell follows a definite pattern of migration between vitreal and ventricular edges of the eye while undergoing the early phases of the cell cycle. During G1, the soma of the cell shuttles towards the vitreal edge of the eye where it proceeds through the S phase of the cell cycle. Once the cell completes DNA synthesis and replication, it migrates back to the ventricular edge of the eye. Here, the cell undergoes mitotic division wherein two daughter cells are produced. At this point, the cells can proceed in one of the following ways, one of the newly born daughter cells leaves the cell cycle and proceeds through differentiation while the other re-enters the cell cycle and continues to proliferate or both the daughter cells can leave the cell cycle towards differentiation or both may re-enter the cell-cycle to continue proliferation. The post mitotic cell migrates to the layer it will eventually occupy in the mature retina and differentiates. The differentiating cell/s then starts its final migration to the position that it will eventually occupy in the mature retina (Figure 2).

During the first wave of retinogenesis, the retinal progenitors gives rise to the ganglion cells, horizontal cells, cones and a subpopulation of amacrine cells. The second wave produces the Müller glial cells and the rest of the amacrine cells and the final wave gives rise to the rods and bipolar cells (Figure 3). This sequence of ‘cell birth’ is highly conserved throughout vertebrates (Lamb, Collin, & Pugh, 2007).

The differentiated cells then together give rise to the formation of a three layered mature retina which will be described in greater detail in a later section. This thesis will contrast two specific early born retinal cells i.e. retinal ganglion cells and the cone photoreceptors with still dividing progenitors. In the next section, the factors that are critical for the development of the retinal ganglion cells will be discussed.

1.3 Retinal ganglion cell development

The retinal ganglion cells are the first neuronal cells that appear in the developing retina. They develop in a regular mosaic as they proceed from the central fundal region of the retina to the periphery. This progress of the 'wave' of differentiation is regulated by the combinatorial influence of Fibroblast growth factor (FGF) and sonic hedgehog (SHH), wherein, FGF regulates the forward progression while Shh negatively regulates the ganglion cell production behind the differentiation wave front (McCabe et al., 1999). Studies have also shown that the Brn3 family of POU-domain transcription factors plays a significant role in the development of the ganglion cells amongst others (Gan et al., 1996). The Brn3 family consists of Brn3a, Brn 3b and Brn 3c proteins of which Brn 3a and 3b are expressed in a larger population of the retinal ganglion cells (Xiang et al., 1996), (Badea et al., 2009, Nadal-Nicolas et al., 2009). The developing ganglion cells express Brn 3b first, followed by Brn 3a and Brn 3c (Xiang, 1998, Liu et al., 2000).

The basic helix-loop-helix (bHLH) proteins comprise a family of transcription factors that bear a distinct structural characteristic i.e. the presence of a DNA binding domain and a helix-loop-helix domain which confers them with the ability to form typically heterodimers of different classes. They have been classified into six different groups based on their distribution patterns, DNA-binding specifications and/or dimerization capabilities. Functionally however, two distinct classes have been identified; activators and repressors. Amongst the activators, homologs of *Drosophila* proneural genes, *acheate-scute* and *atonal*, like *Mammalian achaete-scute (Mash1)* and *Mammalian atonal (Math5),* etc are required for the differentiation of neurons whereas, the repressors, mammalian homologs to *Drosophila hairy* and *Enhancer of Split* genes, like *Hes1* and *Hes5* promote the maintenance of a progenitor population and simultaneously inhibit neurogenesis. *Hes1* and *Hes5* are also directly induced via the Notch pathway thus establishing a link between the extrinsic and intrinsic regulation of neurogenesis. The upregulation of bHLH activator, *Math5,* with the simultaneous downregulation of the *Hes* factors leads to the differentiation of retinal ganglion cells (Hatakeyama and Kageyama, 2004, Pennesi et al., 2006).

1.4 Photoreceptor development

After the retinal ganglion cells, the cone photoreceptors are the next neuronal population that arise in the developing retina followed by the rods in later development. These cells are specialized for phototransduction wherein light energy, received in the form of photons is converted into a chemical signal at the

synaptic termini, further processed by interneurons and then relayed to visual centers in the brain via the activity of retinal ganglion cells. The development of the photoreceptors begins with restricted competence of the proliferating retinal progenitors. The cells are then guided to adopt the photoreceptor precursor cell fate via the transient influence of combinations of multiple bHLH transcription factors like neurogenic differentiation 1 (NEUROD1), NEUROD4, neurogenin2 etc., and expression of an OTX-like homeodomain transcription factor, CRX (Cone-rod homeobox) and inhibition of Notch signaling. Later on in development, the cells that show a higher *Delta* expression and downregulation of Notch signaling are then directed towards the rod cell fate. Retinoic acid, taurine, SHH, etc. are amongst some of the factors that promote the rod cell fate. (Chen et al., 1997, Koike et al., 2007, Lamb et al., 2007, Swaroop et al., 2010)

1.5 The mammalian retina

The mature mammalian retina is a multilayered layered structure with six distinct neuronal cell types and depending on the organism two or three glial cell types. The layers, namely the outer nuclear layer, outer plexiform layer, inner nuclear layer, inner plexiform layer, the ganglion cell layer and nerve fiber layer are arranged in a manner represented in Figure 4 (Cheng et al., 2006). The outer nuclear layer comprises of the photoreceptor population, namely the rods and cones which are responsible for the conversion of light stimuli to an electrical signal. The outer segments of the photoreceptors comprise of stacks of photo-pigment containing disc-like segments which maybe encapsulated by a separate

plasma membrane, like in rod photoreceptors or maybe continuous, like in cone photoreceptors (Sjostrand et al., 1988). The activation of the visual cascade begins with the excitation of the photo-pigment, via light stimuli which activates the following G-protein mediated pathway resulting in hyperpolarization of the cells. Following this, the cells return to their dark state after a series of inactivating reactions of the components of the visual cascade. Both rods and cones are stimulated and recover using similar mechanisms with the difference lying in the specific range of light wavelength to which they respond (Stryer and Bourne, 1986).

The inner nuclear layer is made up of the bipolar cells, horizontal cells, amacrine cells and the cell bodies of the Müller glia, the broad functions of which are as follows. Bipolar cells are named so because of two sets of processes that arise from a central cell body. Each bipolar cell forms a synapse with either the rods or the cones and the ganglion cells. There are two major classes of bipolar neurons in the retina, ON and OFF, which are further subdivided into approximately five classes depending on their responsiveness to a transient or a more sustained influx of information(Lagali et al., 2008, Snellman et al., 2008). The photoreceptors release their synaptic transmission in the form of glutamate as a result of cAMP-gated channels that are open in the dark. During the dark there is more neurotransmitter released. When light hits the retina, the channels are closed as a result of the activation of a phosphodiesterase (PDE). ON bipolar cells arestimulated during light conditions because they are inhibited by

glutamate (Gunhan-Agar et al., 2000). Eventually these signals from the photoreceptors are relayed to the ganglion cells either directly or indirectly, via amacrine cells. There are twenty-nine different types of amacrine cells which are mainly responsible for regulating the ganglion cell responses (Kolb, 1997). They either do this by regulating input from the cone photoreceptors or by creating negative synapses with the bipolar cell axons that make direct contact with the ganglion cells. The dopaminergic amacrines help in regulating the global responsiveness of the ganglion cell layer under different light conditions. The starburst amacrine cells also help fine-tune the ganglion cell response by making stimulatory cholinergic synapses with the ganglion cells (Kolb, 1997, Masland, 2001). The horizontal cells are a group of interneurons in the retina that are responsible for providing feedback to the photoreceptors in a way so as to regulate the contrast between the light and the dark regions (Thoreson et al., 2008). It does this by using the classical center- surround organization of the photoreceptors where if a central cone is stimulated it initiates a negative feedback system for itself and the neighboring ring of cells and thereby adjusting the overall system response to illumination (Nathans, 1999). The cell bodies of the Müller glial cells are also present in the inner nuclear layer of the mature retina. They extend their process through the thickness of the retina to the outer limiting membrane which divides the outer and inner segments of the rods and cones from their cell body and also to the inner limiting membrane which separates the retina from the vitreous matter. They not only provide structural and functional support to the neurons but are also thought to conduct light stimuli

to the photoreceptors with the help of their unique funnel-shaped morphology (Ahmad et al., 2011). In the event of injury they have also been identified as a potential source of stem cells capable of regenerating neuronal cells in addition to themselves (Dyer and Cepko, 2000, Fischer and Reh, 2001, Lindqvist et al., 2010, Otteson and Phillips, 2010). They also contribute to the innate defense mechanism in the retina by recognizing infectious patterns of microbes and responding using the elements in the Toll-Like receptor signaling pathway (Kumar and Shamsuddin, 2012).

The outer and inner plexiform layers contain dendrites and axons that comprise synapses between cell types within the retina. The outer plexiform layer consists of synaptic connections made between photoreceptors using the synaptic spherules of rods, pedicles of the cones, bipolar cells and horizontal cells using their dendritic process and axons (Mariani, 1984). The receptive field center and the classic surround organization that helps generate a visual contrast are first established here (Kolb, 1995). The comparatively thicker inner plexiform layer is where the bipolar cells, amacrine cells and the ganglion cells interact with each other via their processes and dendrites (Kolb, 1995). They also contribute to the receptive field center, light-evoked cell responses, motion and direction sensitivity of the ganglion cells (Lukasiewicz, 2005).

The innermost neuronal layer of the retina is the ganglion cells layer which in addition to a small subset of amacrine cells are the only retinal cell populations

that is capable of producing action potentials. There are at least five different classes, if not more, of ganglion cells namely, midget cells, parasol cells, bistratified cells, photosensitive cells and a population of cells that project to the area of the superior colliculus which helps control fast eye movements (Rockhill et al., 2002, Lin et al., 2004). The axons of the midget ganglion cells extend to and make contact with the parvocellular layers of the lateral geniculate nucleus and are weakly responsive to color changes. The parasol cells send out their axons to make synaptic connections with the magnocellular layers of the lateral geniculate nucleus. These cells respond to rods and cones, have a high conduction velocity and are unresponsive to changes in color (Watanabe and Rodieck, 1989, Jacoby et al., 1996), (Sernagor et al., 2001). The bistratified ganglion cells are moderately responsive to stimuli with a lower velocity of conduction and maybe involved in color vision (Field et al., 2007). Photosensitive ganglion cells containing melanopsin, function in the absence of stimuli from rods and cones and help regulate the circadian rhythm via photoentrainment of the biological clock in the suprachiasmatic nucleus (Pickard and Sollars, 2012). Overall, these ganglion cells are responsible for establishing the physiological link between the retina and the brain.

The development of each of these cell types in the retina is controlled by the activity of specific transcription factors and other molecules. Their expression, however, is regulated by the strategic activation and repression of the genes by modifications occurring on the histone proteins that are associated with them.

This strategic activation or repression involves epigenetic changes which do not involve alterations to the genetic code.

1.6 Epigenetics: Introduction

It has been observed that within the cellular makeup of an organism, even though the cells possess almost identical DNA sequences, the expressed phenotype is vastly different. This may be attributed to the fact that each cell possesses a ‘memory’ of its identity which helps maintain its state, whether differentiated or undifferentiated. The DNA sequences that are transcribed in a cell are a result of this ‘memory’ which is in turn controlled by regulating the transcriptional machinery’s access to the DNA.

Chromosomal DNA is compacted into a eukaryotic nucleus aided by electrostatic interactions with a small family of positively charged proteins known as histones. When the DNA-protein complex tightly interact with each other, the chromatin takes on a closed conformational appearance which is referred to as heterochromatin, wherein the DNA is inaccessible for transcription. Conversely, when the DNA-protein interactions are weakened via modifications occurring on the histone component, the chromatin appears ‘open’. This state of chromatin is referred to as euchromatin, in which the DNA is now accessible for transcription (Figure 5). This forms the basis for the concept of epigenetics. Thus, epigenetics can be broadly defined as the study of reversible, heritable changes that occur in gene expression without altering the DNA sequence (Roloff and Nuber, 2005,

Kiefer, 2007, Ballestar, 2011, Hubner et al., 2012). Epigenetic regulation encompasses methylation of DNA, microRNA (miRNA) and post-translational modifications to histone proteins. The next section will discuss the relationship of DNA to histone proteins.

1.7 Chromosome organization

The DNA-protein complex, referred to as chromatin, allows the large volume of DNA contained in a cell, to efficiently reside in the microscopic nuclear structure. The functional unit of this chromatin is known as the nucleosome. Electron microscopy illustrated this structure as a 'beads on string' conformation with the histone proteins forming each core and the chromosome wrapping around it approximately 1.67 times. This structure is referred to as the first level of organization of chromatin at which point the chromatin fiber has a diameter of 11nm. Condensation of this fiber continues in the form of a solenoid with the help of various SMC (structural maintenance of chromosomes) proteins like condensin and cohesin to give rise to 30 nm fiber which further folds and compacts to 100 and 400nm thick interphase fibers and eventually, the 1400nm thick mitotic chromatid (Figure 6) (Ridgway and Almouzni, 2001, Aragon et al., 2013).

The histone core component of the nucleosome is made up of an octamer consisting of a H3-H4 heterotetramer bound to two H2A-H2B heterodimers. Crystallographic studies have elucidated the histone protein structure to have a

central globular domain and N and C-terminal peptides, the sequences of which are highly conserved from yeast to humans. These sequences are of different lengths and are referred to as histone tails. Although the histone tails are not required for the formation of the histone core octamer, they play a critical role towards those modifications that regulate accessibility of chromatin for transcription (Eickbush and Moudrianakis, 1978, Palter et al., 1979, Alberts, 2010).

The N-terminal of the histone core components serves as the prime target for post-translational modifications like acetylation, phosphorylation and methylation (Figure 7). The lysine residues of these tail regions are the point at which modifications like acetylation, ubiquitination, sumoylation and biotinylation occur, whereas phosphorylation occurs on the serine or threonine residues and methylation occurs on the arginine residues (Bartova et al., 2008, Hubner et al., 2012, Zentner and Henikoff, 2013). The following sections will discuss in detail post-translational modifications to histone tails and enzymes that mediate those modifications.

1.8 Acetylation and deacetylation

Acetylation of histones occurs when an enzyme set known as the histone acetyltransferases (HATs) transfers an acetyl group to the Ɛ- amino group of the lysine residue present on the N-terminal tail regions of core histones (Kurdistani and Grunstein, 2003). This addition of an acetyl group neutralizes the positive

charge on the lysine residue and thereby weakens the interactions between the histone tails and the negatively charged phosphate backbone of DNA. This allows the transcription machinery access to the promoter regions of the DNA leading to gene activation (Struhl, 1998, Sterner and Berger, 2000). There are few HATs that have been identified owing to the low substrate specificity in in vitro studies as well as their roles in acetylation of non-histone proteins. Nevertheless, p300 and CREB Binding Protein (CBP) are amongst those HATs that have been better characterized. Studies have implicated a critical role of these two enzymes in early nervous system development evidenced by the fatality and severe neural tube defects observed in p300/CBP knockout mouse models (Yao et al., 1998, Goodman and Smolik, 2000).

Conversely, the removal of the acetyl groups from the histone tail regions results in the nucleosome becoming tightly packed and inaccessible for transcription. This action is carried out by a family of enzymes known as the Histone deacetylases (HDACs). There are 18 HDACs that have been identified of which eleven are Zinc (Zn^{2+}) dependent and seven that are NAD^{+} dependent. The Zn^{2+} dependent HDACs are referred to as the 'Classical HDAC family' and are further divided into 4 classes, Class I, IIa, Iib, and IV, based on sequence homology to their yeast counterparts. The NAD^{+} dependent HDACs are grouped into Class III and are referred to as 'sirtuins' (Figure 8)(de Ruijter et al., 2003, Lucio-Eterovic et al., 2008, Karagiannis and Ververis, 2012).

HDAC activity has generally been associated with repression of genes; however, recent studies have elucidated an indirect role for these enzymes wherein gene activation was observed. An example of this is described by Dehm et al in 2004 where their studies showed repression of the core SRC promoter when treated with a HDAC inhibitor (Dehm et al., 2004).

1.9 Methylation

Methylation of histones is carried out by transferring a methyl group to either the arginine or the lysine residues. The locus of methylation in the genome is also crucial to be able to determine the effect on gene expression. For example, methylation of histone H3 at lysine 4 (H3K4) results in gene activation whereas methylation of histone H3 at lysine 9 (H3K9) and 27 (H3K27) have been associated with gene repression (Strahl et al., 1999, Zhang and Reinberg, 2001). Histones can be mono-, di- or tri- methylated depending on the histone tail residue being targeted i.e. arginine residues may be mono- or dimethylated and lysine residues can be mono-, di or trimethylated. Heterochromatic regions usually have a higher degree of methylation with histones being predominantly trimethylated whereas euchromatic regions are generally observed to be enriched with mono- or dimethylated histone loci (Robin et al. 2007).

Histone methylation is carried out by histone methyltransferase enzymes (HMT) like Suv39h1 (Suppressor of variegation 39h1), G9a (EuHMTase-2), etc. (Robin et al., 2007). The activity of Suv39h1 has been described to be in the

euchromatic regions i.e. it is associated with mono- and dimethylation of histones. G9a, on the other hand has mostly been observed in the heterochromatic regions wherein its activity results in trimethylation of histone H3 at lysine 9 (H3K9). Effector proteins bind to these repressed sites with the help of specific recognition domains and help in the formation of heterochromatin. For example, HP1, an effector protein possesses a site recognizing chromodomain, which binds to trimethylated lysine residue of histone H3 (H3K9) giving rise to the formation of heterochromatin.

Histone methylation may also be linked to DNA methylation. DNA methylation is mainly observed as 5'methylcytosine on CpG dinucleotide enriched regions on DNA also known CpG Islands. These areas are present in the major groove of the DNA helix, where it is accessible to the sequence specific DNA binding proteins. DNA methyltransferases (DNMT) are responsible for the catalytic reactions resulting in the methylation of CpG nucelotides Depending on the degree of modification, various methyl-CpG-binding proteins may then bind to these methylated CpG islands and recruit transcription repression complexes to the promoter regions resulting in gene silencing. In the retina, DNA methylation plays an important role in the development of photoreceptors by hypomethylation of the genes to be expressed in the fate committed cells and hypermethylation of the same genes in all other retinal cell types (Cheung and Lau, 2005, Cedar and Bergman, 2009).

Recent evidence also suggests that there is methylation that occurs in the exons and introns which are not associated with the CpG islands and maybe involved in RNA-splicing linked to cell-type specific expression patterns (Strathdee et al., 2004).

1.10 Histone phosphorylation

Histone phosphorylation refers to the addition of a negatively charged phosphate group to serine, threonine or tyrosine residues on the histone tail regions. This modification is mostly associated with transcriptional activation due to the weakening of electrostatic interactions between the positively charged histone proteins and negatively charged phosphate backbone of DNA. Protein kinases and protein phosphatases are the enzymes that catalyze this modification. The use of these enzyme groups indicate the presence of crosstalk between epigenetic machinery in a cell and intracellular signaling pathways where kinases and phosphatases are of prime importance.(Nowak and Corces, 2004, Perez-Cadahia et al., 2010, Banerjee and Chakravarti, 2011)

1.11 Histone ubiquitination

Histone ubiquitination is a reversible modification that refers to the addition of a single ubiquitin amino acid group to the core histones, H2A and H2B. This steady state modification is modulated based on the availability of ubiquitin and the appropriate enzymatic machinery. The consequences of this modification on transcription of a gene are dependent on which core histone is ubiquitinated. For

example, ubiquitination of H2A histone results in the repression of a gene, whereas H2B ubiquitination can result in both activation and/or repression.

Addition of an ubiquitin group to a protein requires the sequential action of E1, E2 and E3 ligases. The removal of these ubiquitin groups is carried out by isopeptidases. The E1 enzyme is involved in the ubiquitination of most other proteins but the E2 and E3 enzymes are more specific.

Studies have reported the existence of a distinct cross-talk between ubiquitination and methylation of histones wherein H2B is believed to be necessary for H3 di or tri methylation while H2A ubiqutination has the opposite effect. This interaction extends the effects of ubiquitination to transcriptional control (Shilatifard, 2006, Weake and Workman, 2008, Cao and Yan, 2012).

1.12 Sumoylation

A closely related post-trancriptional modification to ubiquitination is sumoylation i.e. the addition of a SUMO (Small Ubiquitin-related Modifier) to the histone core protein, H4. This process of covalent attachment is modulated by E1, E2 and E3 enzymes and is reversed by proteases. Although mostly referred to as a transcriptional repression marker, sumoylation has been implicated in protein-protein interaction control, exertion of a controlled inhibitory effect on ubiquitin mediated degradation, etc.

Transcription repression, however, is achieved by the recruitment of transcriptional repressor molecules like histone deacetalyses and heterochromatin protein 1 and simultaneous inhibition of histone acetylation (Shiio and Eisenman, 2003, Geiss-Friedlander and Melchior, 2007, Ouyang and Gill, 2009).

1.13 The histone code

Strahl and Allis (2000) proposed that modifications occurring on the histone tails are of prime importance in the study of the activation and repression of genes where some enzymes work to chemically mark the proteins to direct the docking activity of other proteins and some work towards regulating accessibility to the DNA. This hypothesis, now referred to as the Histone Code Hypothesis, describes the post-translational modifications of histones as occurring in three sequential phases; ‘writing’, ‘reading’ and ‘erasing’.

The writing phase involves the activity of the acetylation, methylation and phosphorylation enzymes, the reading phase is characterized by the groups of proteins being recognized by others possessing the recognition-specific sequences and the erasing phase allows the activity of deacetylation, demethylation and protein phosphatase enzymes.

Therefore, the transcriptional control of the genome is heavily dependent on the effect of the appropriate combinations of all the histone modifications as have been described earlier (Strahl and Allis, 2000, Yun et al., 2011).

1.14 Epigenetic regulation in the vertebrate retina

The development of the vertebrate retina requires the synchronous activity of a vast variety of transcription factors. This activity however is subject to the strategic control of the epigenome. The progression from progenitor state to maturation for each of the six neuronal cell types present in the vertebrate retina is tightly regulated by sequential application of the writing, reading and erasing phases as described in the histone code hypothesis.

This study describes the involvement of parts of the 'writing' phase i.e histone acetylation and methylation and the 'erasing' phase with the main emphasis being on deacetylation as carried out by HDACs.

In the mouse retina, it has been shown that HATs like p300 and CBP combine with a number of transcription factors, namely, PAX6, CRX, NeuroD1 amongst others to give rise to a series of gene activation complexes. GCN5 is another HAT enzyme whose activity is seen to be essential especially for the activation of genes critical for the development and maturation of photoreceptors (Peng and Chen, 2007, Chen et al., 2012).

A general model of transcriptional activation, especially at the time of cell fate determination and differentiation of the retinal cell types, incorporates the activities of both transcription factors that bind DNA, as well as chromatin structure modifying molecules. In the heterochromatin state, the DNA binding initiation transcription factors recognize and flag binding sites followed by recruitment of chromatin remodeling complexes. The resulting euchromatin state in those areas then allows the extensive activity of histone tail modifying enzymes which in turn enable the transcriptional machinery to begin synthesizing RNA (Figure 9)(Cvekl and Mitton, 2010).

Transcriptional activation must be complemented with gene repression to avoid aberrant expression of non-specific genes as well as to control the levels of RNA being synthesized in a cell. Histone deacetylases, in combination with other enzymes are responsible for this regulation (Gallinari et al., 2007).

1.15 Classical HDACs

The implication of the activity of the 11 Zn^{2+} dependent histone deactylases, also referred to as the classical HDACs has been the subject of widespread interest especially due to the recent application of HDAC inhibitors as treatment for some forms of cancer. In the vertebrate retina, these HDACs have been found to play a pivotal role in controlling the development of the different cell types. In the developing zebrafish retina, HDAC1, which belongs to the Class I HDAC family, is shown to be essential for the exit of the retinal progenitor from the cell cycle

and progress towards differentiation. This occurs due to the antagonistic influence of HDAC1 on the proliferation promoting canonical WNT pathway. HDAC1 works to repress those genes that are targeted by the WNT pathway, one of them being the *cyclinD1 gene* which encodes the cell cycle promoter protein CYCLIND1. It also competes with β-catenin by increasing the threshold at which downstream targets get activated by Wnt signaling. A mutation in the HDAC1 encoding gene, *add*, resulted in hyperproliferation thereby changing the ratio of proliferating cells to differentiating cells in the developing zebrafish retina (Yamaguchi et al., 2005). Another study described the effects of *hdac1* mutation on the zebrafish retina wherein there was reduced appearance of the retinal ganglion cells, severe reduction in the inner and outer plexiform layers, little to no presence of photoreceptors and aberrant differentiation of Müller glial cells (Stadler et al., 2005a). In contrast, embryonic mice, mutant for *hdac1*, show a decrease in overall proliferation (Lagger et al., 2002) and similarly, a reduced proliferation was observed in the hindbrain of *hdac1* zebrafish (Cunliffe, 2004). This may suggest species specific activity of HDAC1.

A study conducted by Pelzel et al.,2010, described HDAC2 and 3 which are also members of the class I HDAC family, as having an important role in apoptosis following injury in the retina. HDAC2 had an exclusively nuclear expression in the retina under normal conditions as well as post optic nerve crush. HDAC3 was found to have a more diffused cytoplasmic localization with some nuclear scattering in the normal retina, keeping with the previously reported subcellular

localization where HDAC3 is said to translocate between the nucleus and the cytoplasm via non-histone substrates (Gao et al., 2006). After injury however, HDAC3 appeared to adopt a more nuclear pattern of expression and subsequent colocalization pattern studies with γH2AX, used as a marker for apoptotic ganglion cells, revealed that HDAC3 was translocated to the nucleus in the event of imminent cell death (Pelzel et al., 2010). Other studies have highlighted the role of HDAC3 in the initiation of chromatin condensation, which is also considered as a morphological indicator of cell death (Li et al., 2006). In the cytoplasm, HDAC3 has multiple roles including 1) reversing the acetylation of the myocyte enhancing factor 2 (MEF2) found in myogenic and neurogenic cells 2) promotion of PCAF & SRY translocation to the nucleus via deacetylation and interaction with chromosome region maintenance (CRM1) pathway 3) regulation of signal transducer and activator of transcription (STAT) phosphorylation thereby controlling its migration to the nucleus (Kramer et al., 2009, Togi et al., 2009) 4) association with mitotic spindle proteins so as to help regulate the centromeric functions during cell division (Ishii et al., 2008) (Eot-Houllier et al., 2008) (Yao and Yang, 2011)

HDACs 4,5,7 and 9, members of Class IIa of the HDAC family have a MEF binding domain as part of their primary structure which is responsible for their ability to target genomic regions (Jayathilaka et al., 2012). This MEF domain amongst others, gives these HDACs the ability to play important roles in effecting and co-ordinating multiple intracellular trafficking pathways.

The nucleo-cytoplasmic shuttling of HDAC4 is regulated by phosphorylation i.e. in its phosphorylated form HDAC4 binds to the chaperone protein 14-3-3 in the cytoplasm and when dephosphorylated, a pro- nuclear conformational change is observed followed by interactions with MEF2C and DNAJB5 proteins and is thereby translocated to the nucleus. Proteolysis and oxidation may also contribute to the nuclear transport of this HDAC enzyme. (Yao and Yang, 2011)

The cellular localization of HDACs 4 and 5 is described to be highly dynamic and driven by signal response in neuronal cells. They not only associate with the MEF2 transcription factor but their nucleo-cytoplasmic shuttling has also been shown to be regulated via calcium channels and NMDA receptors (Chawla et al., 2003).

HDAC7, described to exert a neuroprotective effect in neuronal cells, does this via a mechanism independent of deacetylase activity. The expression of c-jun, a hallmark of apoptotic cells, is inhibited by HDAC7 leading to protection of the neurons from undergoing apoptosis. This protective mechanism cannot be blocked by most chemical HDAC inhibitors (Ma and D'Mello, 2011). HDAC7 also shuttles between the nucleus and the cytoplasm under hypoxic conditions, the mechanism of which is yet to be identified. HDAC9 associates with MEF2 proteins wherein it exerts a repressive effect to create a negative feedback system during myocyte development. Its nuclear export is under the influence of G-protein mediated phosphorylation i.e. HDAC9 is translocated to the cytoplasm

when acted upon by kinases (Haberland et al., 2007). In the human cone outer segments, HDAC9 may also have anti-aging effects by preventing a stress response and also help maintain structural integrity indirectly via its interaction with cytoskeletal elements (Hornan et al., 2007).

HDACs 6 and 10, members of the Class IIb HDAC family have mostly been described as exclusively cytoplasmic enzymes but recent studies have helped identify some non-histone substrates of HDAC10 in the nucleus.

HDAC6 appears to be dynamically associated with tubulin which may affect lymphocyte chemotaxis (Cabrero et al., 2006), cell-cell- adhesion (Lafarga et al., 2012), stress granule mobility (Bartoli et al., 2011), actin remodeling (Gao et al., 2007) amongst other important functions. Other protein interactions include those with Hsp90, cortactin, β- catenin, peroxiredoxins etc (Yao and Yang, 2011).

The current literature, although able to provide the general role of these HDACs, it is unable to delineate their specific function and subcellular localization in the developing retinal cells. It is also unclear based on the literature what the roles of HDACs are given that there may be tissue and species specific effects.

Some studies have indicated that a global state of acetylation is required for the differentiation of neuronal cells (Hsieh and Gage, 2004). Further, there also appears to be discrepancies in the role of various HDACs in different species.

Here, we test the hypothesis that 1) a combinatorial state of acetylation and deacetylation is required for the development and differentiation of retinal neuronal cells and 2) the HDACs, in combination with transcription factors regulate the cell cycle exit and therefore differentiation within the retina. In this study we have shown 1) a novel tissue specific localization of the classical HDACs as observed in the developing chick and murine retina. 2)HDAC expression is fairly uniform throughout early retinal development when various cell types are generated suggesting that HDAC specificity is at the genomic level rather than cell-type specific level 3) HDAC expression is cell-type specific in the mature retina indicating a potential role in cell type-specific maintenance 4) there is an interesting and novel differential expression in subpopulation of neurons, Müller glia and retinal astrocytes in the mature retina and species specific differences are also seen to highlight this pattern 5) overall HDAC activity appears to be necessary for cell cycle exit in the chick retina.

CHAPTER 2 MATERIALS AND METHODS

2.1 Tissue collection and processing

2.1.1 Chick tissue

White leghorn fertilized chicken eggs were obtained from University of Michigan and stored until ready for use in a biological oxygen demand (BOD) incubator at 16°C (Jeio tech: IL-11A). The eggs were transferred to another incubator which is maintained at a temperature of 38°C (Kuhl, Flemington, NJ) to begin development of embryo. The embryos were collected at specific time points for the study and dissected in PBS. The tissue samples were fixed using 4% paraformaldehyde and then subjected to a series of increasing concentrations of sucrose (5%, 10%, 15% and 20%) made in 0.1M phosphate buffer, pH 7.4. The tissue was then frozen in a solution made with 20% sucrose and Optimal Cutting temperature (OCT) medium (4583Tissue-Tek, Sakura, Torrance CA) in a ratio of 3:1 and stored at -80°C. The frozen blocks were sectioned at 12µm thickness using a Leica CM3050 S cryostat and collected on Superfrost Plus slides (Fisher Scientific, Pittsburgh, PA) pre-coated with Vectabond (Vector Labs, Burlingame, CA), and were stored at -80°C.

2.1.2 Murine tissue

Mice obtained from Jackson labs, CA were mated to produce murine embryos which were removed at embryonic day 16 and pups were used at post natal day 5. The heads of E16 murine embryos and the eyes from P5 were dissected in 1XPBS and fixed overnight in 4% paraformaldehyde. They were then treated with a series of increasing concentrations of sucrose (5%, 10%, 15% and 20%) made in 0.1M phosphate buffer, pH 7.4. The obtained tissue was frozen in a solution made with 20% sucrose and Optimal Cutting temperature (OCT) medium (4583Tissue-Tek, Sakura, Torrance CA) in a ratio of 3:1 and stored at -80°C. The frozen blocks were sectioned at 12µm thickness using a Leica CM3050 S cryostat and collected on Superfrost Plus slides (Fisher Scientific, Pittsburgh, PA) pre-coated with Vectabond (Vector Labs, Burlingame, CA), and were stored at -80°C .

2.2 Flourescence immunohistochemistry

2.2.1 Standard protocol

Slides with the relevant tissue sections were defrosted and allowed to warm till room temperature after removal from the -80 freezer. Liquid blocker PAP pen (Electron Microscope Sciences, Hatfield, PA, and Cat # 71310) was used to outline the slides to contain the reagents added to the area with the tissue. Four percent paraformaldehyde fixation of the tissue sections was carried out for 30 minutes after which the slides were washed two times at intervals of ten minutes each with 1X Phosphate buffer saline (PBS). The sections were then subjected

to permeabilization by methanol for 10 minutes. The slides were then washed twice for 2 minute each with 1X PBS. Antigen retrieval was performed using 1% SDS in 0.01M PBS (Fisher Scientific, Pittsburgh, PA) for 5 minutes followed by three 5 minute washes with 1X PBS. The sections were then treated with 1% sodium borohydrite (Acros, New Jersey) in 1X PBS to reduce autofluorescence for 2 minutes. This was followed by the blocking of the tissue using a solution made with 0.25% triton-X (Biorad, Hercules, CA) made in 1X PBS and 10% donkey serum for 30 minutes. Following this, primary antibodies in the appropriate concentration were made in 2% donkey serum, 0.025% triton-X, diluted in 1X PBS. Sections were incubated with the primary antibodies overnight at 4°C. On the next day, sections were washed two times in 1X PBS followed by application of the appropriate Alexa Flour conjugated secondary antibody (Invitrogen, Grand Island, NY) made in 1X PBS for 1 hour. The sections were further washed in 1X PBS and counterstained for nuclei using Hoeschst Stain (Invitrogen, Cat# H1399). These slides were then mounted using aquapolymount (Vector labs, Burlingame, CA) and sealed with nailpolish (Electron Microscopy Sciences). The immunofluorescence was visualized using an Olympus Confocal FV 1000 microscope. To test the specificity of the primary antibodies used, peptides specific to each HDAC antibody was used. The antibody was pre-absorbed with the relevant peptide for one hour before applying it to the tissue of interest. Also, to account for any background staining that may appear due to the secondary antibody, IgG controls were done wherein tissue sections were incubated with the IgG of the host in which the primary antibody was made, in

place of the primary antibody incubation. Further protocol remained the same. The concentrations of primary antibodies and secondary antibodies used were as listed in Table 1.

2.2.2 Tyramide amplification

This protocol was carried out for immunostaining purposes when both primary antibodies used for co-label were made in the same host organism. Slides with the relevant tissue sections were defrosted after removal from the -80 freezer. Liquid blocker PAP pen (Electron Microscopy Sciences) was used to outline the slides to contain the reagents added to the area with the tissue. 4% paraformaldehyde fixation of the tissue sections was carried out for 30 minutes after which the slides were washed two times at intervals of ten minutes each with 1X Phosphate buffer saline (PBS). The sections were then subjected to permeabilization by methanol for 10 minutes. Sections were further subjected to two 2 minute washes with 1X PBS. Antigen retrieval was performed using 1% SDS in (0.01M PBS) for 5 minutes followed by three 5 minute washes with 1X PBS. The sections were then treated with 1% sodium borohydrite to reduce autofluorescence for 2 minutes. This was followed by the blocking of the tissue using a 10% goat serum solution diluted in 0.25% triton-X made in 1X PBS for 30 minutes. Following this, the first primary antibody was diluted in the appropriate concentration using 2% goat serum, 0.025% triton-X diluted in 1XPBS. Sections were incubated with one of the primary antibodies overnight at 4°C. The following day, sections were washed using 1X PBS and then treated with 3.3% hydrogen

peroxide solution made in methanol to quench endogenous peroxidase for 15 minutes. The sections were washed twice in 1X PBS for 2 minutes each and then incubated with a biotinylated secondary antibody 1:200 (Vector Labs, Burlingame, CA) made in 1XPBS for 1 hour. This was followed by two 5 minute washes in 1X PBS. HRP streptavidin (Vector labs, Burlingame, CA) diluted in 1X PBS, 1:1000, was then applied to the slides and incubated for 1 hour. After this, the sections were washed using TNT buffer. The tyramide reagent (made as per instructions provided in the Tyramide amplification kit, Perkin and Elmer) was then applied to the slides and incubated for 5 minutes and followed up by two 2 minute washes in TNT buffer and two 2 minute washes in 1X PBS. The second primary antibody was then diluted using the serum solution described earlier. The slides were incubated overnight with the second primary antibody at 4°C in the dark. The following day, the slides were washed twice in 1X PBS for 10 minutes each and then incubated with the appropriate Alexa flour conjugated secondary antibody (Invitrogen) (diluted in 1X PBS) for 1 hour at room temperature in the dark.The slides were then washed twice with 1X PBS, counterstained for nuclei using Hoechst Stain (Invitrogen) and mounted using aquapolymount. The immunofluorescence was visualized using an Olympus Confocal Microscope FV1000.

2.3 Real Time-Quantitative PCR (RT-qPCR)

Retina from E5, E8 and E18 chick embryos were used to extract whole RNA (Qiagen, Valencia, CA). These RNA samples were run on a 1% agarose gel to check and confirm the quality of the total RNA. 1µg of total RNA was used to synthesize cDNA for each sample iScript cDNA synthesis kit (Biorad, Hercules, CA). This was performed using the protocol specified by the manufacturer. 7300 RT detection system (Applied Biosystems, Carlsbad, CA) with the Power SYBR green PCR master mix (Invitrogen, Grand Island, NY) was used to perform RT-PCR. The primer pairs used have been listed in Table 2. For each reaction, a total volume of 20 µl including the diluted cDNA, which corresponded to 5ng of initial total RNA and 0.4mM of each primer was used. The cycler conditions used were as listed: 1) initial denaturation at 95°C for 10 minutes 2) 40 cycles of denaturation at 95°C for 15 seconds, 3) annealing at 60°C for 30 seconds 4) extension at 72°C for 30 seconds, 5) final extension at 72°C for 5 minutes. The efficiency of the primers used was calculated by the standard curve method, where efficiency, $E= ((10^{(-1/C_{T2} - C_{T1})}) - 1) \times 100$. A no template control (NTC) and an endogenous control - Beta 2 microglobulin (B2M) were used for every PCR run (Thal et al., 2008). The amplified samples were run on a 2% agarose gel to confirm PCR product size. The fold change in the gene expression levels was determined using the $2^{-\Delta\Delta C_T}$ method, where C_T is the crossing threshold value.

$\Delta C_T = C_{T\ \text{Target gene}} - C_{T\ \text{B2M}}$ and $\Delta\Delta C_T = \Delta C_{T\ \text{treated}} - \Delta C_{T\ \text{control}}$

2.4 Microinjections

Fertilized chicken eggs were transferred to the 38°C and incubated for three days. On day 3 of incubation, the eggs were turned on their sides for 1 hour. These eggs were then opened using a windowing method as standardized earlier in the lab (Belecky-Adams et al., 2012). Briefly, 2-3 ml of albumin was pulled out from the egg using a 3ml syringe with a 20 gauge needle. The area on the shell to be cut open was covered with transpore surgical tape and cut open using curved tungsten carbide scissors (Fine Scientific Tools, Foster city, CA). The vitelline membrane was then subjected to a small slit so as to gain access to the embryo. Injections were carried out using 0.1mm diameter capillary tube pulled using a pipette puller (Sutter Instrument P97 Flaming/ Brown micropipette puller). The needles were then beveled to obtain a 10μm opening at the end of the needle.

These needles were then attached to a picoinjector (Harvard apparatus) and was used to deliver approximately 1μl of Trichostatin- A, a small molecule HDAC inhibitor (Tocris Cat# 1406) diluted in 30% DMSO (Fisher Scientific, Pittsburgh,PA) made in autoclaved 0.9% saline or just vehicle into the eye of the chick embryo. These eggs were then covered with transparent tape and further incubated at 38°C for 24-48 hours. After incubation, the embryos were processed and subjected to the standard protocol of immunohistochemistry as described earlier.

2.5 Cell dissociation and cell counting

Retinae from chick embryos subjected to microinjections were also used for cell dissociation and cell counting. Twenty four to forty-eight hours post- injection, the chick embryos were collected and dissected for the eyes in 1X Hanks balanced salt solution. Following this, the eyes were transferred to 1X calcium- magnesium free Hanks balanced salt solution (1X CMF) (Sigma-Aldrich Cat#H4641) (pH corrected using sodium bicarbonate). The retinae were then isolated from the whole eye tissue and cut into small pieces using tungsten needles to avoid extra damage to the cells. These pieces were then transferred to a tube using siliconized pasteur pipettes, containing warm 1X CMF and incubated in a water bath at 37°C for 10 minutes. After the incubation, the 1X CMF was removed and the cells were treated with 0.5% trypsin (Gibco) and DNAse (Qiagen, Maryland, USA) made in DMEM, for 20 minutes in a 37°C water bath. Following this, the cells were washed twice with DMEM. The cells were then passed through a reduced bore pipet to create a single- cell suspension and then filtered using a 50micron nitex filter. The cells were then counted using a hematocytometer and diluted to obtain 5×10^5 cells per ml. 200µl of the cell suspension was then used to load into a cytospin funnel attached to slides pre-treated with vectabond and centrifuged using a cytocentrifuge (ThermoShandon, Ashvile,NC &Cat#873WIDB) at 800 rpm for 3 minutes. The cells were fixed using 4% paraformaldehyde for 30 minutes and then subjected to the standard protocol of immunohistochemistry as described earlier.

CHAPTER 3 RESULTS: CHICK RETINA

3.1 Combinatorial state of heterochromatin and euchromatin in the developing chick retina

To reveal potential differences in the state of the chromatin during differentiation of the retina, we immunolabeled sections of retina at specific developmental stages with anitbodies that recognize epitopes on post-translationally modified histones that represent euchromatin and heterochromatin. For the chick, we chose embryonic days 3, 5, 8 and 18 (E3, E5, E8 and E18) for analysis. E3 chick retina is representative of a highly proliferative retina with the presence of a high number of progenitors, E5 representative of early differentiation with the appearance of the early born ganglion cells and photoreceptors but also highly proliferative, E8 representative of a more differentiated retina and reduced proliferation and finally, E18 was used to represent the mature retina with all the differentiated cell types. These sections were analyzed for the presence of heterochromatin and euchromatin domains with antibodies specific to acetylated histone 3 at lysine 18 (AcH3K18), a marker for euchromatin, and tri-methylated Histone 3 at lysine 9 (H3K9me3), a marker for heterochromatin. In the early stages of development represented by the E3 and E5 chick retina, almost all the cells appear to show overlapping label for both the euchromatin marker

(AcH3K18) and the heterochromatin marker (H3k9me3). At E8, in addition to overlap of the two labels (Figure10 I), a small population of cells towards the inner developing layers showed very weak to no label for acetylation and no apparent label for methylation (Figure10 G-H). In the mature retina (E18) there appeared to be comparatively less label overlap of the AcH3K18 and H3K9me3 marks (Figure 10 L). The co-labeled cells were observed in the outer part of the INL where horizontal cells lie, amacrine cells and ganglion cells. Cells present between the outer part of the INL and the innermost part of the INL appear to be primarily methylated (Figure 10 K). The photoreceptor nuclei and a small population of the bipolar cells showed weak label for both the markers (Figure 10).

Closer scrutiny of the immunolabel also revealed that some of the mitotic cells towards the ventricular edge of the chick retina especially at E3, E5 were singly labeled for either for AcH3k18 or H3K9me3.

These results indicated that not only was acetylation critical for the differentiation of retinal neurons but that de-acetylation and methylation were also critical. To explore the role histone deacetylase enzymes might have during the development of the chick retina. For this purpose, it was necessary to 1) check for the presence of *Hdac* mRNA in the chick 2) characterize and classify the localization of these proteins in the developing and mature chick retina.

3.2 RT-qPCR analysis of the *hdac* mRNA levels in the developing chick retina

To check for the presence of *hdac* mRNA in the developing chick retina, whole RNA was extracted from the retinas of E5, E8 and E18 chick embryos. This RNA was reverse transcribed to generate c-DNA which was then used for RT-qPCR. Analysis of the Ct values was carried out via delta-delta ct method which revealed the following trends in the fold change relative to mRNA levels in the E5 retina (Figure 11).

hdacs 3, 4, 7, 10 and 11 did not show a statistically different fold change relative to E5 at E8 and at E18. *hdacs* 1 and 9 appeared to show a decrease in the mRNA levels as development progressed with the highest level of mRNA observed at E5 and the lowest at E18. *hdac*2 mRNA levels was the only one to show an increase in the mRNA level at E18 as compared to E5.

This confirmed that *hdac* genes in the chick retina were being transcribed. To determine if this mRNA was being translated into the respective proteins, western blots and immunohistochemistry on the chick retinal sections was performed.

3.3 Classical histone deacetylase localization patterns in the chick retina

To assess the localization patterns of the HDAC proteins in the developing chick retina, the retinal sections from E3, E5, E8 and E18 were co-immunolabeled with available antibodies specific to each classical HDAC. As a control, western blots

using protein extracts from the developing chick retina were done to test the specificity of the HDAC antibodies earlier by Mahesh Shivanna, a post-doc in the lab. Further, to compare the localization patterns of these classical HDACs in still dividing retinal progenitors and some early differentiated cell types, we co-labeled the sections with each of the following markers 1) SOX2, a progenitor marker during early development at E3,5 and 8 and a marker for a subset of amacrine cells, retinal astrocytes and Müller glia in the mature retina, 2) RA4- a marker for early differentiating cells at E3 in the chick, 3) BRN3C- a nuclear marker for ganglion cells at E5,E8 and E18 and 4) VISININ- a cytoplasmic marker for early photoreceptors. These sections were then counterstained for nuclei with Hoechst stain. The potential interraction of each HDAC could be predicted by determining whether the proteins were localized to the nucleus of these cell types at various developmental stages in the chick retina.

The initial analysis of immunolabeled sections led to categorizing the localization patterns of each HDAC into predominantly nuclear and nuclear and cytoplasmic (Table 3). This analysis revealed the following; 1) HDACs 1 and 2 were predominantly nuclear in localization at all stages examined and 2) HDACs 3-11 appeared to be nuclear and cytoplasmic. These HDACs also showed some variation in localization depending on the stage examined. HDAC5 appeared to have a weak nuclear signal at E5 but went on to show a stronger nuclear label at E18. HDAC8 also appeared to be weakly labeling the nucleus of the ganglion cells at E5 but goes on to show no nuclear label by E18. HDAC10 showed

nuclear label at both E5 and E18, but appeared to have no nuclear label at E8. Further we also observed some common patterns of localization between stages E3 and E8. Many of the HDACs appeared to be higher at the vitreal and scleral edges and less abundant in the neuroblast layers in between. This was readily apparent in sections that were co-labeled with SOX2, which at E8 labels progenitor cell, many of which were weakly labeled with HDACs of interest. Further at E18, localization patterns emerged that appeared to be more cell type specific. For instance, many of the HDACs labeled nuclei in the ganglion cell layer, the inner part of the inner nuclear layer, where the amacrine cells reside and a layer of inner nuclear cells adjacent to the outer plexiform layer (presumptive horizontal cells). Very few if any of the HDACs appeared to be present in the nuclei of SOX2 labeled cells and Muller glial cells in the center of the inner nuclear layer whereas retinal astrocytes (labeled with SOX2 in the ganglion cell layer) appeared to have HDACs 1-3, 6, 8 and 9 co-localized to the nucleus. Universally, HDAC localization to the photoreceptor nuclei was very weak to non-existent. HDACs 1, 2, 3, 5 and 8 were the only HDACs that appeared to show a weak nuclear label in the E18 ONL, however, all but HDAC1 were present in the inner/outer segment and other photoreceptor processes (Table 4).

In the following sections, the HDACs have been separated by the localization patterns in the chick mentioned earlier. The localization of each HDAC in the chick is briefly described in the appropriate sections.

3.4 Predominantly nuclear histone deacetylases in the chick retina

HDAC1 and 2 showed similar localization patterns in the developing chick retina (Figure 12 A-C; 15 A-C; 18 and 19) E3 sections were co-labeled with SOX2 to mark the progenitor cells or RA4 to mark the newly differentiating cells. At E3 HDACs 1 and 2 were observed to co-localize with SOX2 labeled retinal progenitors and were also seen to appear in the nucleus of the RA4 labeled cells.

At E5, HDAC1 and HDAC2 co-localized with SOX 2 (neuroblasts), Brn 3c (Ganglion cells) and visinin (photoreceptors). At E8, HDAC 1 and 2 appeared to be more abundant in the presumptive outer nuclear layer, ganglion cell layer and markedly less abundant in the neuroblast layer. By E-18 HDAC1 appeared to be restricted permanently to presumptive horizontal cells, amacrine cells, ganglion cells and retinal astrocytes. HDAC2 showed a similar localization pattern; with the exception that immunolabel was more widespread in the inner nuclear layer than there was HDAC1 label. Müller glia did not express either HDAC1 or 2.

3.5 Nuclear and cytoplasmic histone deacetylases in the chick retina

HDACs 3-11, earlier observed as having nuclear and cytoplasmic localization patterns in the developing chick retina were also further analyzed for localization patterns in the progenitors and early differentiated cell types.

At E3, the chick retina, did not show nuclear localization of HDAC3 with the retinal progenitors (Figure 12 H-J) but showed some nuclear signal in the RA4-marked cells (Figure 15 D-F).

In the E5 chick retina, HDAC3 did not localize to the nucleus of progenitor cells but went on to have a nuclear and cytoplasmic localization pattern in the early born retinal ganglion cells and weakly in the photoreceptor population (Figure 20 A-C). At E8, nuclear and cytoplasmic localization was observed in the progenitor cells as well as the ganglion cells and photoreceptors (Figure 20 D-F). In the mature retina, HDAC3 was partially localized to the nucleus of some of the retinal astrocytes as well as a subset of cholinergic amacrine cells. Weak nuclear and cytoplasmic localization was observed in the retinal ganglion cells (Figure 20 G-I). HDAC4 at E3 appeared to be cytoplasmic in the neuroblast cells marked by SOX2 (Figure 12 J-L) but there was some nuclear label observed in the cells marked by RA4 (Figure 15 H-J).

At E5, HDAC4 appeared to be localized to the cytoplasm of the progenitor population of cells labeled by SOX2 and then goes on to have a nuclear localization in the Brn3c labeled cells as well as weak nuclear localization in the VISININ marked cells (Figure 21 A-C). The E8 chick retina co-labeled for HDAC4 showed some nuclear signal overlap in the neuroblast, a stronger nuclear and cytoplasmic signal in the ganglion cells and little to no signal in the visinin-marked photoreceptors (Figure 21: D-F).

The mature E18 chick retina labeled with HDAC4 showed no nuclear signal in the retinal astrocytes, SOX2 labeled amacrine cells or in the műller glial cells. Nuclear localization was observed in the ganglion cells co-labeled with Brn3c but there was no nuclear signal detected for HDAC4 in the photoreceptor nuclei. HDAC4 also labeled a population of presumptive amacrine cells in the inner part of the inner nuclear layer. Cytoplasmic signal was also observed in the inner plexiform layer where the synapses between the various neuronal cell types are made (Figure 21 G-I).

HDAC5 was found to be cytoplasmic in localization in the progenitor population of the E3 retina and weak nuclear label was observed in the RA4 labeled cells (Figure 13 J-L; Figure 15 A-C). HDAC 5 was observed to be predominantly cytoplasmic in the progenitor cells in the E5 and E8 and retinal astrocytes and cholinergic amacrine cells at E18. However, a nuclear and cytoplasmic localization pattern was observed in both the retinal ganglion cells in the developing (E5, E8) and mature retina (E18) (Figure 22).

HDAC6 in the developing retina (E3, E5, 8) showed a predominantly cytoplasmic localization pattern in the progenitor cells (Figure 13 D-F; Figure 23 A-D). In the mature retina, retinal astrocytes and cholinergic amacrine cells showed a nuclear and cytoplasmic localization. There was high intensity of labeling in the ganglion cell layer between E5 and E18, however, close scrutiny of the indicated the labeling was not nuclear (Figure 23 G-I).

HDAC8 appeared to have a cytoplasmic localization pattern in the progenitor population of the developing retina as observed in the E3, E5 and E8 retinal sections (Figure 13 G-I; Figure 24 A-D). RA4 labeled cells at E3 also did not show nuclear localization (Figure 16 A-C). Weak nuclear localization was observed in the retinal astrocytes and cholinergic amacrine cells in the mature retina. Cells within the ganglion cell layer showed an exclusively cytoplasmic localization pattern in both the developing and the mature retina. The photoreceptor population, on the other hand, was observed to have weak nuclear localization along with a strong cytoplasmic localization especially in the mature retina (Figure 24). HDAC9 followed a similar pattern of cytoplasmic localization in the progenitor population (Figure 13 J-L; Figure 25 A, D, G) in the developing and mature retina as observed with HDAC8. The retinal ganglion cells and the photoreceptor population in the developing retina appeared to have a cytoplasmic localization pattern of HDAC9 (Figure 25 B, C, E, F, H and I). HDAC 10 was found to be predominantly cytoplasmic in the progenitor population of the developing retina (Figure 14 A-C; Figure 26 A, D) as well the retinal astrocytes and cholinergic amacrine cells in the mature retina (Figure 26 G). The retinal ganglion cells at E18 however showed the presence of weak nuclear signal (Figure 14 A-C; Figure 16 G-I; Figure 26). The localization pattern of HDAC11 in the progenitor population in developing retina at E3, E5 and E8, and the retinal astrocyte and cholinergic amacrine cells in the mature retina appeared to be cytoplasmic with some nuclear label observed in the ganglion cells of the mature retina (Figure 14 D-F; Figure 17A-C; Figure 27).

In order to explore the species type differences or similarities in the role of the HDAC enzymes, we studied the global acetylation and methylation patterns as well as the localization of the HDAC enzymes in the developing murine retina.

3.6 Cell Dissociation and cell counting post TSA injection

To determine if HDACs were involved in cell cycle exit and/or differentiation of retinal progenitors, embryos were microinjected with HDAC inhibitor, Trichostatin-A (TSA). A range of concentrations from 50nM to 1μM was initially tested to determine the effective range of the inhibitor. Following injection of the vehicle (30% DMSO) or TSA, embryos were collected 24 or 48 hours post-injection, embedded, cryosectioned and immunolabeled for AcH3K18 or H3K9me3 to determine overall acetylation levels. Figure 28 shows that TSA (500nM) injected embryos showed an increase in acetylation and decrease in in methylation in comparison to vehicle-injected, as would be expected if TSA injection was successful. Injection of TSA above the concentrations of 500nM did not appear to increase effectiveness by immunofluorescence. Further, the levels of apoptosis were also assessed in embryos injected with a range of TSA concentrations. At 500nM and below, no apoptosis was observed in vehicle or TSA-treated embryos 24 or 48 hours post injection. However, above 500nM TSA, increasing numbers of apoptotic cells were observed as well as thinning retina in comparison to the vehicle-treated controls (not shown). Thus 500nM TSA was chosen for further evaluations.

To evaluate changes in progenitor cells and early differentiating ganglion cells and cone photoreceptors, E3 embryos were injected with vehicle or TSA, and embryos were collected 24 or 48 hours post-injection for further analysis. Embryos were analyzed using 2 methods; tissue was embedded, cryosectioned and immunolabeled using cell-type specific markers, or retina were isolated, enzymatically treated, dissociated and cytospun onto slides to be immunolabeled for quantitative estimation of cell types. For these analyses, we used three markers, SOX2 for progenitors, BRN3C for ganglion cells and VISININ for photoreceptors. The analysis of the sections showed that there appeared to be an overall increase in the thickness of TSA- injected embryos 48 hours post-injection (Figure 29) . An examination of the cell type- specific markers did not appear to show a marked change in either the BRN3C or VISININ labeled cells. Likewise, counts of control and TSA-injected retina showed no statistically significant changes of ganglion cells or cone photoreceptors (Figure 30 B). SOX2 labeled cells appeared to increase slightly, but more counts must be done to complete the data set (Figure 30 A)

CHAPTER 4 RESULTS: MURINE RETINA

4.1 Global acetylation and methylation pattern in the developing murine retina

In order to elucidate the global patterns of acetylation and methylation in the developing murine retina, a study similar to that performed on the chick retina was carried out. Retinal sections from embryonic mice at E16, which is representative of a highly proliferative retina with early born ganglion cells appearing, and P5, which was representative of a more differentiated retina, were labeled with acetylated H3K18 (marker for euchromatin) and methylated H3K9 (marker for heterochromatin). The co-localization of the two marks indicated that the developing murine retina had the presence of euchromatin and heterochromatin in the cells, in very close proximity to each other (Figure 31).

Further, to contrast the differences and/or similarities in the localization of the HDACs in the murine retina with respect to that observed in the chick retina, retinal sections from E16 and P5 murine retina were immunolabeled with antibodies specific to each classical HDAC along with SOX2 and Brn3. SOX2 labels the progenitor cells at E16 and goes onto label the retinal astrocytes, a subset of amacrine cells and also the Müller glia at P5. Visinin, the marker used

for chick retinal studies in Chapter 3 does not label mouse retina hence, we are developing markers to label developing mouse photoreceptors in future studies. As in chick retinal studies, RT-qPCR studies were done to determine which HDAC were present and immunoblots were used to distinguish whether antibodies recognized the proper molecular weight proteins (unpublished results). These studies were started by Mahesh Shivanna, a post doc in the lab, and will not be described in this thesis. A general description of the localization patterns of each of the classical HDACs in the developing murine retina will be described in the following section.

4.2 Localization patterns of the classical HDACs in the developing murine retina

Murine retina sections from E16 and P5 were labeled for the classical HDACs with the antibodies that were used for the chick studies earlier and co-labeled with SOX2 and BRN3A or BRN3C to check for their presence in the progenitor cells and the ganglion cells respectively. Broadly, all the HDACs were present in the E16 and P5 retina and appeared to have either nuclear or nuclear and cytoplasmic localization patterns. Some of the HDACs also appeared to have a differential pattern of localization depending on the age and the cell types studied. Therefore, to further distinguish between these patterns, the HDACs were categorized based on the similarity of localization in the cell types that were studied (Table 5). The localization of each HDAC will be described in the appropriate category.

Four of the five categories that the HDACs have been grouped into are based on cells that are labeled by SOX2. It labels more than one type of cell depending on the age of the animal. At E16, retinal progenitors are labeled and at P5, cholinergic amacrine cells, retinal astrocytes and Müller glia are labeled by SOX2. Also, BRN3C was used to label E16 ganglion cells and BRN3A was used to label ganglion cells in the P5 murine retina because the BRN3C antibody used did not label the P5 ganglion cells and similarly BRN3A did not label the ganglion cells at E16.

HDACs 2, 4, 5, 6, and 8 follow a similar pattern of localization where all of them labeled the nucleus of the retinal progenitors in the developing murine retina where HDAC2 (Figure 33) was the only one that showed a weaker label. They also labeled the nucleus of the cholinergic amacrine cells present in the inner nuclear layer of the retina. Here, HDAC5 (Figure 36) showed a weaker nuclear label as compared to the others in the cholinergic amarine cells. All these HDACs also strongly labeled the nuclei of the retinal astrocytes. HDACs 4 (Figure 35), 5, 6 (Figure 37) and 8 (Figure 38) showed nuclear label in the ganglion cells of the murine retina. The presence of HDAC2 in the ganglion cells was not determined. None of these HDACs labeled the Müller glia.

HDACs 1 (Figure 32), 10 (Figure 40) and 11 (Figure 41) also follow a comparable pattern of localization in the developing murine retina. These HDACs did not co-localize with SOX2 in the nuclei of the progenitor cells however, the cholinergic

amacrine cells and the retinal astrocytes showed positive nuclear label. HDAC1 and 10 showed nuclear label in the ganglion cells of the developing retina but there was very weak to no nuclear signal of HDAC11 in the ganglion cells. These HDACs also did not co-label the Müller glia.

HDAC3 (Figure 34) and HDAC9 (Figure 39) were somewhat similar in their pattern of localization. Both showed a nuclear label in the progenitors but HDAC3 had a weak signal. Further, they showed a nuclear label in the cholinergic amacrine cells, retinal astrocytes and the ganglion cells. These two HDAC enzymes were also the only ones that appeared to weakly co-localize with nuclei of the Müller glia.

CHAPTER 5 DISCUSSION

5.1 A combination of acetylation and deacetylation are necessary for the developing chick and murine retina

To initially characterize the euchromatin and hetreochromatin state pattern in the developing chick retina, sections from E3, E5, E8 and E18 chick embryos were immunolabeled with antibodies specific to acetylated H3K18 and tri-methylated H3K9. These antibodies labeled euchromatin and heterochromatin marks respectively. A clear co-localization of these two epigenetic marks was observed at all stages, with E3 and E5 showing widespread co-localization, indicating that euchromatin and heterochromatin states did exist alongside each other in the nuclei of the developing retinal cells. The co-localization patterns, also showed that the open and closed chromatin states in these cells were in very close proximity to each other as opposed to the spatial restriction of heterochromatin to the periphery of the nucleus and euchromatin centrally, that is generally described (Towbin et al.). A similar pattern of co-localization was also observed in the murine retina where acetylated H3K18 and tri-methylated H3K9 marks co-localized with each other. This pattern observed in the progenitor cells of the developing chick and murine retina may be indicating that the regions in the nuclei that show both acetylated and methylated marks contain bivalent chromatin domains. Bivalent domains in the nuclei of progenitor cells have been

previously described to be important for lineage control. Here, multiple modifications to the histone occur in a manner wherein the genes that control the final lineage of the cell are repressed in the pluripotent state but also keeps them 'poised' for activation when differentiation begins (Vastenhouw and Schier, 2012). For repression and subsequent activation to occur, the presence and activity of the appropriate enzyme must be necessary. This also coincides with our initial hypothesis that the HATs and HDACs may be working in a combinatorial manner to guide the retinal progenitors to their ultimate cell fate.

In addition to the co-localization patterns observed, a closer scrutiny of the chick retinal sections at E3 and E5 revealed that some of the mitotic cells present at the ventricular edge of the retina were either exclusively labeled for AcH3K18 or H3K9me3. These observations suggest that the chromatin state in the nuclei of the dividing cells play a very important role in their progression through the cell cycle and also control the timing of their exit. The HATs and HDACs have been implicated earlier in regulating the progression of the cell through the cell cycle in the other model systems like yeast (Legube and Trouche, 2003), Xenopus (Tseng et al., 2011)and zebrafish (Tseng et al., 2011). Given that there may be some species or tissue specific variations in the particulars of which modification and enzymes may be responsible for the cell cycle progression and exit, it remains important to further explore this mechanism in the species of interest, in this case, the chick retina.

Further, the retinal sections from the E8 chick retina revealed that there were some cells that showed a stronger acetylation label while some showed a stronger methylation label. As has been mentioned in an earlier section, E8 chick retina was used to represent a progressive point in development where proliferation has been completed in the central retina and differentiation occurs at a higher rate.

The differential labeling pattern of the two epigenetic marks may be reflective of this progression in development where a greater population of retinal cells is directed towards their cell fate with the help of the changes in the histone modification status. At E18, a greater number of cells were observed to have a stronger methylation label. E18 retina, as previously mentioned, is representative of the mature retina. Here, the cells in the retina have adopted their cell fate and have migrated to their appropriate positions. It is important for these cells now, to maintain their identity for which the genes unrelated to their lineage must be repressed while the genes allowing them to perform their cell-type function must be active.

Studies have shown that methylation and deacetylation of lineage unrelated genes is key to maintenance of the cell identity (Hublitz et al., 2009). This may explain the patterns of acetylation and methylation that we observed in the E18 chick retina wherein the cells showing a comparatively higher degree of methylation may possibly be doing so in order to maintain their identity.

Therefore, it was clear to us that methylation and deacetylation were equally important for the development of retina as was acetylation.

In order to further understand the role of deacetylation we chose to explore the role of the classical HDACs in the development of the chick retina. Also, to account for the possible species specific differences in the localization and roles of these enzymes we contrasted our findings from the chick retina to those obtained from the developing murine retina.

5.2 Classical HDACs in the developing chick and murine retina show species specificity

To study the localization patterns of the classical HDACs in the developing chick and murine retina, antibodies specific to each HDAC were used for immunohistochemistry analysis. These sections were further co-labeled for SOX2, RA4, BRN3 and VISININ to elucidate cell type specific localization in progenitors and differentiated cell types respectively. Broadly, the localization patterns of the HDACs in both the chick and the murine retina could be divided into two distinct classes, predominantly nuclear and nuclear and cytoplasmic. However the differences lay in the specific HDACs that belonged to each category and cell specific localization patterns.

HDAC1 and HDAC2 localization in the chick retina in all the stages of development studied was found to be predominantly nuclear. In the cell types

that were studied in the chick retina, namely retinal progenitors, ganglion cells, and early photoreceptors in the developing retina with the addition of cholinergic amacrine cells, retinal astrocytes and Müller glia in the mature retina, HDACs1 and 2 appeared to be localized to their nucleus with the exception of the Müller glia. On the other hand, with the cell types that were studied in the developing mouse retina, namely the retinal progenitors and early ganglion cells at E16 with the addition of retinal astrocytes, cholinergic amacrine cells and Müller glia at P5, showed that HDAC1 was nuclear and cytoplasmic in localization. Also, at E16, the nuclear label in the retinal progenitors and the ganglion cells for HDAC1 was weak in contrast to E3, E5 and E8 chick retinal sections. A stronger nuclear label was observed at P5 in the retinal astrocytes, cholinergic amacrine cells and the ganglion cells and no nuclear label in the Müller glia which was similar to the chick retina. HDAC2 was the only protein that appeared to be predominantly nuclear in localization in the developing murine retina, similar to the nuclear localization observed in the chick retina.

HDACs3-11 were nuclear and cytoplasmic in localization with stage dependent variability, in the chick retina for instance, HDAC9 weakly labeled the nucleus of newly differentiating cells marked by RA4 at E3 and the ganglion cells at E5 and E8, but then goes on to have a strong nuclear label at E18. This localization pattern and variability was also observed in the developing murine retina where HDACs 1, 3, 4, 5 and 6 appeared to be predominantly cytoplasmic in localization at E16 but went on to having a strong nuclear localization at P5. Further, Müller

glial cells in the chick retina did not show any nuclear localization with any of the HDACs studied but in the mouse retina, at P5, HDAC3 and HDAC9 appeared to be weakly nuclear in the same cell type.

These observations, with respect to the differences observed in the two tissue types studied demonstrates that the classical HDAC enzyme localization in the developing retina varies according to the species in which they are found which also suggests that they may have species-specific activity. The differences in the HDAC localization between the early developing chick and mouse was also observed where the investigators studied the differences in spatial distribution of the class I HDACs, namely HDACs 1, 2, 3 and 8 during their development (Murko et al., 2010).

5.3 Classical HDACs show differential localization in the mature chick retina

The broad profile study of localization of the classical HDACs in the developing chick retina at E3, E5 and E8 seemed to retain general similarities. However, the mature chick retina at E18 with the appearance of all the cell types was more specific and showed differences in comparison to the developing retina. Our observations showed that 1) HDACs 1, 2, 3, 5 and 8 appeared weakly in the nuclei of the photoreceptors 2) HDACs 1, 2, 3, 4, 6, 8 and 9 appeared to be present in the nucleus of the retinal astrocytes 3) HDACs 1, 2, 3, 4, 5, 6, 9 and 11 were present in the nucleus of the ganglion cells 4) none of the HDACs were present in the nuclei of the Müller glia. The roles of these HDAC enzymes in the

mature retina may be more inclined towards maintenance of the cell types as the differentiation and maturation of the cell types has already occurred.

These results bring forth a novel categorization of the classical HDACs in the developing and mature chick retina providing the knowledge based on which the unique roles of these HDACs in each of the retinal cell types and their interaction with the genes necessary for the development of those cell types may be further elucidated.

5.4 Inhibition of class I and II HDACs may lead to inability of the dividing retinal cells to leave the cell cycle.

We hypothesized based on previous studies in the central nervous system that the HDAc activity would be critical for cell cycle exit in the developing chick retina. If this hypothesis were true, one might expect that an inhibition of HDAC activity mght lead to an increase in the progenitor cell population and an inhibition in cellular differentiation. In the TSA injected embryos, thepercentage of SOX2 labeled progenitors seemed to show an increase in the TSA treated embryonic eyes as compared to that of the control. This suggested that HDAC inhibition possibly led to the cells being unable to differentiate or that some of the dividing cells were unable to leave the cell cycle and continued to proliferate.

This observation was consistent to a certain extent, with studies that were conducted on the zebrafish which showed that HDAC, a member of the class I

HDAC superfamily, was involved in the transcription of proteins that regulate the cell cycle exit of dividing cells and that a loss of HDAC1 would lead to the inability of the cells to leave the cell cycle (Stadler et al., 2005b). We were thus also able to describe a novel method of HDAC inhibition in the developing chick retina wherein a decrease in HDAC activity possibly led to the retinal cells being unable to leave the cell cycle.

On the other hand, the percentage of the early differentiated cell types remained comparable, which suggested that there may have been some cells that were already committed to their cell fate but did not differentiate until later, before the injection of the inhibitor was performed. It may also be possible that the effect of the inhibitor was transient wherein the cells overcame the effect of the inhibitor over a period of time and continued to develop as the designated cell type. Further, the other HDACs that were not inhibited, namely HDAC classes III and IV which may have been able to compensate activity to some degree. These possibilities will be addressed in future studies as is broadly described in the next sections in addition to the future scope of this thesis based on the conclusions drawn.

CHAPTER 6 CONCLUSIONS

We have shown here that in contrast to some studies, euchromatin and heterochromatin states are present in close proximity in the developing retina and therefore acetylation and deactylation may be equally important for the development of the chick and murine retina. Also, the classical HDACs were present in the developing chick and murine retina with differential expression according to species and developmental stage thus enabling us to suggest that these enzymes may have unique species and age-dependent roles. Our preliminary observation with regard to HDAC inhibition in the chick retina also tells us that overall HDAC activity is required for the cell to exit the cell cycle. Thus, from this study we can conclude that the classical HDACs have unique roles in the developing chick and murine retina and that their activity may be necessary for cell cycle exit.

CHAPTER 7 FUTURE DIRECTIONS

To further advance this study we hope to achieve the following in the future

1) Examine co-localization of HDACs in the photoreceptors of the developing mouse.
2) Elucidate the localization patterns of HDACs in the mature murine retina.
3) Quantify HDAC inhibition using specific assays.
4) Knockout studies for each of the classical HDACs to identify unique roles.
5) Gene interaction studies for the classical HDACs with respect to each cell type.

REFERENCES

REFERENCES

1. Ahmad I, Del Debbio CB, Das AV, Parameswaran S (2011) Muller glia: a promising target for therapeutic regeneration. Investigative Ophthalmology and Visual Sciences 52:5758-5764.
2. Alberts B (2010) Cell biology: the endless frontier. Molecular Biology of the Cell 21:3785.
3. Aragon L, Martinez-Perez E, Merkenschlager M (2013) Condensin, cohesin and the control of chromatin states. Current Opinion in Genetics & Development. (In the Press)
4. Badea TC, Cahill H, Ecker J, Hattar S, Nathans J (2009) Distinct roles of transcription factors brn3a and brn3b in controlling the development, morphology, and function of retinal ganglion cells. Neuron 61:852-864.
5. Ballestar E (2011) An Introduction to Epigenetics. In: Epigenetic Contributions in Autoimmune Disease, volume. 711 (Ballestar, E., ed), pp 1-11: Springer US.
6. Banerjee T, Chakravarti D (2011) A peek into the complex realm of histone phosphorylation. Molecular and Cellular Biology 31:4858-4873.
7. Bartoli KM, Bishop DL, Saunders WS (2011) The role of molecular microtubule motors and the microtubule cytoskeleton in stress granule dynamics. International Journal of Cell Biology 2011:939848.
8. Bartova E, Krejci J, Harnicarova A, Galiova G, Kozubek S (2008) Histone modifications and nuclear architecture: a review. The journal of Histochemistry and Cytochemistry : Official Journal of the Histochemistry Society 56:711-721.
9. Belecky-Adams TL, Hudson SR, Tiwari S (2012) In ovo eye electroporation. Methods in Molecular Biology 884:71-89.
10. Cabrero JR, Serrador JM, Barreiro O, Mittelbrunn M, Naranjo-Suarez S, Martin-Cofreces N, Vicente-Manzanares M, Mazitschek R, Bradner JE, Avila J, Valenzuela-Fernandez A, Sanchez-Madrid F (2006) Lymphocyte chemotaxis is regulated by histone deacetylase 6, independently of its deacetylase activity. Molecular biology of the cell 17:3435-3445.
11. Cao J, Yan Q (2012) Histone ubiquitination and deubiquitination in transcription, DNA damage response, and cancer. Frontiers in Oncology 2:26.
12. Cedar H, Bergman Y (2009) Linking DNA methylation and histone modification: patterns and paradigms. Nature reviews Genetics 10:295-304.

13. Chawla S, Vanhoutte P, Arnold FJ, Huang CL, Bading H (2003) Neuronal activity-dependent nucleocytoplasmic shuttling of HDAC4 and HDAC5. Journal of neurochemistry 85:151-159.Chen S, Wang QL, Nie Z, Sun H, Lennon G, Copeland NG, Gilbert DJ, Jenkins NA, Zack DJ (1997) Crx, a novel Otx-like paired-homeodomain protein, binds to and transactivates photoreceptor cell-specific genes. Neuron 19:1017-1030
14. .Chen YC, Gatchel JR, Lewis RW, Mao CA, Grant PA, Zoghbi HY, Dent SY (2012) Gcn5 loss-of-function accelerates cerebellar and retinal degeneration in a SCA7 mouse model. Human Molecular Genetics 21:394-405.
15. Cheng H, Nair G, Walker TA, Kim MK, Pardue MT, Thulé PM, Olson DE, Duong TQ (2006) Structural and functional MRI reveals multiple retinal layers. Proceedings of the National Academy of Sciences 103:17525-17530.
16. Cheung P, Lau P (2005) Epigenetic regulation by histone methylation and histone variants. Molecular Endocrinology 19:563-573.
17. Cunliffe VT (2004) Histone deacetylase 1 is required to repress Notch target gene expression during zebrafish neurogenesis and to maintain the production of motoneurones in response to hedgehog signalling. Development 131:2983-2995.
18. Cvekl A, Mitton KP (2010) Epigenetic regulatory mechanisms in vertebrate eye development and disease. Heredity 105:135-151.
19. De Ruijter AJ, van Gennip AH, Caron HN, Kemp S, van Kuilenburg AB (2003) Histone deacetylases (HDACs): characterization of the classical HDAC family. The Biochemical Journal 370:737-749.
20. Dehm SM, Hilton TL, Wang EH, Bonham K (2004) SRC proximal and core promoter elements dictate TAF1 dependence and transcriptional repression by histone deacetylase inhibitors. Molecular and Cellular Biology 24:2296-2307.
21. Doh ST, Hao H, Loh SC, Patel T, Tawil HY, Chen DK, Pashkova A, Shen A, Wang H, Cai L (2010) Analysis of retinal cell development in chick embryo by immunohistochemistry and in ovo electroporation techniques. Biomedical Developmental Biology 10:8.
22. Dyer MA, Cepko CL (2000) Control of Muller glial cell proliferation and activation following retinal injury. Nature Neuroscience 3:873-880.
23. Eickbush TH, Moudrianakis EN (1978) The histone core complex: an octamer assembled by two sets of protein-protein interactions. Biochemistry 17:4955-4964.
24. Eot-Houllier G, Fulcrand G, Watanabe Y, Magnaghi-Jaulin L, Jaulin C (2008) Histone deacetylase 3 is required for centromeric H3K4 deacetylation and sister chromatid cohesion. Genes & Development 22:2639-2644.

25. Field GD, Sher A, Gauthier JL, Greschner M, Shlens J, Litke AM, Chichilnisky EJ (2007) Spatial properties and functional organization of small bistratified ganglion cells in primate retina. The Journal of neuroscience : The Official Journal of the Society for Neuroscience 27:13261-13272.
26. Fischer AJ, Reh TA (2001) Muller glia are a potential source of neural regeneration in the postnatal chicken retina. Nature Neuroscience 4:247-252.
27. Gallinari P, Di Marco S, Jones P, Pallaoro M, Steinkuhler C (2007) HDACs, histone deacetylation and gene transcription: from molecular biology to cancer therapeutics. Cell Research 17:195-211.
28. Gan L, Xiang M, Zhou L, Wagner DS, Klein WH, Nathans J (1996) POU domain factor Brn-3b is required for the development of a large set of retinal ganglion cells. Proceedings of the National Academy of Sciences of the United States of America 93:3920-3925.
29. Gao YS, Hubbert CC, Lu J, Lee YS, Lee JY, Yao TP (2007) Histone deacetylase 6 regulates growth factor-induced actin remodeling and endocytosis. Molecular and Cellular Biology 27:8637-8647.
30. Gao Z, He Q, Peng B, Chiao PJ, Ye J (2006) Regulation of nuclear translocation of HDAC3 by IkappaBalpha is required for tumor necrosis factor inhibition of peroxisome proliferator-activated receptor gamma function. The Journal of Biological Chemistry 281:4540-4547.
31. Geiss-Friedlander R, Melchior F (2007) Concepts in sumoylation: a decade on. Nature reviews Molecular Cell Biology 8:947-956.
32. Goodman RH, Smolik S (2000) CBP/p300 in cell growth, transformation, and development. Genes & Development 14:1553-1577.
33. Gunhan-Agar E, Kahn D, Chalupa LM (2000) Segregation of on and off bipolar cell axonal arbors in the absence of retinal ganglion cells. The Journal of Neuroscience : The Official Journal of the Society for Neuroscience 20:306-314.
34. Haberland M, Arnold MA, McAnally J, Phan D, Kim Y, Olson EN (2007) Regulation of HDAC9 gene expression by MEF2 establishes a negative-feedback loop in the transcriptional circuitry of muscle differentiation. Molecular and Cellular Biology 27:518-525.
35. Harada T, Harada C, Parada LF (2007) Molecular regulation of visual system development: more than meets the eye. Genes & Development 21:367-378.
36. Hatakeyama J, Kageyama R (2004) Retinal cell fate determination and bHLH factors. Seminars in Cell & Developmental biology 15:83-89.
37. Hornan DM, Peirson SN, Hardcastle AJ, Molday RS, Cheetham ME, Webster AR (2007) Novel retinal and cone photoreceptor transcripts revealed by human macular expression profiling. Investigative Ophthalmology & Visual Science 48:5388-5396.
38. Hsieh J, Gage FH (2004) Epigenetic control of neural stem cell fate. Current Opinion in Genetics & Development 14:461-469.

39. Hublitz P, Albert M, Peters AH (2009) Mechanisms of transcriptional repression by histone lysine methylation. The International Journal of Developmental Biology 53:335-354.
40. Hubner MR, Eckersley-Maslin MA, Spector DL (2012) Chromatin organization and transcriptional regulation. Current Opinion in Genetics & Development.
41. Ishii S, Kurasawa Y, Wong J, Yu-Lee LY (2008) Histone deacetylase 3 localizes to the mitotic spindle and is required for kinetochore-microtubule attachment. Proceedings of the National Academy of Sciences of the United States of America 105:4179-4184.
42. Jacoby R, Stafford D, Kouyama N, Marshak D (1996) Synaptic inputs to ON parasol ganglion cells in the primate retina. The Journal of neuroscience : The Official Journal of the Society for Neuroscience 16:8041-8056.
43. Jayathilaka N, Han A, Gaffney KJ, Dey R, Jarusiewicz JA, Noridomi K, Philips MA, Lei X, He J, Ye J, Gao T, Petasis NA, Chen L (2012) Inhibition of the function of class IIa HDACs by blocking their interaction with MEF2. Nucleic Acids Research 40:5378-5388.
44. Karagiannis TC, Ververis K (2012) Potential of chromatin modifying compounds for the treatment of Alzheimer's disease. Pathobiology of Aging & Age Related Diseases 2: 10.3402.
45. Kiefer JC (2007) Epigenetics in development. Developmental dynamics : An Official Publication of the American Association of Anatomists 236:1144-1156.
46. Koike C, Nishida A, Ueno S, Saito H, Sanuki R, Sato S, Furukawa A, Aizawa S, Matsuo I, Suzuki N, Kondo M, Furukawa T (2007) Functional roles of Otx2 transcription factor in postnatal mouse retinal development. Molecular and Cellular Biology 27:8318-8329.
47. Kolb H (1995) Inner Plexiform Layer. In: Webvision: The Organization of the Retina and Visual System (Kolb, H. et al., eds) Salt Lake City (UT). NBK92606
48. Kolb H (1997) Amacrine cells of the mammalian retina: neurocircuitry and functional roles. Eye 11 (Pt 6):904-923.
49. Kramer OH, Knauer SK, Greiner G, Jandt E, Reichardt S, Guhrs KH, Stauber RH, Bohmer FD, Heinzel T (2009) A phosphorylation-acetylation switch regulates STAT1 signaling. Genes & Development 23:223-235.
50. Kumar A, Shamsuddin N (2012) Retinal Muller glia initiate innate response to infectious stimuli via toll-like receptor signaling. PLOS One 7:e29830.
51. Kurdistani SK, Grunstein M (2003) Histone acetylation and deacetylation in yeast. Nature Reviews Molecular Cell Biology 4:276-284.
52. Lafarga V, Mayor F, Jr., Penela P (2012) The interplay between G protein-coupled receptor kinase 2 (GRK2) and histone deacetylase 6 (HDAC6) at the crossroads of epithelial cell motility. Cell Adhesion & Migration 6:495-501.

53. Lagali PS, Balya D, Awatramani GB, Munch TA, Kim DS, Busskamp V, Cepko CL, Roska B (2008) Light-activated channels targeted to ON bipolar cells restore visual function in retinal degeneration. Nature Neuroscience 11:667-675.
54. Lagger G, O'Carroll D, Rembold M, Khier H, Tischler J, Weitzer G, Schuettengruber B, Hauser C, Brunmeir R, Jenuwein T, Seiser C (2002) Essential function of histone deacetylase 1 in proliferation control and CDK inhibitor repression. The European Molecular Biology Journal 21:2672-2681.
55. Lamb TD, Collin SP, Pugh EN, Jr. (2007) Evolution of the vertebrate eye: opsins, photoreceptors, retina and eye cup. Nature Reviews Neuroscience 8:960-976.
56. Legube G, Trouche D (2003) Regulating histone acetyltransferases and deacetylases. The European Molecular Biology Reports 4:944-947.
57. Li Y, Kao GD, Garcia BA, Shabanowitz J, Hunt DF, Qin J, Phelan C, Lazar MA (2006) A novel histone deacetylase pathway regulates mitosis by modulating Aurora B kinase activity. Genes & development 20:2566-2579.
58. Lin B, Wang SW, Masland RH (2004) Retinal ganglion cell type, size, and spacing can be specified independent of homotypic dendritic contacts. Neuron 43:475-485.
59. Lindqvist N, Liu Q, Zajadacz J, Franze K, Reichenbach A (2010) Retinal glial (Muller) cells: sensing and responding to tissue stretch. Investigative Ophthalmololgy Visual Sciences 51:1683-1690.
60. Liu W, Khare SL, Liang X, Peters MA, Liu X, Cepko CL, Xiang M (2000) All Brn3 genes can promote retinal ganglion cell differentiation in the chick. Development 127:3237-3247.
61. Lucio-Eterovic AK, Cortez MA, Valera ET, Motta FJ, Queiroz RG, Machado HR, Carlotti CG, Jr., Neder L, Scrideli CA, Tone LG (2008) Differential expression of 12 histone deacetylase (HDAC) genes in astrocytomas and normal brain tissue: class II and IV are hypoexpressed in glioblastomas. Biomedical Cancer 8:243.
62. Lukasiewicz PD (2005) Synaptic mechanisms that shape visual signaling at the inner retina. Progress in brain research 147:205-218.
63. Ma C, D'Mello SR (2011) Neuroprotection by histone deacetylase-7 (HDAC7) occurs by inhibition of c-jun expression through a deacetylase-independent mechanism. The Journal of Biological Chemistry 286:4819-4828.
64. Mariani AP (1984) The neuronal organization of the outer plexiform layer of the primate retina. International review of cytology 86:285-320.
65. Masland RH (2001) The fundamental plan of the retina. Nature Neuroscience 4:877-886.
66. McCabe KL, Gunther EC, Reh TA (1999) The development of the pattern of retinal ganglion cells in the chick retina: mechanisms that control differentiation. Development 126:5713-5724.

67. Morrow EM, Chen CM, Cepko CL (2008) Temporal order of bipolar cell genesis in the neural retina. Neural Development 3:2.
68. Murko C, Lagger S, Steiner M, Seiser C, Schoefer C, Pusch O (2010) Expression of class I histone deacetylases during chick and mouse development. The International Journal of Developmental Biology 54:1527-1537.
69. Nadal-Nicolas FM, Jimenez-Lopez M, Sobrado-Calvo P, Nieto-Lopez L, Canovas-Martinez I, Salinas-Navarro M, Vidal-Sanz M, Agudo M (2009) Brn3a as a marker of retinal ganglion cells: qualitative and quantitative time course studies in naive and optic nerve-injured retinas. Investigative Ophthalmology & Visual science 50:3860-3868.
70. Nathans J (1999) The evolution and physiology of human color vision: insights from molecular genetic studies of visual pigments. Neuron 24:299-312.
71. Nowak SJ, Corces VG (2004) Phosphorylation of histone H3: a balancing act between chromosome condensation and transcriptional activation. Trends in Genetics : TIG 20:214-220.
72. Otteson DC, Phillips MJ (2010) A conditional immortalized mouse muller glial cell line expressing glial and retinal stem cell genes. Investigative Ophthalmolology and Visual Sciences 51:5991-6000.
73. Ouyang J, Gill G (2009) SUMO engages multiple corepressors to regulate chromatin structure and transcription. Epigenetics : Official Journal of the DNA Methylation Society 4:440-444.
74. Palter KB, Foe VE, Alberts BM (1979) Evidence for the formation of nucleosome-like histone complexes on single-stranded DNA. Cell 18:451-467.
75. Pelzel HR, Schlamp CL, Nickells RW (2010) Histone H4 deacetylation plays a critical role in early gene silencing during neuronal apoptosis. Biomedical Neuroscience 11:62.
76. Peng GH, Chen S (2007) Crx activates opsin transcription by recruiting HAT-containing co-activators and promoting histone acetylation. Human Molecular Genetics 16:2433-2452.
77. Pennesi M, Bramblett D, Cho J-H, Tsai M-J, Wu S (2006) A Role for bHLH Transcription Factors in Retinal Degeneration and Dysfunction. In: Retinal Degenerative Diseases, vol. 572 (Hollyfield, J. et al., eds), pp 155-161: Springer US.
78. Perez-Cadahia B, Drobic B, Khan P, Shivashankar CC, Davie JR (2010) Current understanding and importance of histone phosphorylation in regulating chromatin biology. Current Opinion in Drug Discovery & Development 13:613-622.
79. Pickard GE, Sollars PJ (2012) Intrinsically photosensitive retinal ganglion cells. Reviews of Physiology, Biochemistry and Pharmacology 162:59-90.
80. Ridgway P, Almouzni G (2001) Chromatin assembly and organization. Journal of Cell Science 114:2711-2712.

81. Robin P, Fritsch L, Philipot O, Svinarchuk F, Ait-Si-Ali S (2007) Post-translational modifications of histones H3 and H4 associated with the histone methyltransferases Suv39h1 and G9a. Genome Biology 8:R270.
82. Rockhill RL, Daly FJ, MacNeil MA, Brown SP, Masland RH (2002) The diversity of ganglion cells in a mammalian retina. The Journal of neuroscience : The Official Journal of the Society for Neuroscience 22:3831-3843.
83. Roloff TC, Nuber UA (2005) Chromatin, epigenetics and stem cells. European Journal of Cell Biology 84:123-135.
84. Sernagor E, Eglen SJ, Wong ROL (2001) Development of Retinal Ganglion Cell Structure and Function. Progress in Retinal and Eye Research 20:139-174.
85. Shiio Y, Eisenman RN (2003) Histone sumoylation is associated with transcriptional repression. Proceedings of the National Academy of Sciences of the United States of America 100:13225-13230.
86. Shilatifard A (2006) Chromatin modifications by methylation and ubiquitination: implications in the regulation of gene expression. Annual Review of Biochemistry 75:243-269.
87. Sjostrand FS, Candipan RC, Durstenfeld A (1988) The surface structure of photoreceptor outer segment disks. Journal of Ultrastructure and Molecular Structure Research 101:40-50.
88. Snellman J, Kaur T, Shen Y, Nawy S (2008) Regulation of ON bipolar cell activity. Progress in Retinal and Eye Research 27:450-463.
89. Stadler JA, Shkumatava A, Norton WH, Rau MJ, Geisler R, Fischer S, Neumann CJ (2005a) Histone deacetylase 1 is required for cell cycle exit and differentiation in the zebrafish retina. Developmental Dynamics : an Official Publication of the American Association of Anatomists 233:883-889.
90. Stadler JA, Shkumatava A, Norton WHJ, Rau MJ, Geisler R, Fischer S, Neumann CJ (2005b) Histone deacetylase 1 is required for cell cycle exit and differentiation in the zebrafish retina. Developmental Dynamics 233:883-889.
91. Sterner DE, Berger SL (2000) Acetylation of histones and transcription-related factors. Microbiology and Molecular Biology Reviews : MMBR 64:435-459.
92. Strahl BD, Allis CD (2000) The language of covalent histone modifications. Nature 403:41-45.
93. Strahl BD, Ohba R, Cook RG, Allis CD (1999) Methylation of histone H3 at lysine 4 is highly conserved and correlates with transcriptionally active nuclei in Tetrahymena. Proceedings of the National Academy of Sciences of the United States of America 96:14967-14972.
94. Strathdee G, Davies BR, Vass JK, Siddiqui N, Brown R (2004) Cell type-specific methylation of an intronic CpG island controls expression of the MCJ gene. Carcinogenesis 25:693-701.

95. Struhl K (1998) Histone acetylation and transcriptional regulatory mechanisms. Genes & Development 12:599-606.
96. Stryer L, Bourne HR (1986) G proteins: a family of signal transducers. Annual Review of Cell Biology 2:391-419.
97. Swaroop A, Kim D, Forrest D (2010) Transcriptional regulation of photoreceptor development and homeostasis in the mammalian retina. Nature Reviews Neuroscience 11:563-576.
98. Thal SC, Wyschkon S, Pieter D, Engelhard K, Werner C (2008) Selection of endogenous control genes for normalization of gene expression analysis after experimental brain trauma in mice. Journal of Neurotrauma 25:785-794.
99. Thoreson WB, Babai N, Bartoletti TM (2008) Feedback from horizontal cells to rod photoreceptors in vertebrate retina. The Journal of neuroscience : The Official Journal of the Society for Neuroscience 28:5691-5695.
100. Togi S, Kamitani S, Kawakami S, Ikeda O, Muromoto R, Nanbo A, Matsuda T (2009) HDAC3 influences phosphorylation of STAT3 at serine 727 by interacting with PP2A. Biochemical and Biophysical Research Communications 379:616-620.
101. Towbin BD, Gonzalez-Sandoval A, Gasser SM Mechanisms of heterochromatin subnuclear localization. Trends in Biochemical Sciences. 38(7):356-63.
102. Tseng AS, Carneiro K, Lemire JM, Levin M (2011) HDAC activity is required during Xenopus tail regeneration. PLOS one 6:e26382
103. Vastenhouw NL, Schier AF (2012) Bivalent histone modifications in early embryogenesis. Current Opinion in Cell Biology 24:374-386.
104. Watanabe M, Rodieck RW (1989) Parasol and midget ganglion cells of the primate retina. The Journal of Comparative Neurology 289:434-454.
105. Weake VM, Workman JL (2008) Histone ubiquitination: triggering gene activity. Molecular Cell 29:653-663.
106. Xiang M (1998) Requirement for Brn-3b in early differentiation of postmitotic retinal ganglion cell precursors. Developmental Biology 197:155-169.
107. Xiang M, Gan L, Zhou L, Klein WH, Nathans J (1996) Targeted deletion of the mouse POU domain gene Brn-3a causes selective loss of neurons in the brainstem and trigeminal ganglion, uncoordinated limb movement, and impaired suckling. Proceedings of the National Academy of Sciences of the United States of America 93:11950-11955.
108. Yamaguchi M, Tonou-Fujimori N, Komori A, Maeda R, Nojima Y, Li H, Okamoto H, Masai I (2005) Histone deacetylase 1 regulates retinal neurogenesis in zebrafish by suppressing Wnt and Notch signaling pathways. Development 132:3027-3043.

109. Yao T-P, Oh SP, Fuchs M, Zhou N-D, Ch'ng L-E, Newsome D, Bronson RT, Li E, Livingston DM, Eckner R (1998) Gene Dosage Dependent Embryonic Development and Proliferation Defects in Mice Lacking the Transcriptional Integrator p300. Cell 93:361-372.
110. Yao YL, Yang WM (2011) Beyond histone and deacetylase: an overview of cytoplasmic histone deacetylases and their nonhistone substrates. Journal of Biomedicine & Biotechnology 2011:146493.
111. Yun M, Wu J, Workman JL, Li B (2011) Readers of histone modifications. Cell Research 21:564-578.
112. Zentner GE, Henikoff S (2013) Regulation of nucleosome dynamics by histone modifications. Nature Structural & Molecular Biology 20:259-266.
113. Zhang Y, Reinberg D (2001) Transcription regulation by histone methylation: interplay between different covalent modifications of the core histone tails. Genes & Development 15:2343-2360.

TABLES

TABLES

Table 1 List of antibodies used for immunohistochemistry

HDAC	Antibody Supplier	Concentration used	Peptide supplier
Rabbit Anti-HDAC 1 (Cat # ab33278)	ABCAM (Cambridge, MA)	1:300	ABCAM (Cambridge, MA)
Mouse Anti-HDAC 2 (Cat # ab12169)	ABCAM (Cambridge, MA)	1:350	ABCAM (Cambridge, MA)
Rabbit Anti-HDAC 3 (Cat # ab16047)	ABCAM (Cambridge, MA)	1:300	ABCAM (Cambridge, MA)
Rabbit Anti-HDAC4 (Cat# NBP2-22151)	Novus Biologicals (Littleton, Co)	1:500	-
Rabbit Anti-HDAC 5 (Cat # ab53693)	ABCAM (Cambridge, MA)	1:100	Santa Cruz (Santa Cruz, CA)
Rabbit Anti-HDAC 6 (Cat #LSB5253)	Life Span Biosciences (Seattle, WA)	1:250	Santa Cruz (Santa Cruz, CA)
Rabbit Anti-HDAC 8 (Cat # sc11405)	Life Span Biosciences (Seattle, WA)	1:500	Life Span Biosciences (Seattle, WA)
Rabbit Anti-HDAC 9 (Cat # ab59718)	ABCAM (Cambridge, MA)	1:250	ABCAM (Cambridge, MA)
Rabbit Anti-HDAC 10 (Cat # NB100-91801)	Novus Biologicals (Littleton, Co)	1:100	Santa Cruz (Santa Cruz, CA)
Rabbit Anti-HDAC 11 (Cat #GTX116403)	GeneTex (Irvine, CA)	1:100	Santa Cruz (Santa Cruz, CA)
Rabbit Anti-Acetylated histone (Cat# ab1191)	ABCAM (Cambridge, MA)	1:1000	N/A
Mouse Anti-methylated histone (cat# ab1220)	ABCAM (Cambridge, MA)	1:300	N/A
Goat Anti- Brn 3c C-14(sc-6026(	Santa Cruz (Santa Cruz CA)	1:100	N/A
Mouse anti- Visinin	Developmental studies Hybridoma Bank (Iowa)	1:30	N/A
Goat Anti-Sox2 (Cat # sc17320)	Santa Cruz (Santa Cruz, CA)	1:250	N/A
Mouse anti-BRN3A	Chemicon International (Ternacula, CA)	N/A	N/A
Mouse anti-RA4	Gift from Steve McLoon	1:1000	N/A

Table 2 List of primer used for RT- qPCR for chick HDAC mRNA		
HDAC	FORWARD/ REVERSE	PRIMER SEQUENCE
HDAC1	Forward	CGTGGGGAGGCAGGAAAATG
	Reverse	CGGATCCTGTGGGGCTTCAT
HDAC2	Forward	CTATGGCGTACAGTCAGGGC
	Reverse	TTTCATTGGATGCCCTTGTCCA
HDAC3	Forward	CTTTCAACGTGGGCGATGAC
	Reverse	GTTGTTCAGCTGCGTTGCTC
HDAC4	Forward	GGCCCTCCAGCAGTTAGTG A
	Reverse	AGCTGGCTCGTTGGGTTTTG
HDAC7	Forward	GCAGGGATTCTGTCACAGCG
	Reverse	TGGCCACTTTGAAGGCCAAC
HDAC9	Forward	CCACCCCAAGCTCTGGTAC
	Reverse	AGCCGTTTTACGGAGTGGGA
HDAC10	Forward	TGTTGCTGTTGCACTGAGAC
	Reverse	CATTCCCGTCAGCATCCTCT
HDAC11	Forward	ACCTCTGCGAACCCAGACAG
	Reverse	CACGTTGATTGCCCAGCCTC
Beta2 microglobulin	Forward	CAAGGACGACTGGACCTTCC
	Reverse	CGGGATCCCACTTGAAGAC

Table 3 Categorization of HDAC localization in the developing chick retina	
Predominantly nuclear	Nuclear and cytoplasmic
HDAC1	HDAC3
HDAC2	HDAC4
	HDAC5
	HDAC6
	HDAC8
	HDAC9
	HDAC10
	HDAC11

Table 4 Localization of HDACs in the mature chick retina

HDAC	Outer nuclear layer	Cholinergic amacrine cells	Müller Glia	Retinal astrocytes	Retinal ganglion cells
HDAC1	+/-	+	-	+	+
HDAC2	+/-	+	-	+	+
HDAC3	+/-	+	-	+	+
HDAC4	-	-	-	-	+
HDAC5	+/-	-	-	-	+
HDAC6	-	+	-	+	+
HDAC8	+/-	+/-	-	+	+
HDAC9	-	+/-	-	+	+
HDAC10	-	-	-	-	+/-
HDAC11	-	-	-	-	-

- No nuclear label, +/- Weak nuclear label, + Nuclear label

Table 5 Classical HDAC localization in the developing murine retinal cell types

	Progenitors	Cholinergic amacrine Cells	Retinal astrocytes	Ganglion cells	Müller glia
HDAC1	-	+	+	+	-
HDAC2	+/-	+	+	ND	-
HDAC3	-	+	+	+	+
HDAC4	+	+	+	+	-
HDAC5	+	+/-	+	+	-
HDAC6	+	+	+	+	-
HDAC8	+	+	+	+	-
HDAC9	+/-	+	+	+	+
HDAC10	-	+	+	+	-
HDAC11	-	+	+	-	-

- No nuclear label, +/- Weak nuclear label, + Nuclear label, ND Not determined

FIGURES

FIGURES

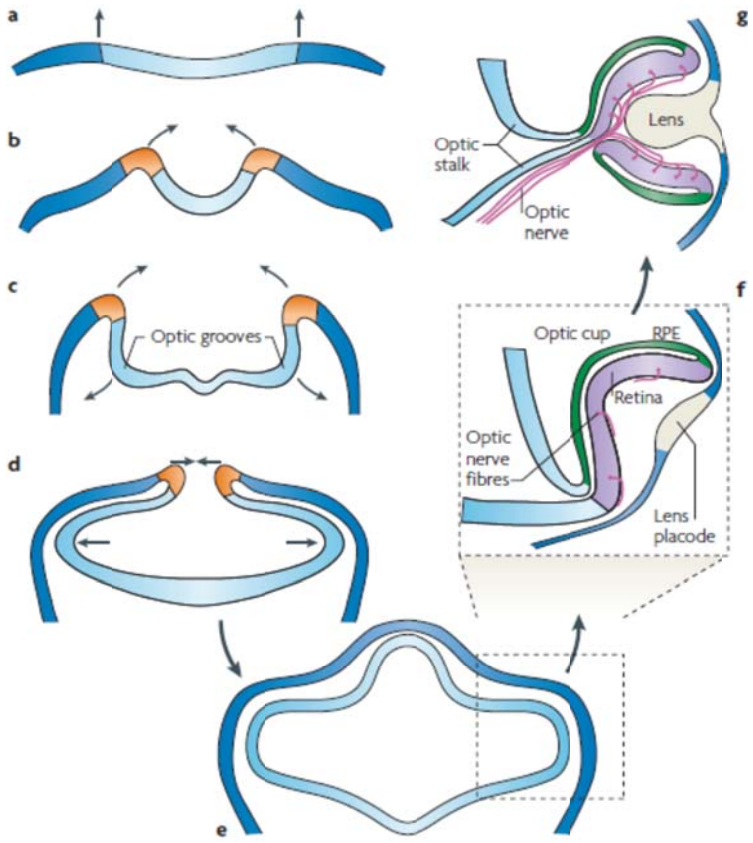

Figure 1 Development of the vertebrate eye (Lamb, Collin, & Pugh, 2007). Development of the vertebrate eye starts with (a) Induction of the neural plate (light blue) (b) Under the influence of transcription factors, the neural plate folds upwards and inwards to form the neural tube (light blue). (c) Evagination and bisecting of the presumptive eye field then follows with the appearance of distinct

optic grooves. (d) Optic grooves enlarge followed by (e-f) closure of the neural tube and the developing optic vesicle then makes contact with the overlying surface ectoderm with the simultaneous induction of the lens placode. Invagination of the optic vesicle resulting in the formation of a double layered optic cup where the inner layer is presumptive neural retina and the outer layer is the presumptive RPE. (g) Ganglion cells from the neural retina then send out axons which leave the eye in the form of an optic nerve.

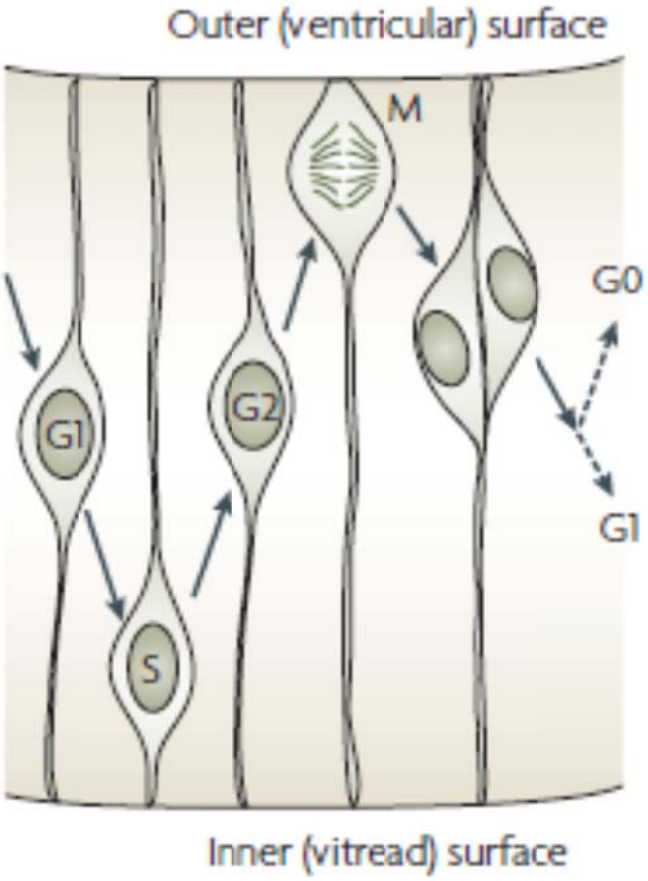

Figure 2 Retinal progenitors in cell cycle (Lamb, Collin, & Pugh, 2007). The developing retinal cells follow a distinct path of movement while undergoing various stages of the cell cycle. The cell undergoes the 'S' phase of the cell cycle when at the vitreal edge eventually followed by mitotic division at the ventricular edge of the retina. The daughter cells then either terminally differentiate or re-enter the cell cycle.

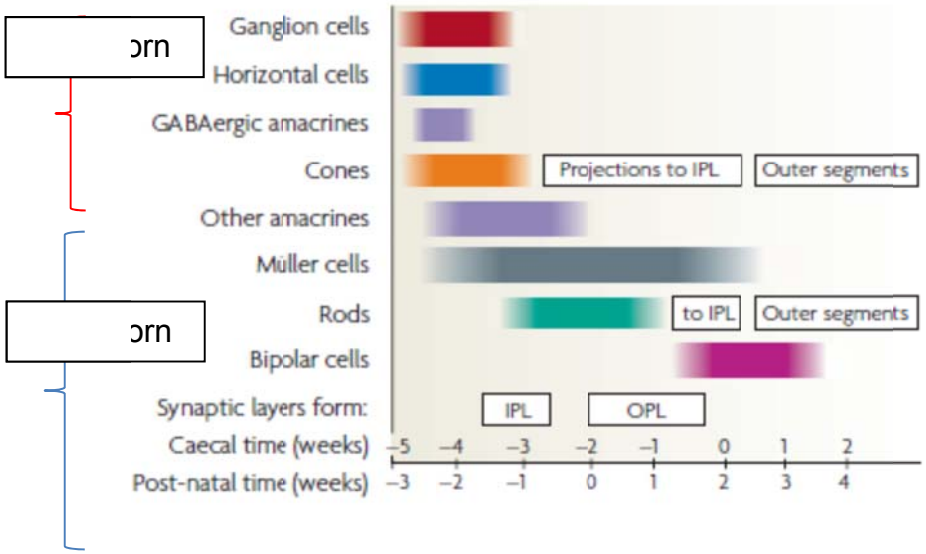

Figure 3 Graphical representation of the timeline of 'birth' of retinal cells in the vertebrate retina (Lamb, Collin, & Pugh, 2007). Cells can be roughly divided into two classes- 'early born' and 'later born'.

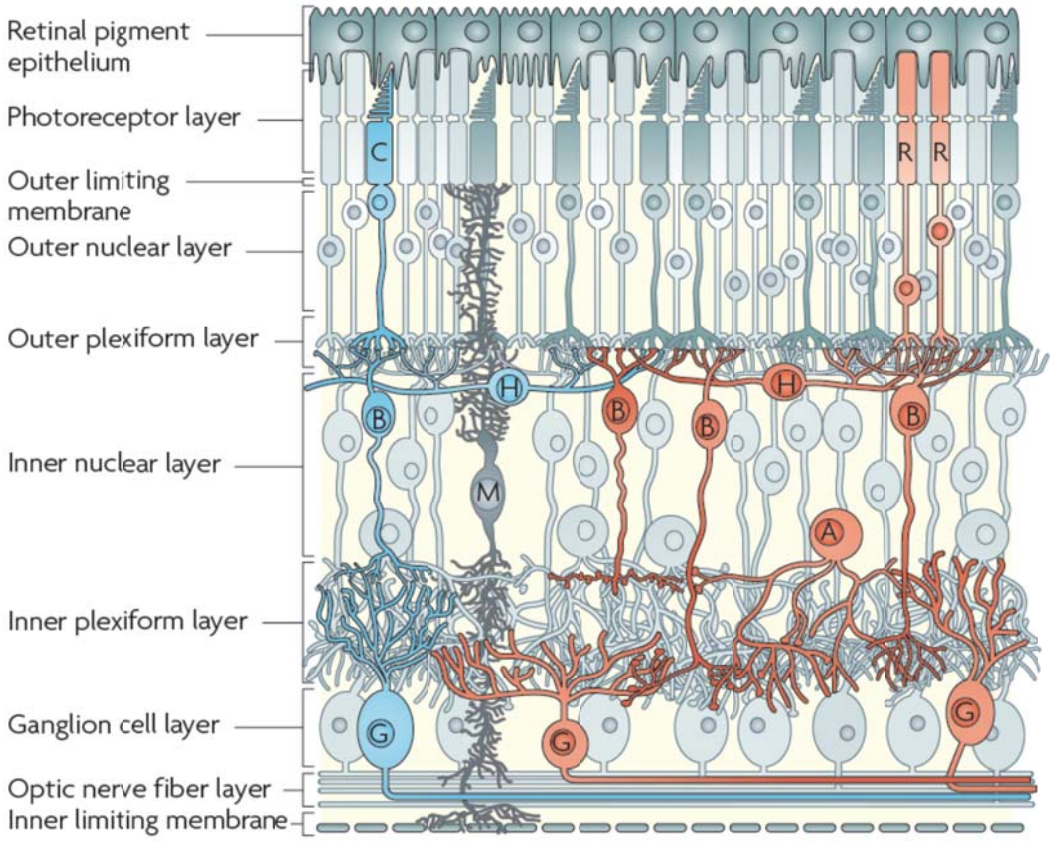

Figure 4 The multilayered structure of the mature mammalian retina (Cheng et al., 2006).

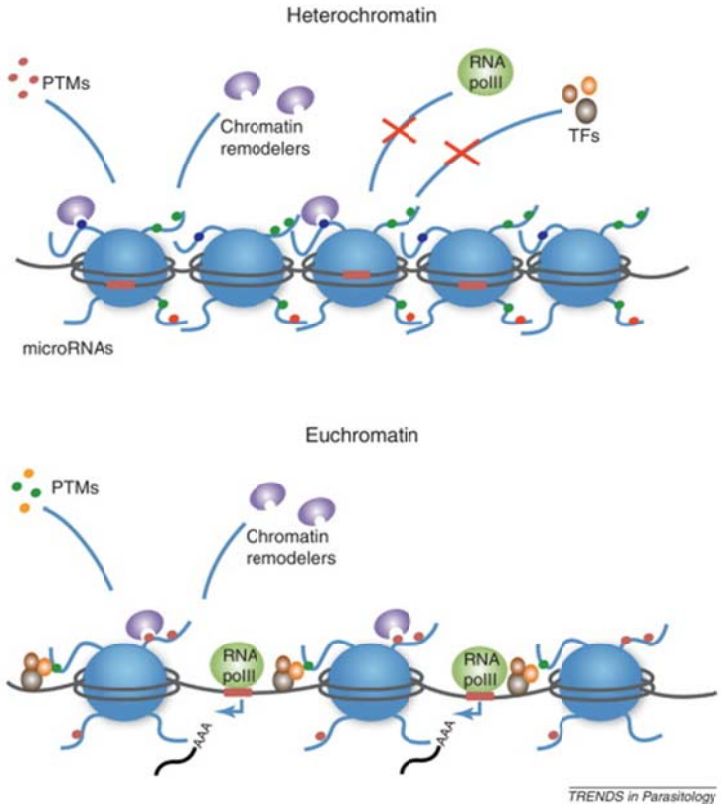

Figure 5 Schematic representation of heterochromatin and euchromatin states of DNA in a eukaryotic cell (Croken et al., 2012).

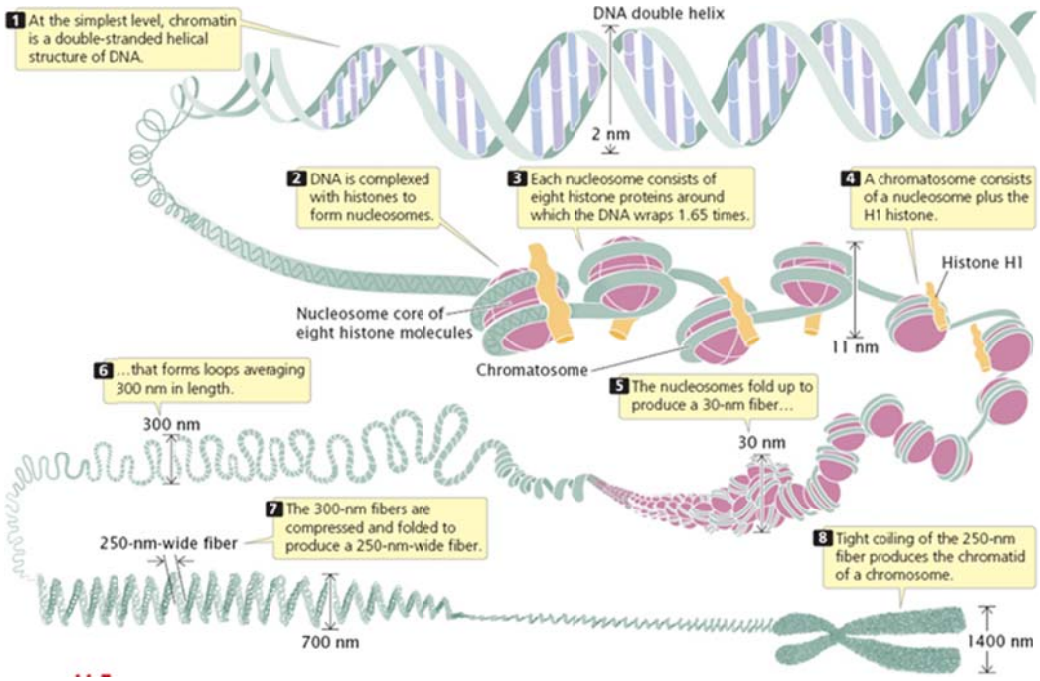

Figure 6 Chromosomal organization inside the nucleus of a eukaryotic cell (W. H. Freeman Pierce and Benjamin, 2011). Initially, chromatin is the double helical structure of DNA. It interacts with a protein core and wraps around this structure approximately 1.67 times to give rise to a 11nm fiber. This complex, now referred to as a 'nucleosome' undergoes multiple condensations with the help of structural proteins. In its most condensed form, the chromatin is referred to as the mitotic chromatid which is a 250nm thick fiber.

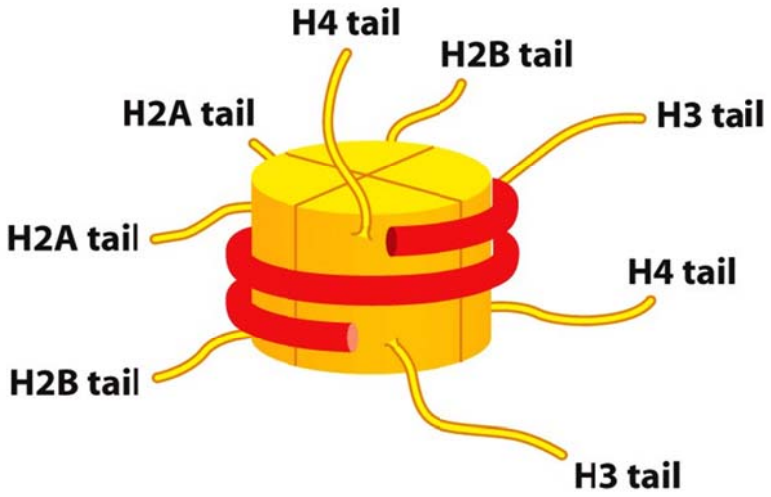

Figure 7 Schematic representation of a core histone with the N-terminal tail regions and DNA wrapped around the globular domain 1.67 times (Alberts et al., 2008).

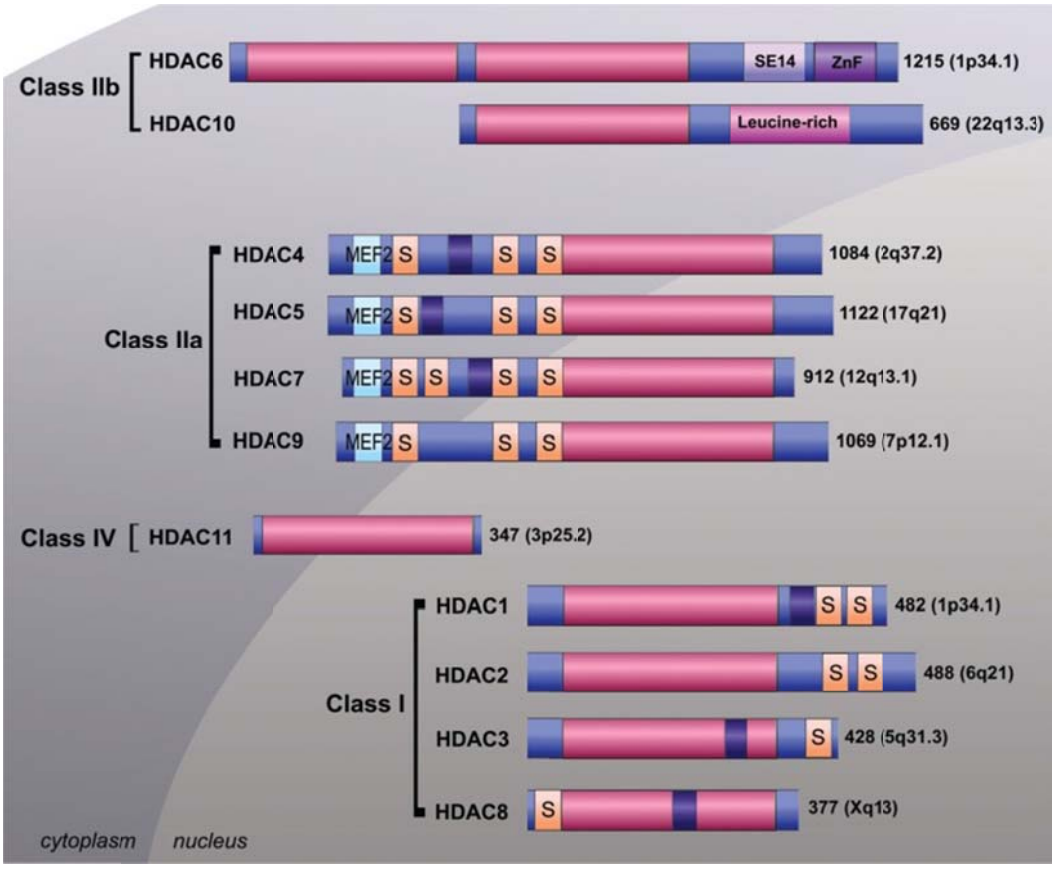

Figure 8 Classification of histone deacetylases (Karagiannis & Ververis, 2012). This classification is based on the sequence homology of the enzymes to the yeast counterparts. Class I includes HDACs 1, 2, 3 and 8. Class II is further divided into two classes, IIa and IIb. Class IIa includes HDACs 4, 5, 7 and 9 and Class IIb includes HDACs 6 and 10. Class IV has only HDAC11.

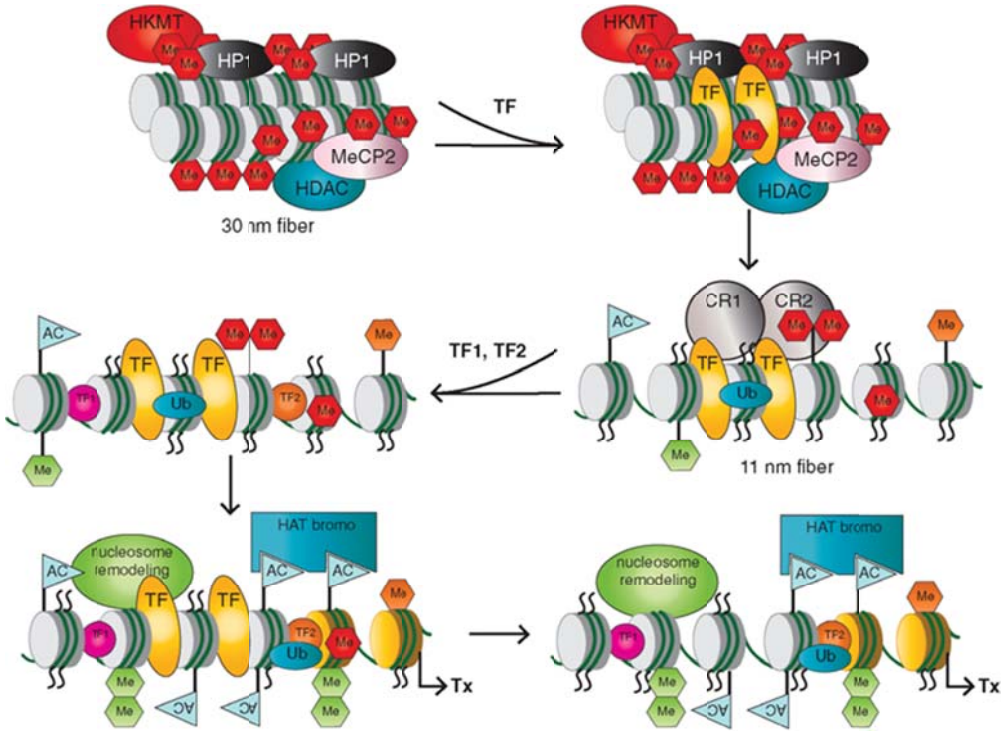

Figure 9 A schematic model for genetic activation in embryonic eye development (Cvekl & Mitton, 2010). Red octagons indicate heterochromatin state maintaining modifications in the 30nm fiber; Methylated marks and presence of Histone deacetylases. Yellow Transcription factors (TFs) with the ability to recognize and flag binding sites on heterochromatin for future transcription machinery to act. Chromatin remodeling enzymes- CR1 and CR2 recruitment for conversion of heterochromatin to euchromatin (Open conformation) with the help of other post translational histone modification like acetylation, activating methylations, etc. Transcriptional machinery is now allowed to bind previously flagged sites on DNA for 'reading'.

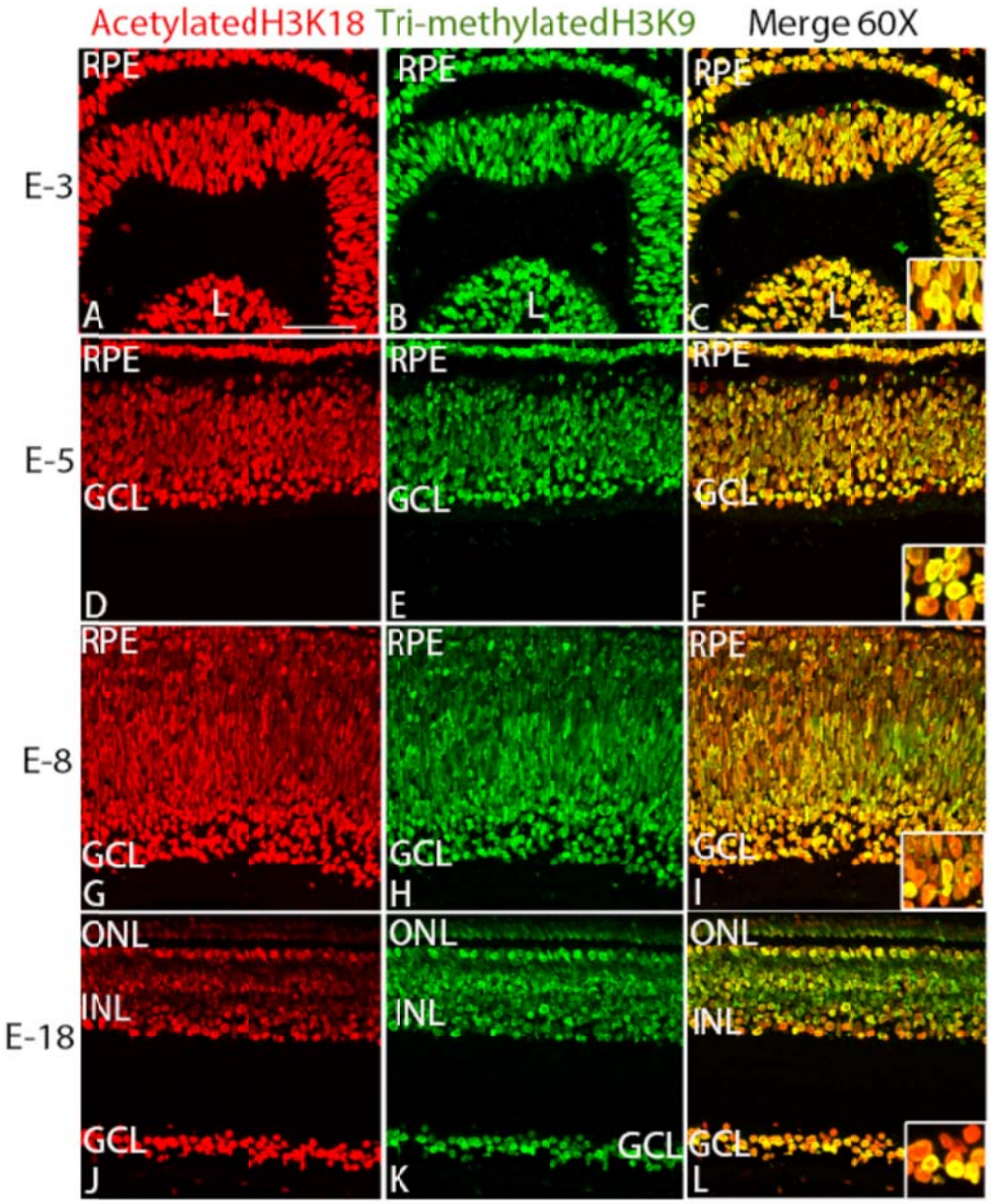

Figure 10 Histone acetylation and trimethylation localization in the developing chick retina. Global patterns of acetylation were labeled with antibody that recognizes AcH3K18 (Red) and double labeled with antibody that recognizes methylated histone3(K9) in the developing and mature chick retina.

The developing retina is represented by E3 (A-C), E5 (D-F) and E8 (G-I). The mature retina is represented by E18 (J-L). Merged images show the presence as a combination of active and inactive states of chromatin in the developing retina. Insets show higher magnification of labeled cells (C, F, I and L). Scale bar of 50μm shown in (A) representative of all images in the figure.

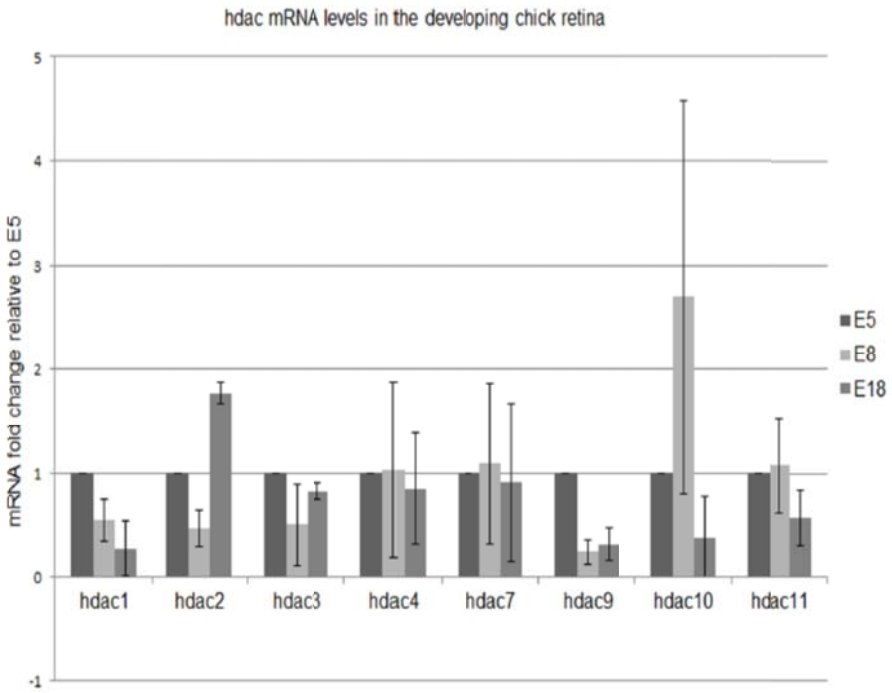

Figure 11 RT-qPCR analysis of hdac mRNA levels in the developing chick retina. hdac mRNA levels in the developing chick retina was calculated as fold change relative to E5. The analysis was done by delta-delta ct method. hdacs 3, 4, 7, 10 and 11did not show a statistically different fold change relative to E5. hdacs 1 and 9 appeared to show decrease in mRNA levels as development progressed. hdac2 mRNA levels were the only one to show an increase in the mRNA level at E18.

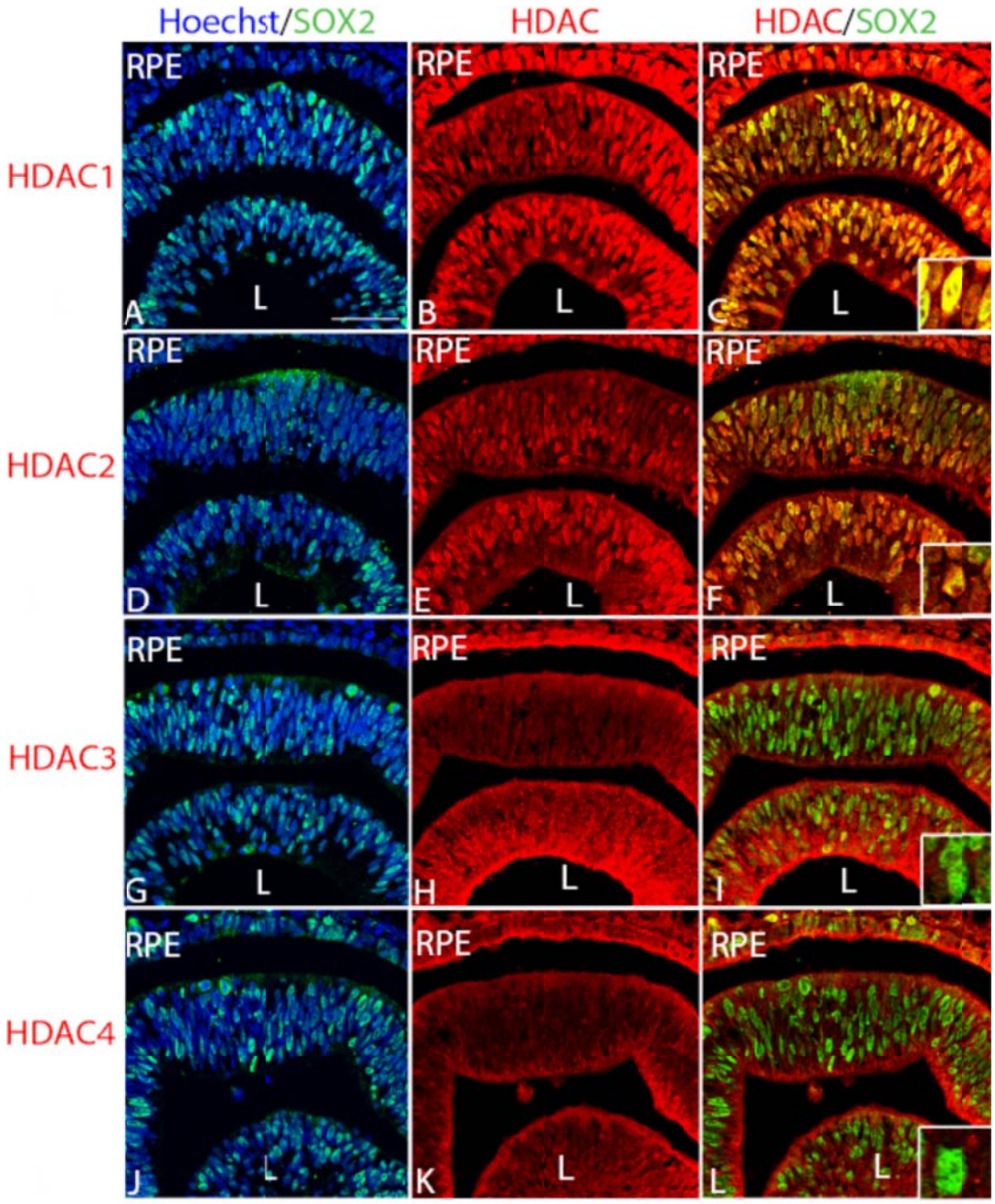

Figure 12 HDAC 1-4 co-labeled with SOX2 in the E3 retina. HDAC1 co-localized with SOX2 labeled progenitor cells (A-C).HDAC2 showed some nuclear co-label with SOX2 (D-F). HDAC3 (G-I) and HDAC4 (J-L) showed no nuclear label in the progenitor cells. Insets show a higher magnification of labeled cells. Scale bar measuring 50μm shown (A) representative of all images.

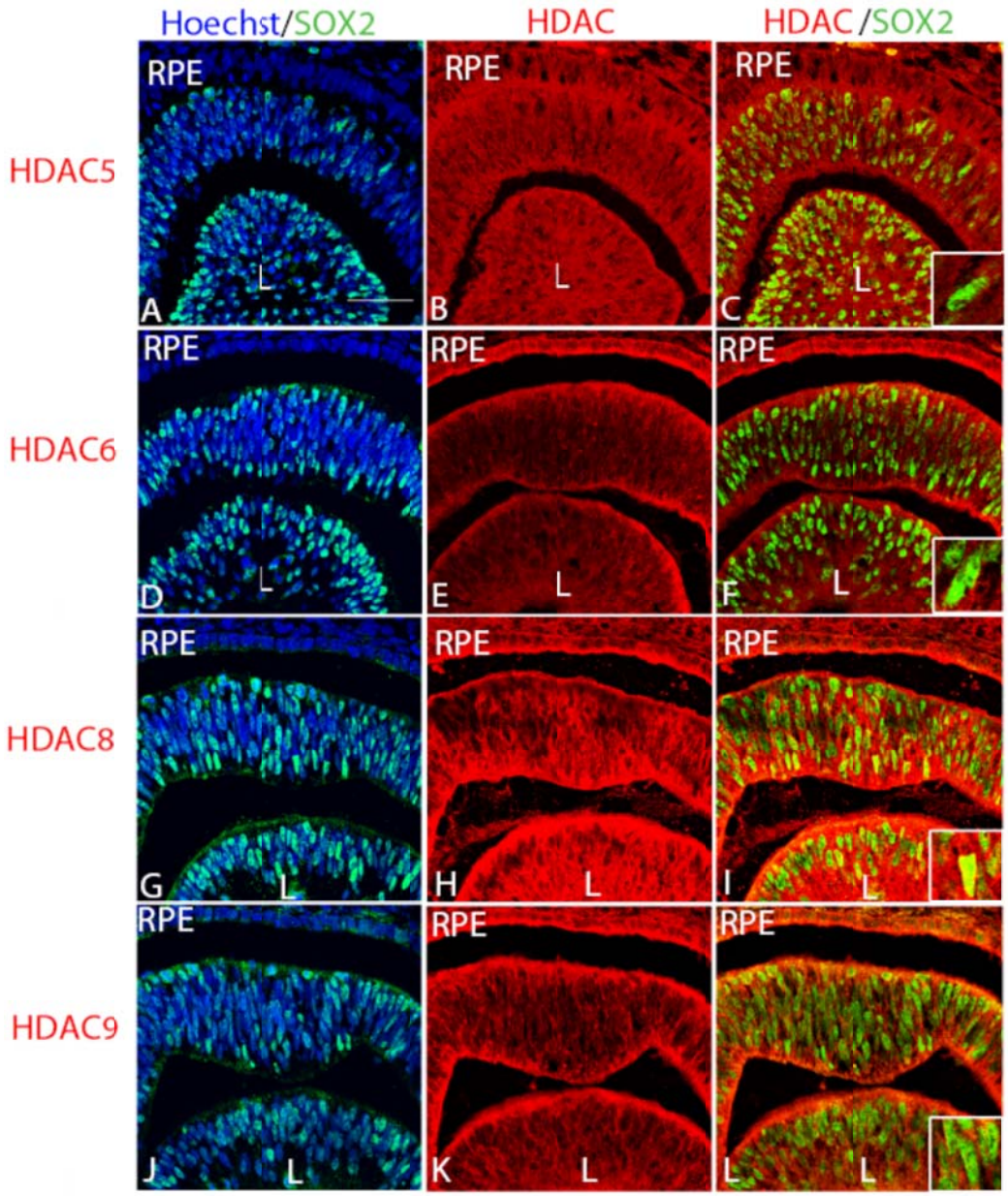

Figure 13 HDACs 5, 6, 8 and 9 co-labeled with SOX2 in the E3 retina. HDAC5 (A-C), HDAC6 (D-F) and HDAC9 (J-L) did not show any nuclear co-label with the SOX2 labeled progenitor cells.

HDAC8 (G-I) showed weak nuclear co-label in the progenitor cells. Insets show magnified labeled cells. Scale bar measuring 50μm shown (A) representative of all images.

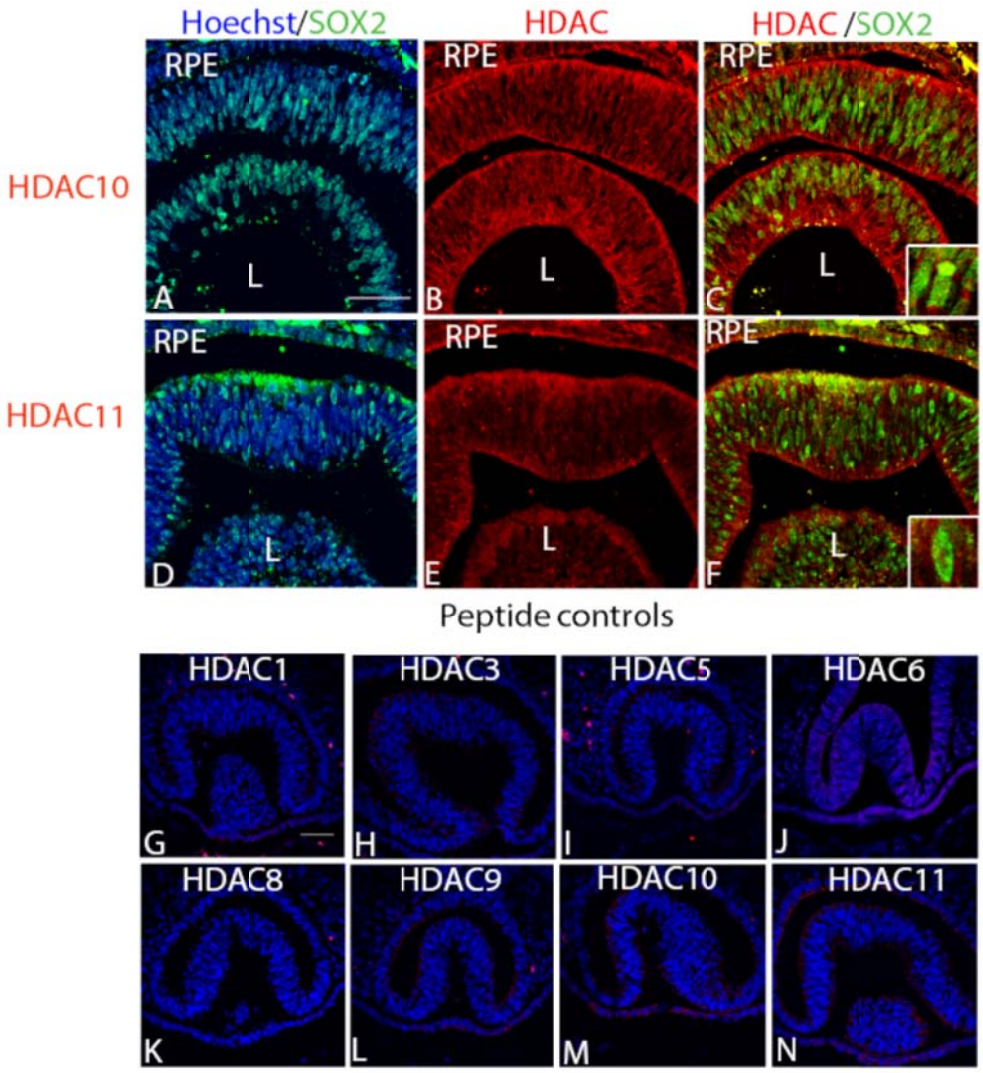

Figure 14 HDAC10 and HDAC11 localization in the E3 chick retina. HDAC10 (A-C) and HDAC11 (D-F) did not show any nuclear label in SOX2-labeled progenitor cells. Insets show a magnified view of the labeled cells. Scale bar of 50 μm shown in A representative of A-F. G-N show peptide controls that were conducted for the HDAC antibodies used to show specificity of the antibody. Scale bar of 50μm shown in G representative of G-N.

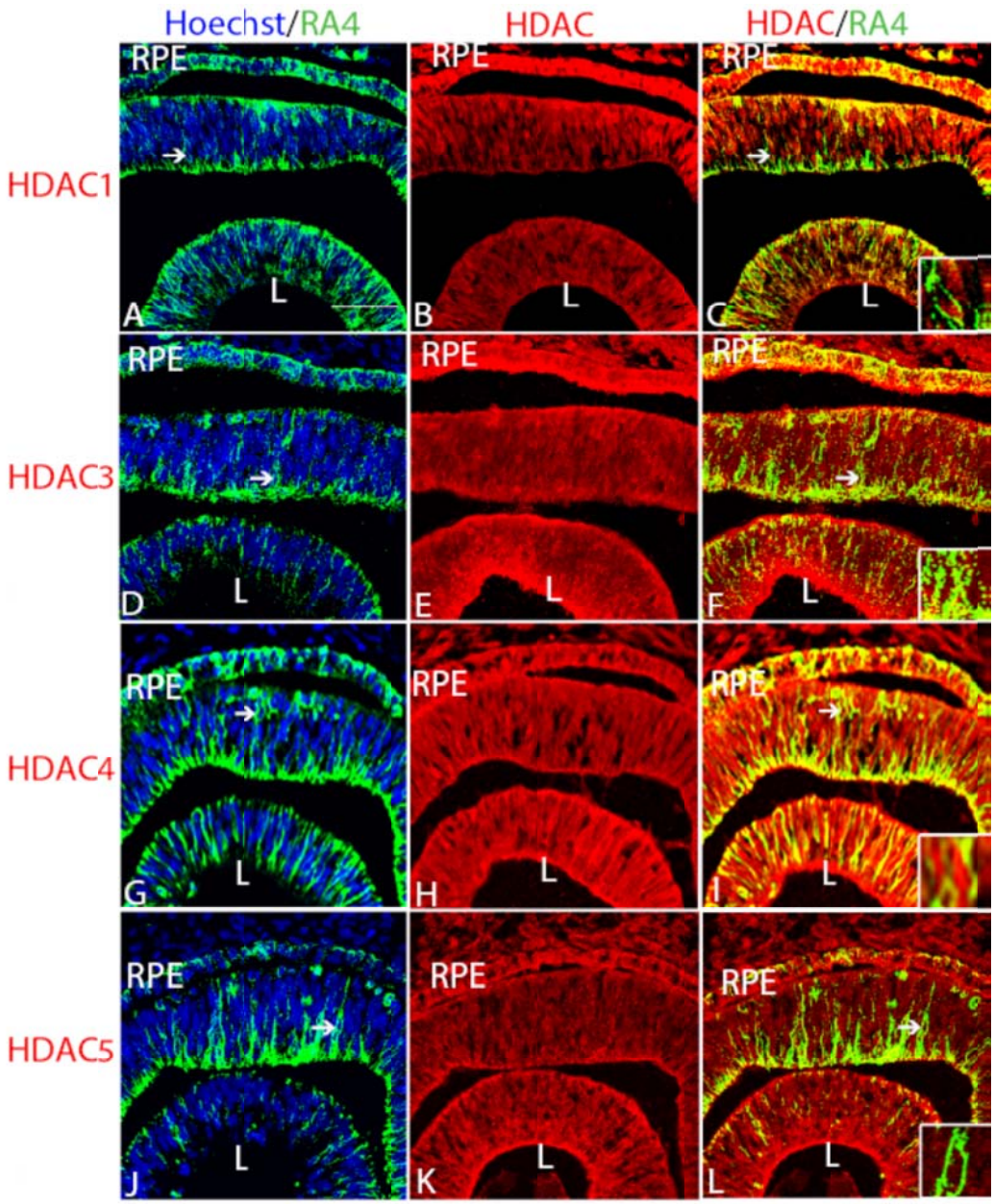

Figure 15 Localization of HDACs 1, 3, 4 and 5 in RA4 labeled newly differentiating cells in the E3 chick retina. RA4 is a cytoplasmic marker for newly differentiating cells. HDAC1 (A-C), HDAC3 (D-F), HDAC4 (G-I) and HDAC5 (J-L) did not co-localize in the RA4 labeled cytoplasm of the newly differentiating cells. Arrows point to cells that have been magnified in the insets (C, F, I and L). Scale bar measuring 50μm shown in A representative of all images in this figure.

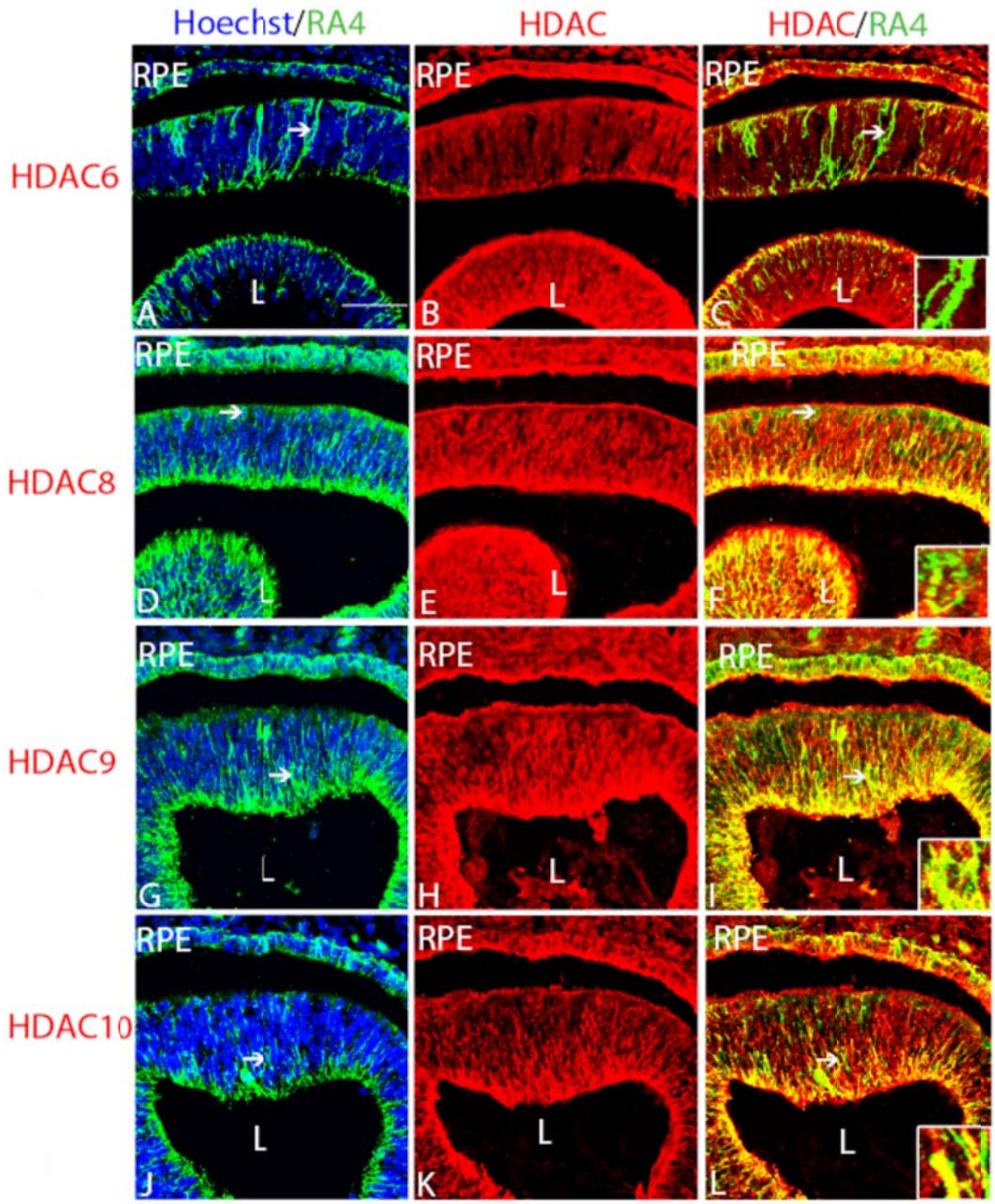

Figure 16 Localization of HDACs 6, 8, 9 and 10 in the in RA4 labeled newly differentiating cells in the E3 chick retina. RA4 is a cytoplasmic marker for newly differentiating cells. HDAC6 (A-C) did not co-localize with RA4. HDAC8 (D-F) HDAC9 (G-I) and HDAC10 (J-L) showed partial cytoplasmic co-localization with RA4. Arrows point to cells that have been magnified in the insets (C, F, I and L). Scale bar measuring 50μm shown in A representative of all images in this figure.

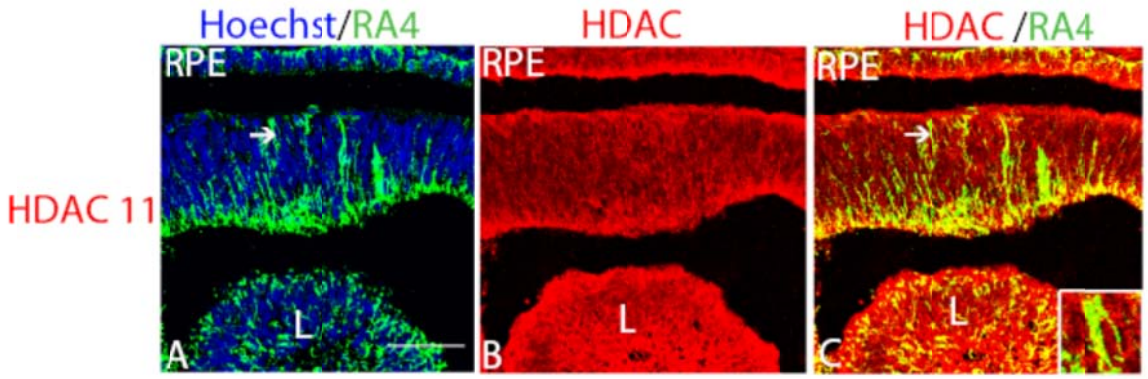

Figure 17 Localization of HDAC11in the in RA4 labeled newly differentiating cells in the E3 chick retina. RA4 is a cytoplasmic marker for newly differentiating cells. HDAC11 partially co-localized with RA4 in the cytoplasm of these cells. Arrows point to cells that have been magnified in the inset (C). Scale bar measuring 50μm shown in A representative of all images in this figure.

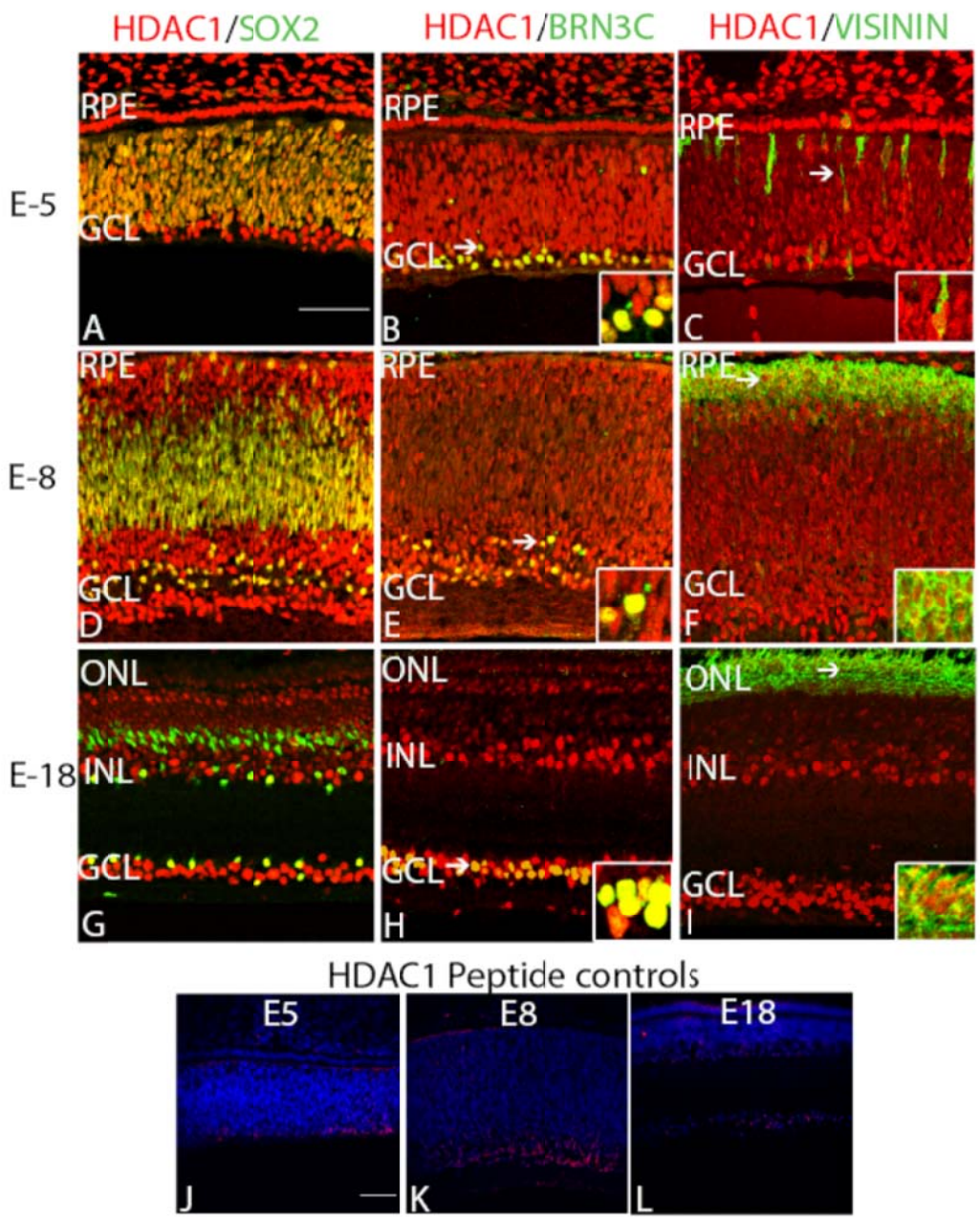

Figure 18 Localization of HDAC1 in the developing chick retina. Localization of HDAC1 in E5 (A-C), E8 (D-F) and E18 (G-I) was predominantly nuclear in pattern. Nuclear-co-localization of HDAC1 with SOX2 labeled progenitors at E5 (A) and E8 (D) was observed. At E18 (G), SOX2 labeled the retinal astrocytes, cholinergic amacrine cells and the Müller glia. HDAC1 co-localized with SOX2 in

the retinal astrocytes, weakly co-labeled the cholinergic amacrine cells and did not label the nuclei of the Müller glia. HDAC1 co-localized with BRN3C, a nuclear ganglion cell marker at E5 (B), E8 (E) and E18 (H). VISININ, a cytoplasmic marker was used to label photoreceptors. HDAC1 did not co-localize with VISININ at E5 (C), E8 (F) or E18 (I). Arrows in B, E and H point to co-labeled cells magnified in the insets. Arrows in C, F and I point to cells magnified in the insets. Peptide controls for HDAC1 were performed on E5 (J), E8 (K), and E18 (L) retinal sections to test the specificity of the antibody used. Scale bar of 50μm shown in A representative for images A-I. 50μm scale bar shown in J representative of J-L.

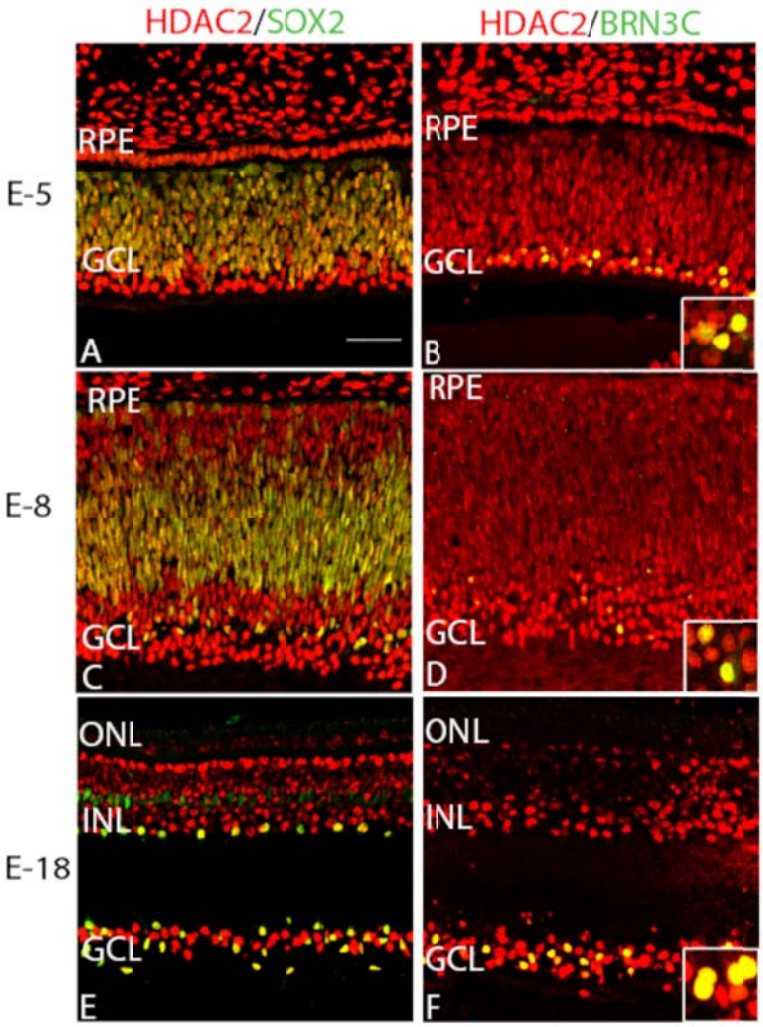

Figure 19 Localization of HDAC2 in the developing chick retina. HDAC2 localization at E5 (A-B), E8 (C-D) and E18 (E-F) was predominantly nuclear in pattern. Nuclear-co-localization of HDAC2 with SOX2 labeled progenitors at E5 (A) and E8 (C) was observed. At E18 (E), SOX2 labeled the retinal astrocytes, cholinergic amacrine cells and the Müller glia. HDAC2 co-localized with SOX2 in the retinal astrocytes and cholinergic amacrine cells but did not label the nuclei of the Müller glia. HDAC2 co-localized with BRN3C, a nuclear ganglion cell marker at E5 (B), E8 (D) and E18 (F). Scale bar of 50μm shown in A representative for images A-F.

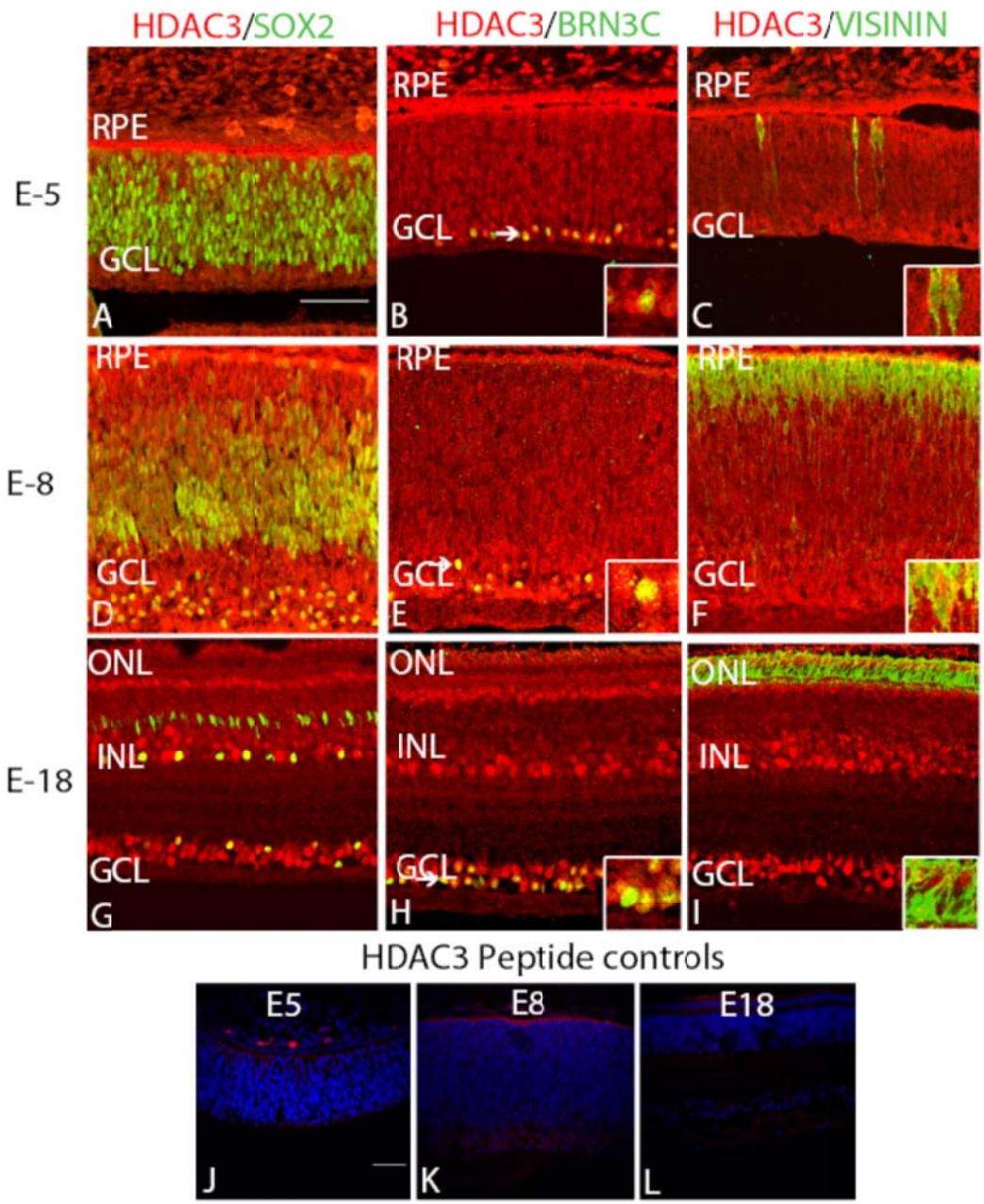

Figure 20 Localization of HDAC3 in the developing chick retina. Localization of HDAC3in E5 (A-C), E8 (D-F) and E18 (G-I) was nuclear and cytoplasmic in pattern. Nuclear-co-localization of HDAC1 with SOX2 labeled progenitors at E5 (A) and E8 (D) was not observed. At E18 (G), SOX2 labeled the retinal astrocytes, cholinergic amacrine cells and the Müller glia. HDAC3 co-localized

with SOX2 in the retinal astrocytes, the cholinergic amacrine cells but did not label the nuclei of the Müller glia. HDAC3 co-localized with BRN3C, a nuclear ganglion cell marker at E5 (B), E8 (E) and E18 (H). VISININ, a cytoplasmic marker was used to label photoreceptors. HDAC3 did not co-localize with VISININ at E5 (C) or E18 (I) but partially co-localization was observed at E8 (F). Arrows in B, E and H point to co-labeled cells magnified in the insets. Insets show a magnified view of the labeled cells in (C, F and I). Peptide controls for HDAC3 were performed on E5 (J), E8 (K), and E18 (L) retinal sections to test the specificity of the antibody used. Scale bar of 50μm shown in A representative for images A-I. 50μm scale bar shown in J representative of J-L.

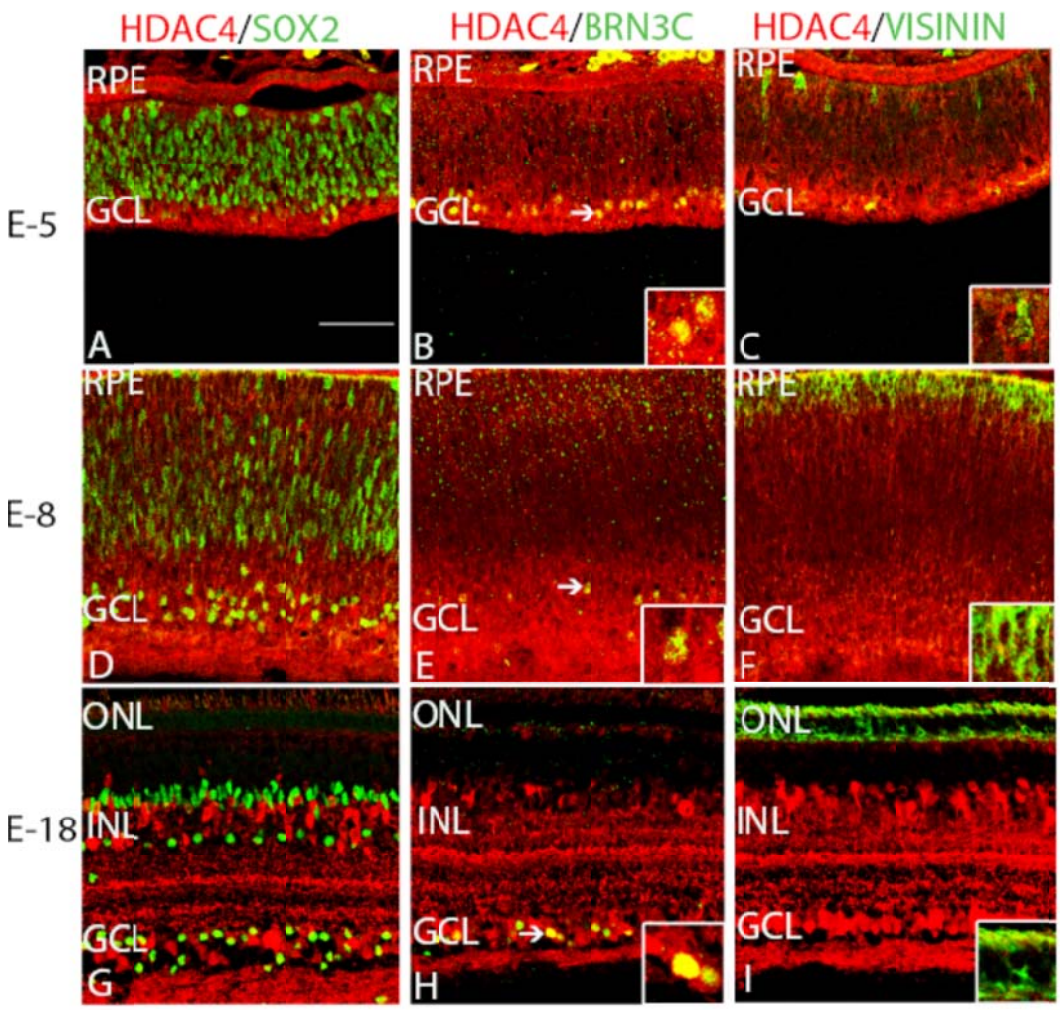

Figure 21 Localization of HDAC4 in the developing chick retina. Localization of HDAC4in E5 (A-C), E8 (D-F) and E18 (G-I) was nuclear and cytoplasmic in pattern. Nuclear-co-localization of HDAC4 with SOX2 labeled progenitors at E5 (A) and E8 (D) was not observed. At E18 (G), SOX2 labeled the retinal astrocytes, cholinergic amacrine cells and the Müller glia. HDAC4 did not co-localize with SOX2 in the retinal astrocytes, the cholinergic amacrine and nuclei of the Müller glia. HDAC4 co-localized with BRN3C, a nuclear ganglion cell marker at E5 (B), E8 (E) and E18 (H). VISININ, a cytoplasmic marker was used to label photoreceptors. HDAC4 did not co-localize with VISININ E18 (I) but weak

co-localization was observed at E5 (C) and E8 (F). Arrows in B, E and H point to co-labeled cells magnified in the insets. Insets show a magnified view of labeled cells in C, F and I. Scale bar of 50μm shown in A representative for images A-I.

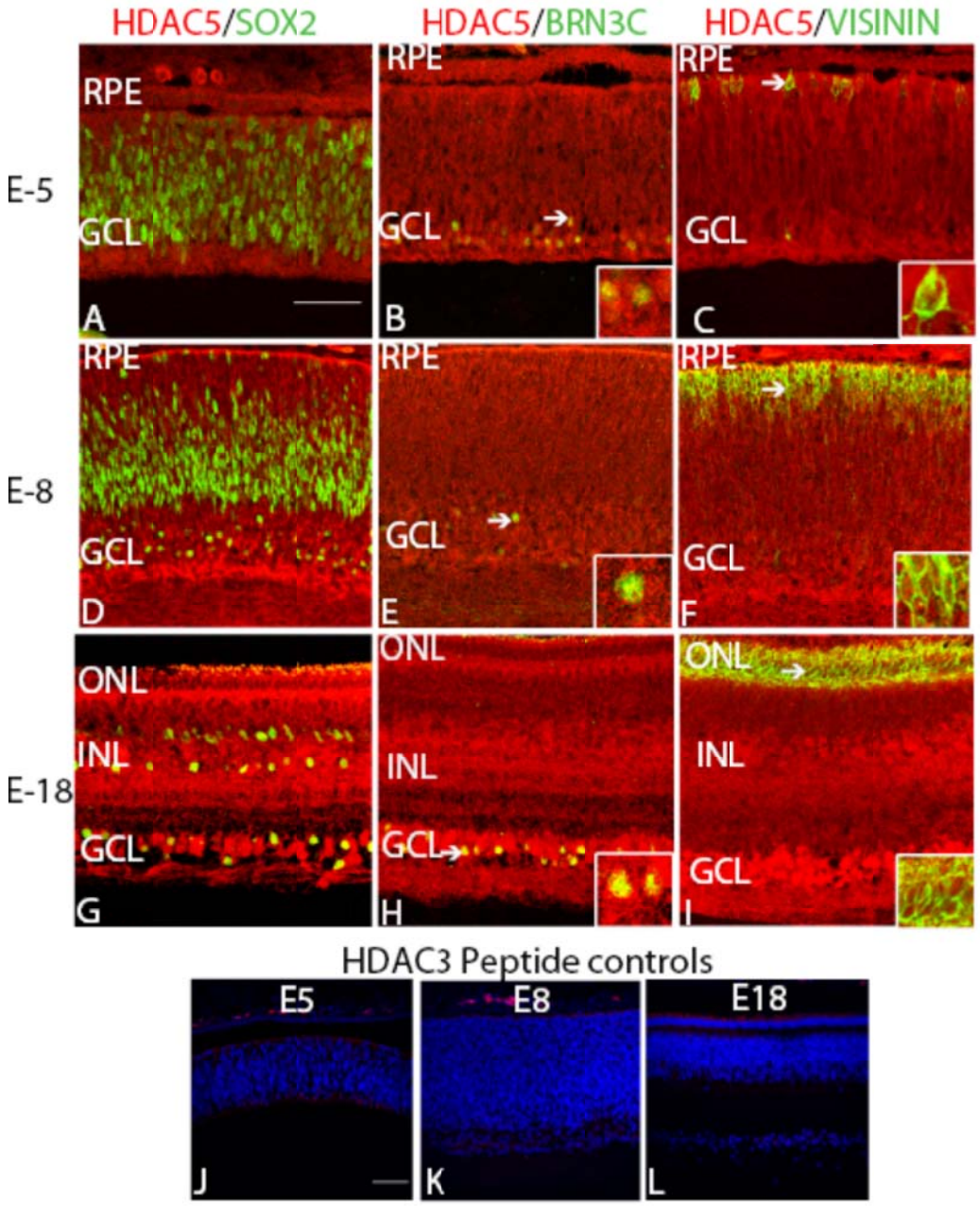

Figure 22 Localization of HDAC5 in the developing chick retina. Localization of HDAC5 in E5 (A-C), E8 (D-F) and E18 (G-I) was nuclear and cytoplasmic in pattern. Nuclear-co-localization of HDAC5 with SOX2 labeled progenitors at E5 (A) and E8 (D) was not observed. At E18 (G), SOX2 labeled the retinal astrocytes, cholinergic amacrine cells and the Müller glia. HDAC5 co-localized

with SOX2 in the retinal astrocytes, the cholinergic amacrine cells but did not label the nuclei of the Müller glia. HDAC5 weakly co-localized with BRN3C, a nuclear ganglion cell marker at E5 (B) and E8 (E) but strong nuclear label was observed at E18 (H). VISININ, a cytoplasmic marker was used to label photoreceptors. HDAC5 did not co-localize with VISININ at E5 (C) or E18 (I) but partial co-localization was observed at E8 (F). Arrows point to labeled cells that were magnified in the insets (B, E, H, C, F and I). Peptide controls for HDAC5 were performed on E5 (J), E8 (K), and E18 (L) retinal sections to test the specificity of the antibody used. Scale bar of 50μm shown in A representative for images A-I. 50μm scale bar shown in J representative of J-L.

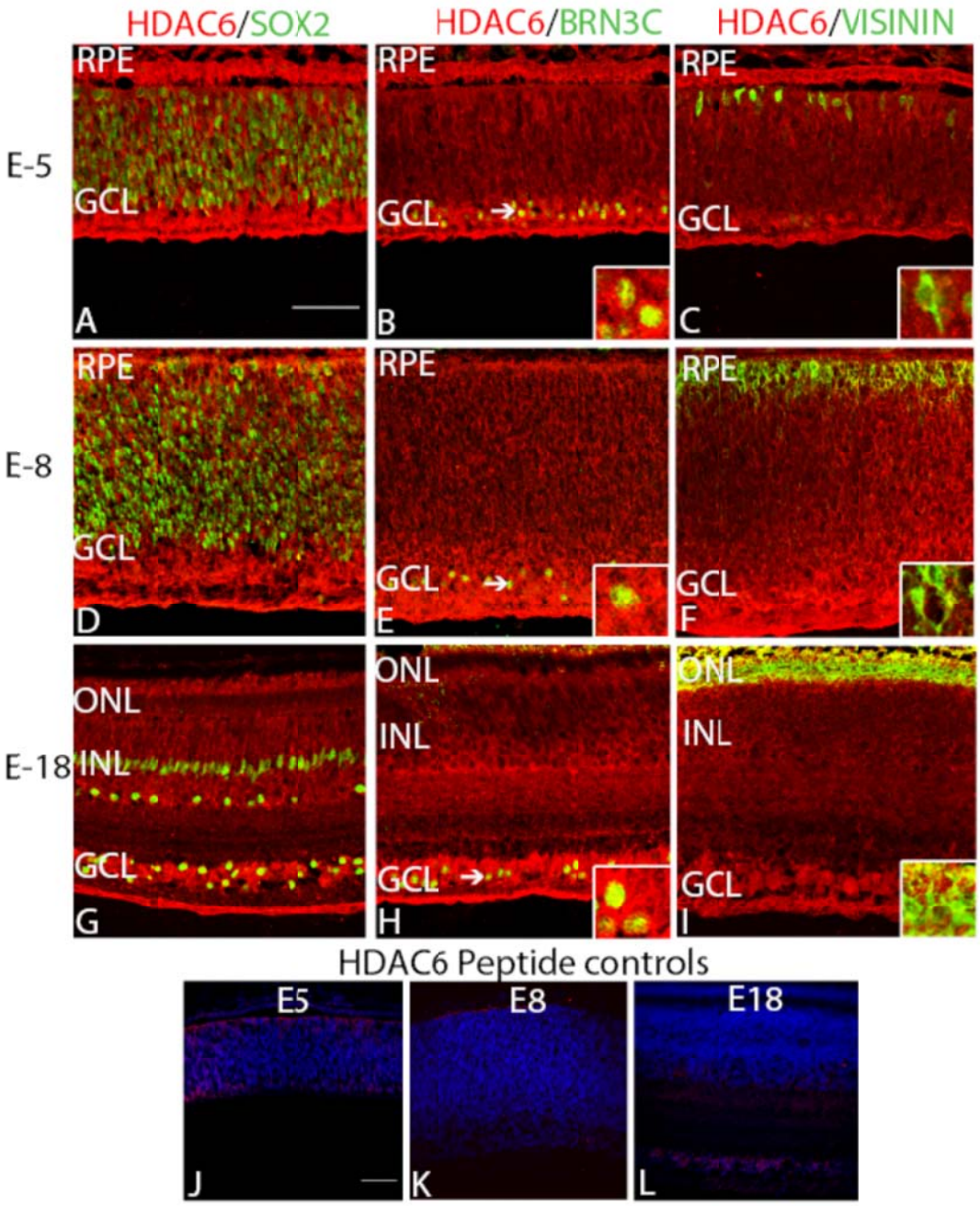

Figure 23 Localization of HDAC6 in the developing chick retina. Localization of HDAC6 in E5 (A-C), E8 (D-F) and E18 (G-I) was nuclear and cytoplasmic in pattern. Nuclear-co-localization of HDAC6 with SOX2 labeled progenitors at E5 (A) and E8 (D) was not observed. At E18 (G), SOX2 labeled the retinal astrocytes, cholinergic amacrine cells and the Müller glia. HDAC6 co-localized

with SOX2 in the retinal astrocytes, the cholinergic amacrine cells but did not label the nuclei of the Müller glia. HDAC6 co-localized with BRN3C, a nuclear ganglion cell marker at E5 (B), E8 (E) and E18 (H). VISININ, a cytoplasmic marker was used to label photoreceptors. HDAC6 partially co-localized with VISININ at E5 (C), E8 (F) and E18 (I). Arrows point to labeled cells that were magnified in the insets (B, E, H, C, F and I). Peptide controls for HDAC6 were performed on E5 (J), E8 (K), and E18 (L) retinal sections to test the specificity of the antibody used. Scale bar of 50μm shown in A representative for images A-I. 50μm scale bar shown in J representative of J-L.

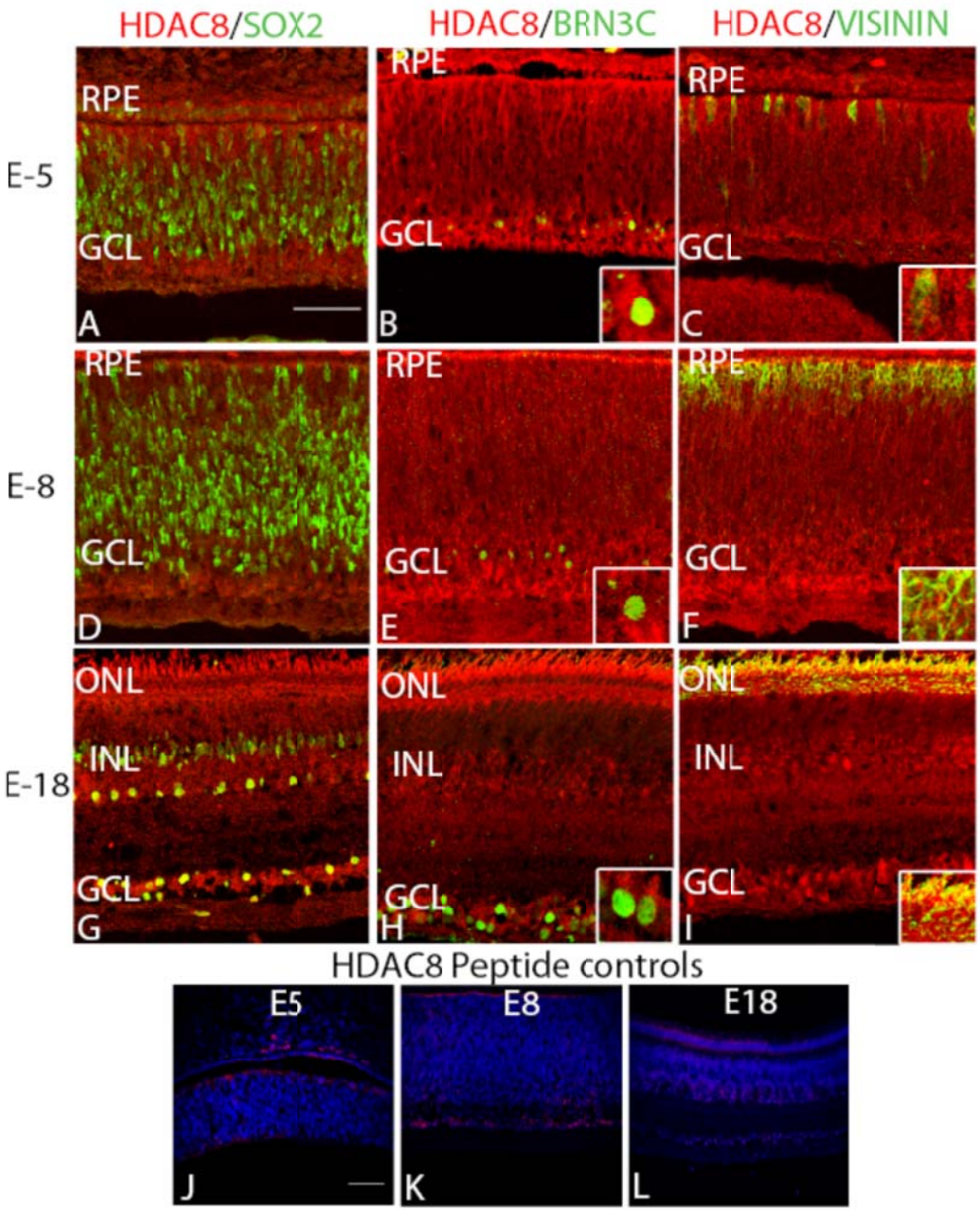

Figure 24 Localization of HDAC8 in the developing chick retina. Localization of HDAC8 in E5 (A-C), E8 (D-F) and E18 (G-I) was nuclear and cytoplasmic in pattern. Nuclear-co-localization of HDAC8 with SOX2 labeled progenitors at E5 (A) and E8 (D) was not observed. At E18 (G), SOX2 labeled the retinal astrocytes, cholinergic amacrine cells and the Müller glia. HDAC8 co-localized

with SOX2 in the retinal astrocytes, the cholinergic amacrine cells but did not label the nuclei of the Müller glia. HDAC8 co-localized with BRN3C, a nuclear ganglion cell marker at E5 (B) but did not show a nuclear co-label at E8 (E) and E18 (H). VISININ, a cytoplasmic marker was used to label photoreceptors. HDAC8 partially co-localized with VISININ at E5 (C), E8 (F) and E18 (I). Insets show a magnified view of labeled cells (B, E, H, C, F and I). Peptide controls for HDAC8 were performed on E5 (J), E8 (K), and E18 (L) retinal sections to test the specificity of the antibody used. Scale bar of 50μm shown in A representative for images A-I. 50μm scale bar shown in J representative of J-L.

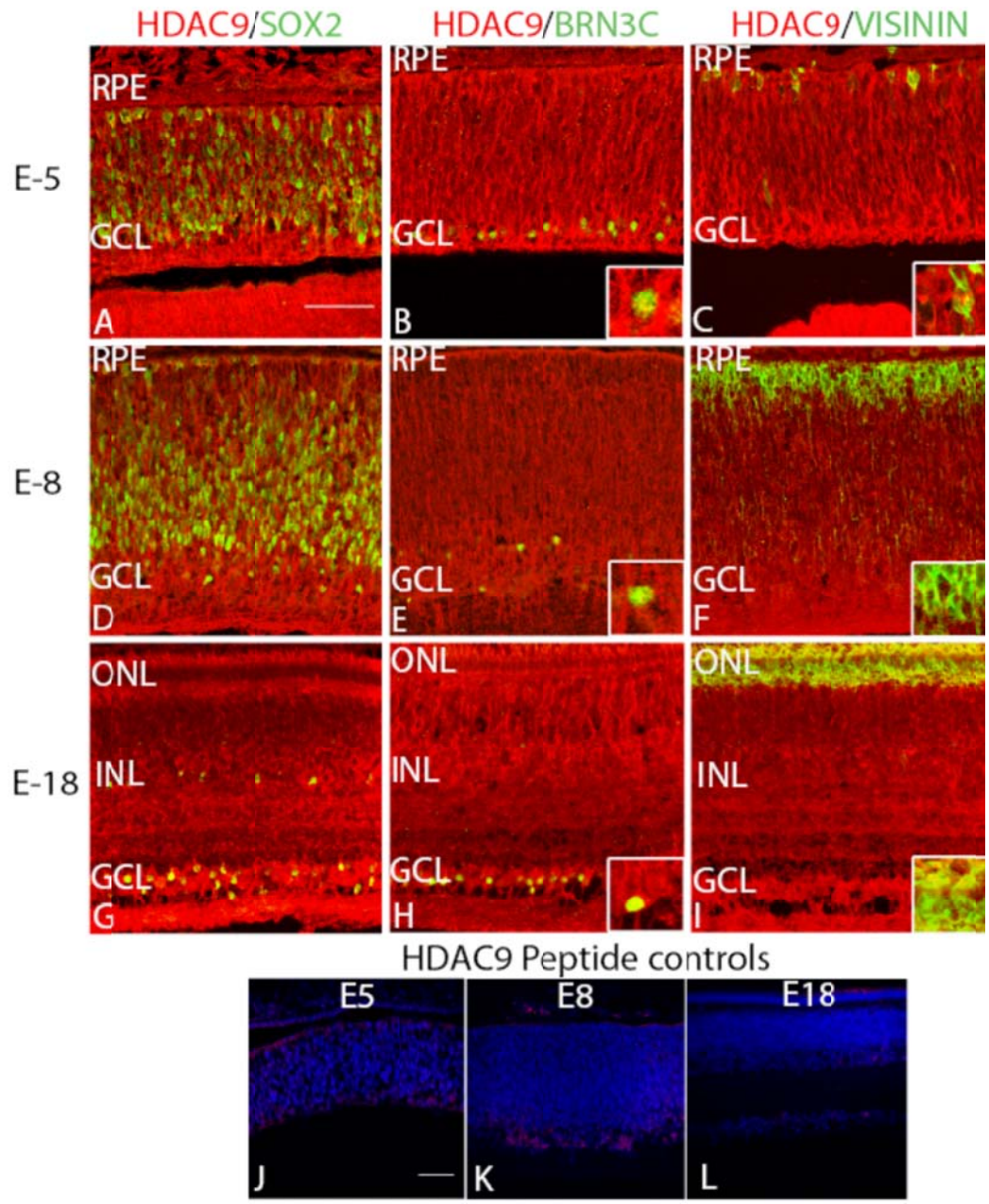

Figure 25 Localization of HDAC9 in the developing chick retina. Localization of HDAC9 in E5 (A-C), E8 (D-F) and E18 (G-I) was nuclear and cytoplasmic in pattern. Nuclear-co-localization of HDAC9 with SOX2 labeled progenitors at E5 (A) and E8 (D) was not observed. At E18 (G), SOX2 labeled the retinal astrocytes, cholinergic amacrine cells and the Müller glia. HDAC9 co-localized

with SOX2 in the retinal astrocytes, the cholinergic amacrine. HDAC9 co-localized with BRN3C, a nuclear ganglion cell marker at E18 (H) and showed a weak co-label at E5 (B) and E8 (E). VISININ, a cytoplasmic marker was used to label photoreceptors. HDAC9 partially co-localized with VISININ at E5 (C), E8 (F) and E18 (I). Insets show a magnified view of labeled cells (B, E, H, C, F and I). Peptide controls for HDAC9 were performed on E5 (J), E8 (K), and E18 (L) retinal sections to test the specificity of the antibody used. Scale bar of 50μm shown in A representative for images A-I. 50μm scale bar shown in J representative of J-L.

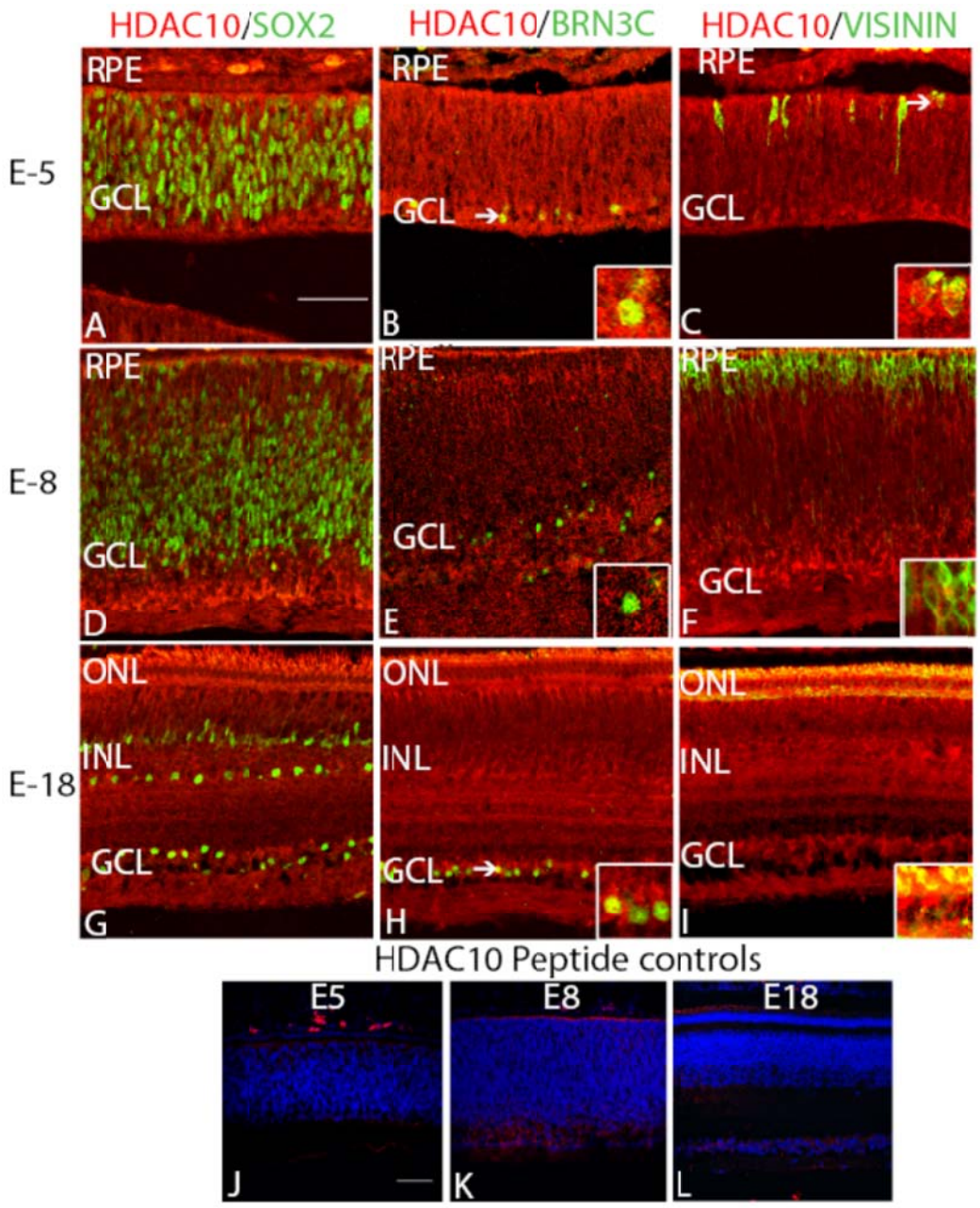

Figure 26 Localization of HDAC10 in the developing chick retina. Localization of HDAC10 in E5 (A-C), E8 (D-F) and E18 (G-I) was nuclear and cytoplasmic in pattern. Nuclear-co-localization of HDAC10 with SOX2 labeled progenitors at E5 (A) and E8 (D) was not observed. At E18 (G), SOX2 labeled the retinal astrocytes, cholinergic amacrine cells and the Müller glia. HDAC10 did not co-

localize with SOX2 in the retinal astrocytes, the cholinergic amacrine cells and the Müller glia. HDAC10 co-localized with BRN3C, a nuclear ganglion cell marker at E5 (B) and E18 (H) but not at E8 (E). VISININ, a cytoplasmic marker was used to label photoreceptors. HDAC10 partially co-localized with VISININ at E5 (C), E8 (F) and co-localized in the presumptive outer segments of the photoreceptors at E18 (I). Arrows point to labeled cells that were magnified in the insets (B, E, H, C). Magnified view of the labeled cells is seen in the insets (F and I). Peptide controls for HDAC10 were performed on E5 (J), E8 (K), and E18 (L) retinal sections to test the specificity of the antibody used. Scale bar of 50μm shown in A representative for images A-I. 50μm scale bar shown in J representative of J-L.

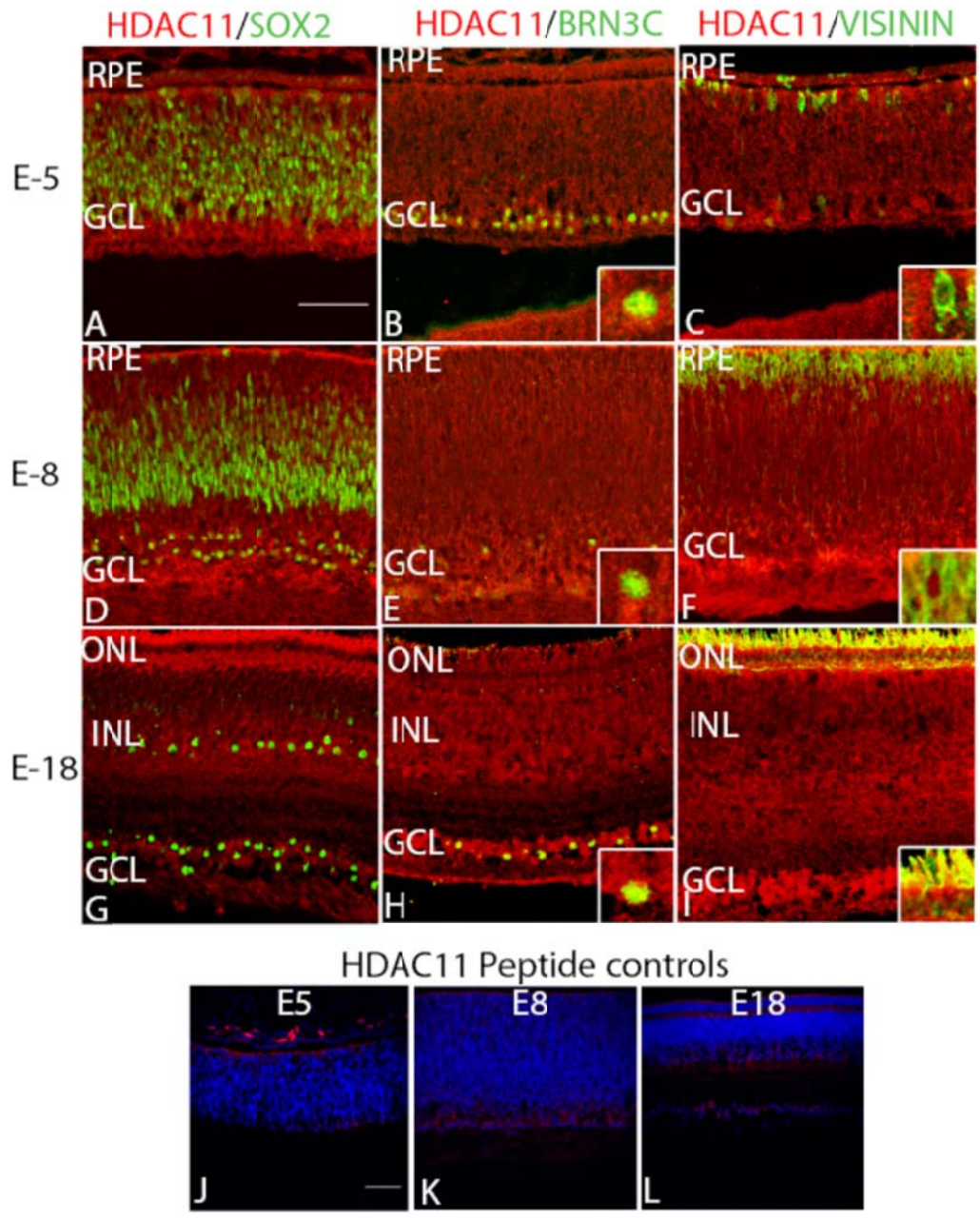

Figure 27 Localization of HDAC11 in the developing chick retina. Localization of HDAC11 in E5 (A-C), E8 (D-F) and E18 (G-I) was nuclear and cytoplasmic in pattern. Nuclear-co-localization of HDAC11 with SOX2 labeled progenitors at E5 (A) and E8 (D) was not observed. At E18 (G), SOX2 labeled the retinal astrocytes, cholinergic amacrine cells and the Müller glia. HDAC11 did not co-

localize with SOX2 in the retinal astrocytes, the cholinergic amacrine cells and the Müller glia. HDAC11 weakly co-localized with BRN3C, a nuclear ganglion cell marker at E5 (B) and E8 (E) and showed a strong nuclear label at E18 (H). VISININ, a cytoplasmic marker was used to label photoreceptors. HDAC11 partially co-localized with VISININ at E5 (C), E8 (F) and co-localized in the presumptive outer segments of the photoreceptors at E18 (I). Insets show a magnified view of the labeled cells (B, E, H, C, F and I). Peptide controls for HDAC11 were performed on E5 (J), E8 (K), and E18 (L) retinal sections to test the specificity of the antibody used. Scale bar of 50μm shown in A representative for images A-I. 50μm scale bar shown in J representative of J-L.

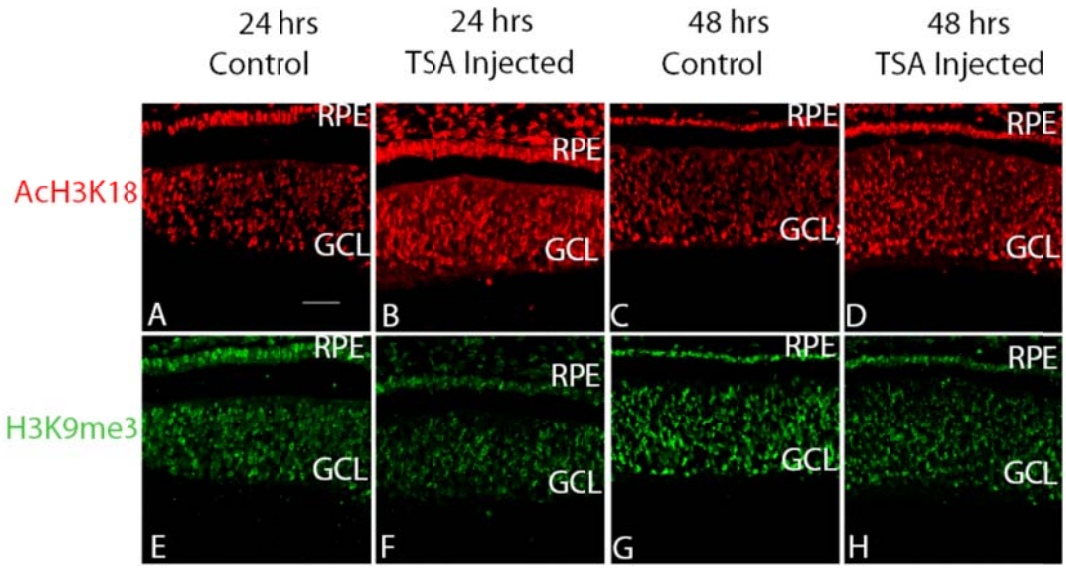

Figure 28 Trichostatin A microinjections into developing eye. Effect of inhibition of class I and II HDACs on the developing chick retina was observed 24 and 48 hours post-injection. Vehicle treated embryos harvested 24hours post injection labeled for AcH3K18 (euchromatin marker) (A) and H3K9me3 (Heterochromatin marker) (E). TSA treated chick retina 24 hours post injection labeled for AcH3K18 showed hyperacetylation (B) and hypomethylation (F) of cells compared to the control (A, E). Vehicle treated embryos harvested 48hours post injection labeled for AcH3K18 (C) and H3K9me3 (G). TSA treated chick retina 24 hours post injection labeled for AcH3K18 (D) showed similar changes in acetylation (D) and methylation (H) compared to the control as was observed after 24 hours post injection. Scale bar of 50μM shown in A representative for all images.

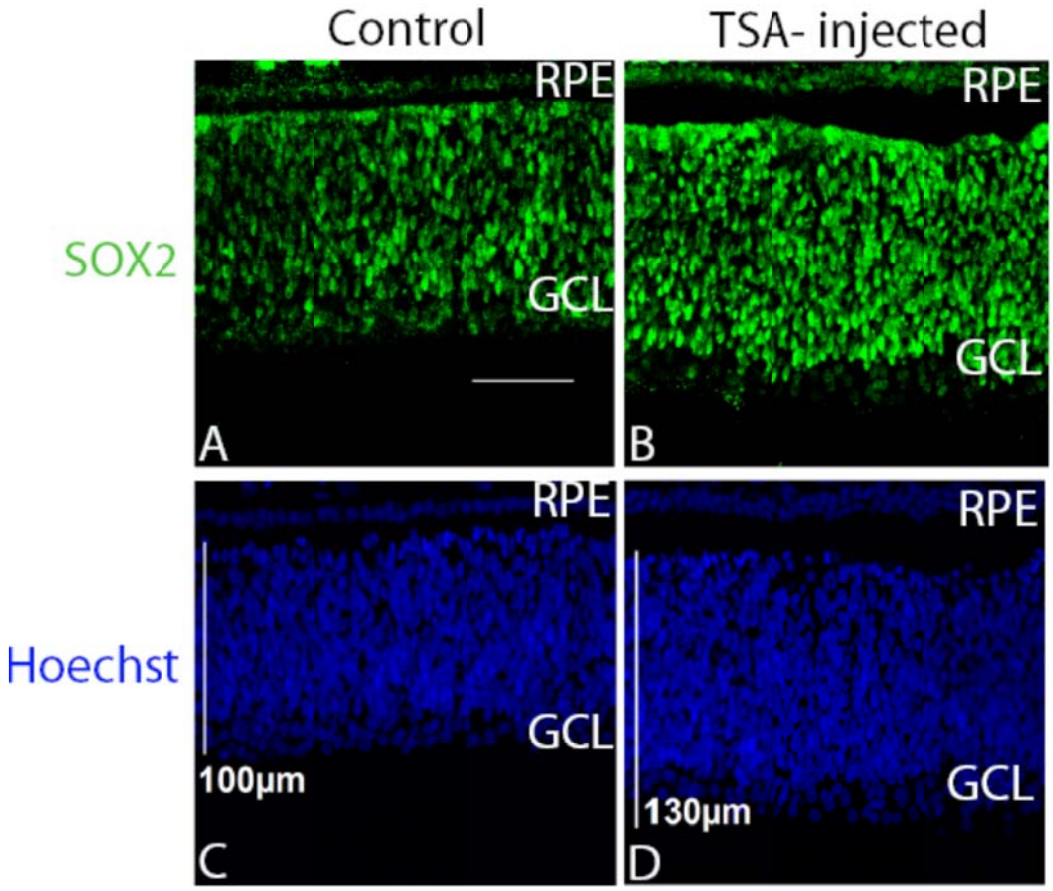

Figure 29 SOX2 labeled progenitors in the chick retina, 48 hours post vehicle and TSA injection. Vehicle treated chick retina (A, C) and 500nM TSA injected retina (B, D) were labeled with SOX2 to visualize progenitor population in the samples respectively. The overall number SOX2 labeled cells in the vehicle treated retina (A) appeared to be less than 500nM TSA treated retina (B). Scale bar of 50µM representative of all images.

C and D show the Hoechst stained nuclei of the retina. Scale bars depicting the thickness of the Control (C) and the TSA injected (D) suggest that the retina of the TSA injected retina is more than that of the control (C).

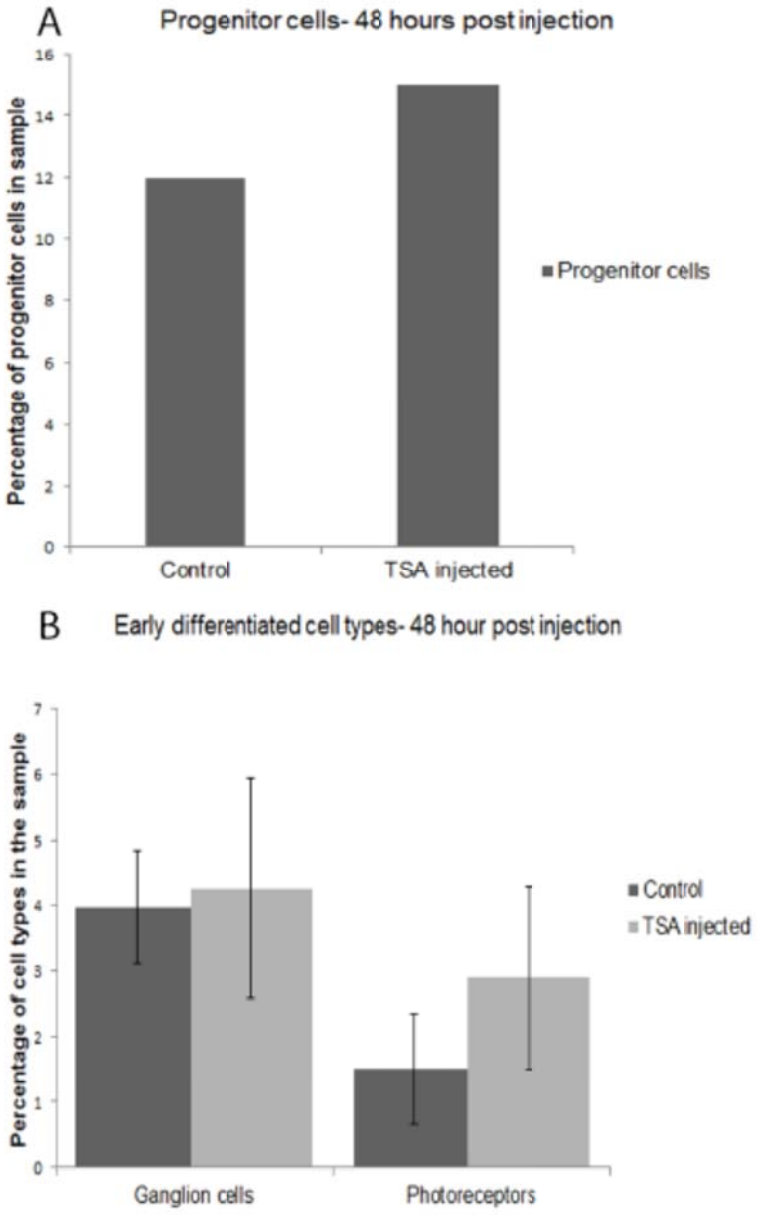

Figure 30 Quantitative estimation of cell types in the chick retina 48hours post vehicle and TSA injection. Graph A shows the quantitative comparison of SOX2 labeled progenitor cells counted in the vehicle injected control and the TSA injected chick retinas. Data set is yet to be completed but preliminary results are

suggestive of an increase in the number of progenitor cells in the TSA treated retinas. Graph B shows the quantitative comparison of early differentiated cells types in the vehicle injected control and the TSA injected chick retinas. The comparison of the ganglion cell and photoreceptor percentages in the control and the TSA injected retina did not show a significant change.

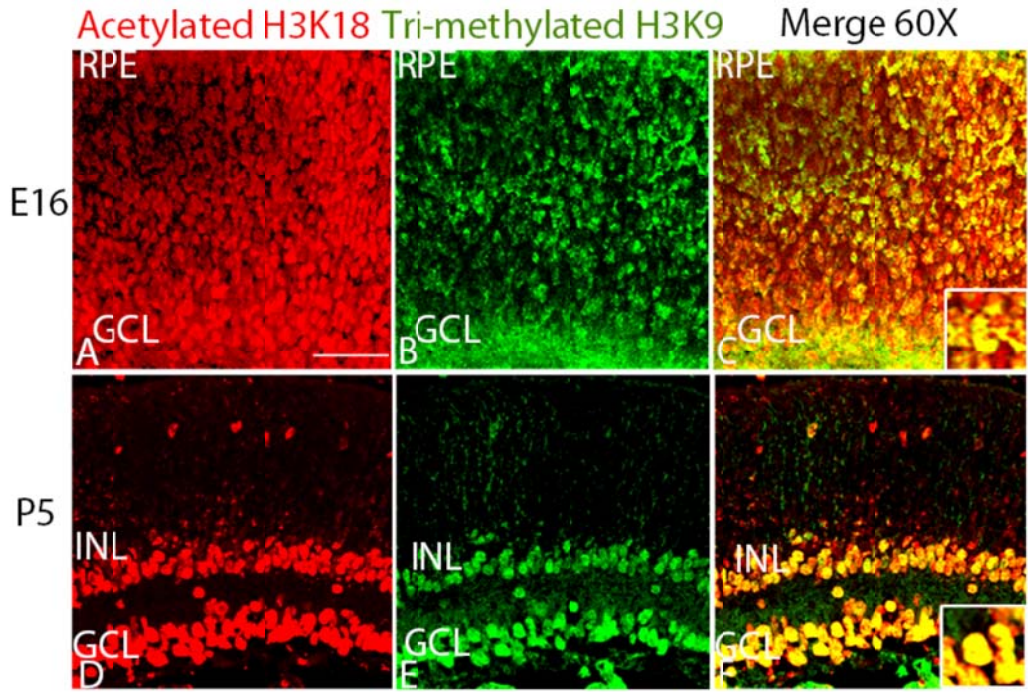

Figure 31 Euchromatin and heterochromatin in the developing murine retina. Global acetylation and methylation patterns in the developing murine retina. Acetylated H3K18 (red) marker for euchromatin, and methylated H3K9 (green), marker for heterochromatin co-label performed on developing murine retina at E16 (A and B) and P5 (D and E). At E16 (C), the merged images showed co-localization of the acetylated and methylated marks indicating presence of euchromatin and heterochromatin in the same cells. At P5 (I), co-labeled cells were also detected however, both the tri-methylated and acetylated markers were restiricted primarily to the ganglion cell layer and a subpopulation of cell in the inner nuclear layer.

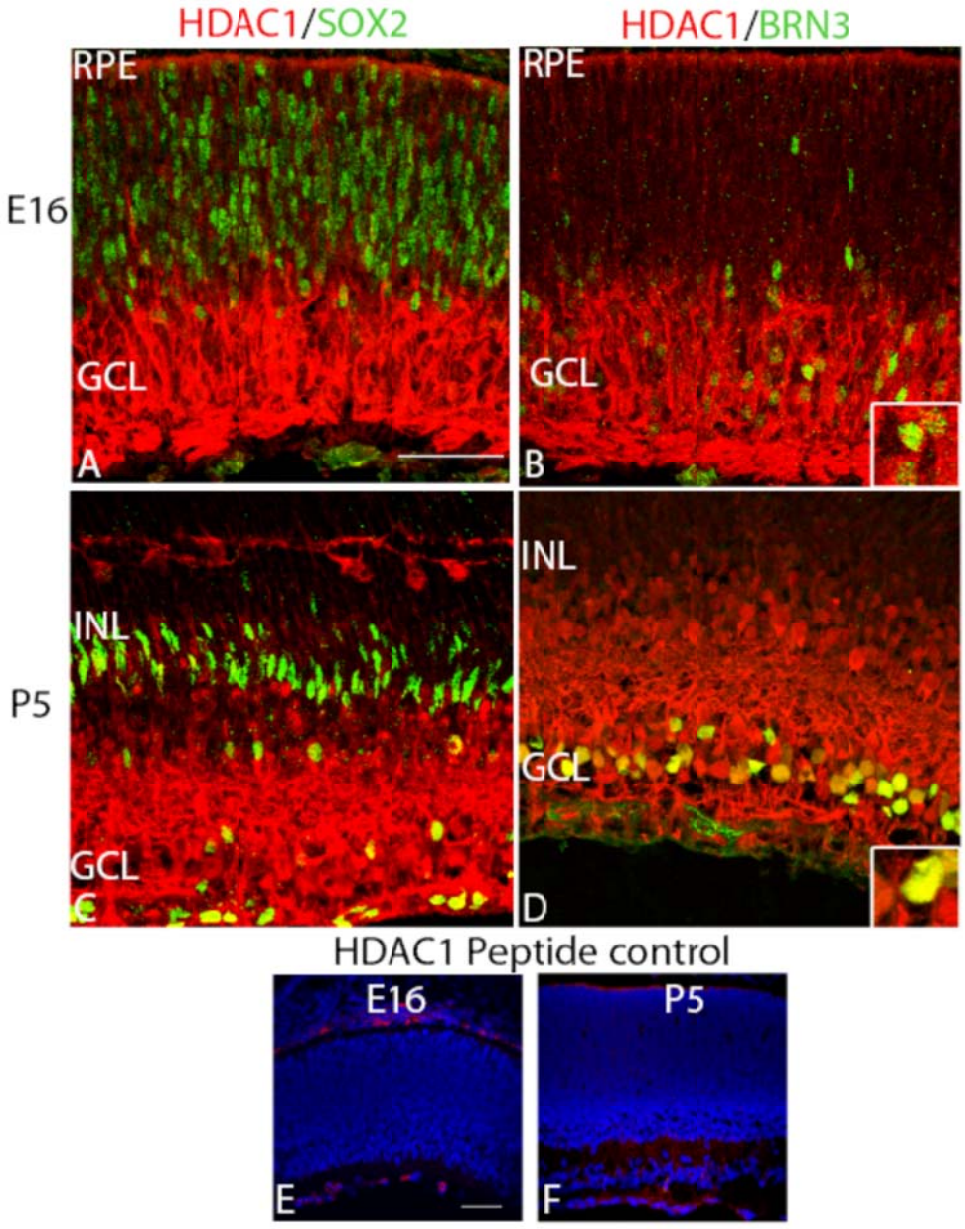

Figure 32 HDAC1 in the developing murine retina. HDAC1 localization in the developing and murine retina was nuclear and cytoplasmic. No detectable HDAC1 was present in the nucleus of the SOX2 labeled cells at E16 (A) and Müller glia at P5 (C). Co-label was detected in cholinergic amacrine cells at the edge of the inner nuclear layer and inner plexiform layers and in the SOX2

labeled retinal astrocytes found in the ganglion cell layer (C). BRN 3C (B) and BRN3A (D) co-localized with HDAC1 to the ganglion cell nucleiat E16 and P5 respectively. Insets show magnified view of labeled ganglion cells (B, D). Peptide controls for HDAC1 were performed on E16 (E) and P5 (F) retinal sections to test the specificity of the antibody used. Scale bar of 50μm shown in A representative for images A-D. 50μm scale bar shown in E representative of E-F.

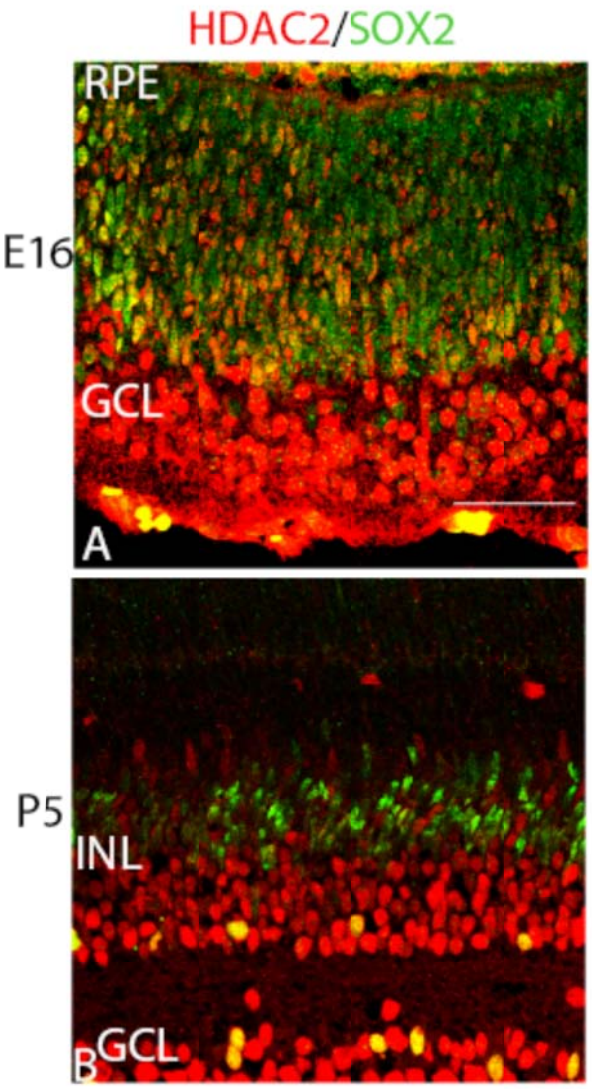

Figure 33 HDAC2 in the developing murine retina. E16 and P5 murine retina were co-labeled with HDAC2 and SOX2 (A and B).The staining pattern showed HDAC2 to be nuclear. At E16, HDAC2 showed nuclear localization in the progenitor cells marked by SOX2 (A). At P5, HDAC2 showed nuclear localization in the retinal astrocytes and cholinergic amacrine cells marked by SOX2. There was no overlap of signal with the Müller glia, also marked by SOX2 (B). Scale bar of 50μm shown in A representative for images A-B.

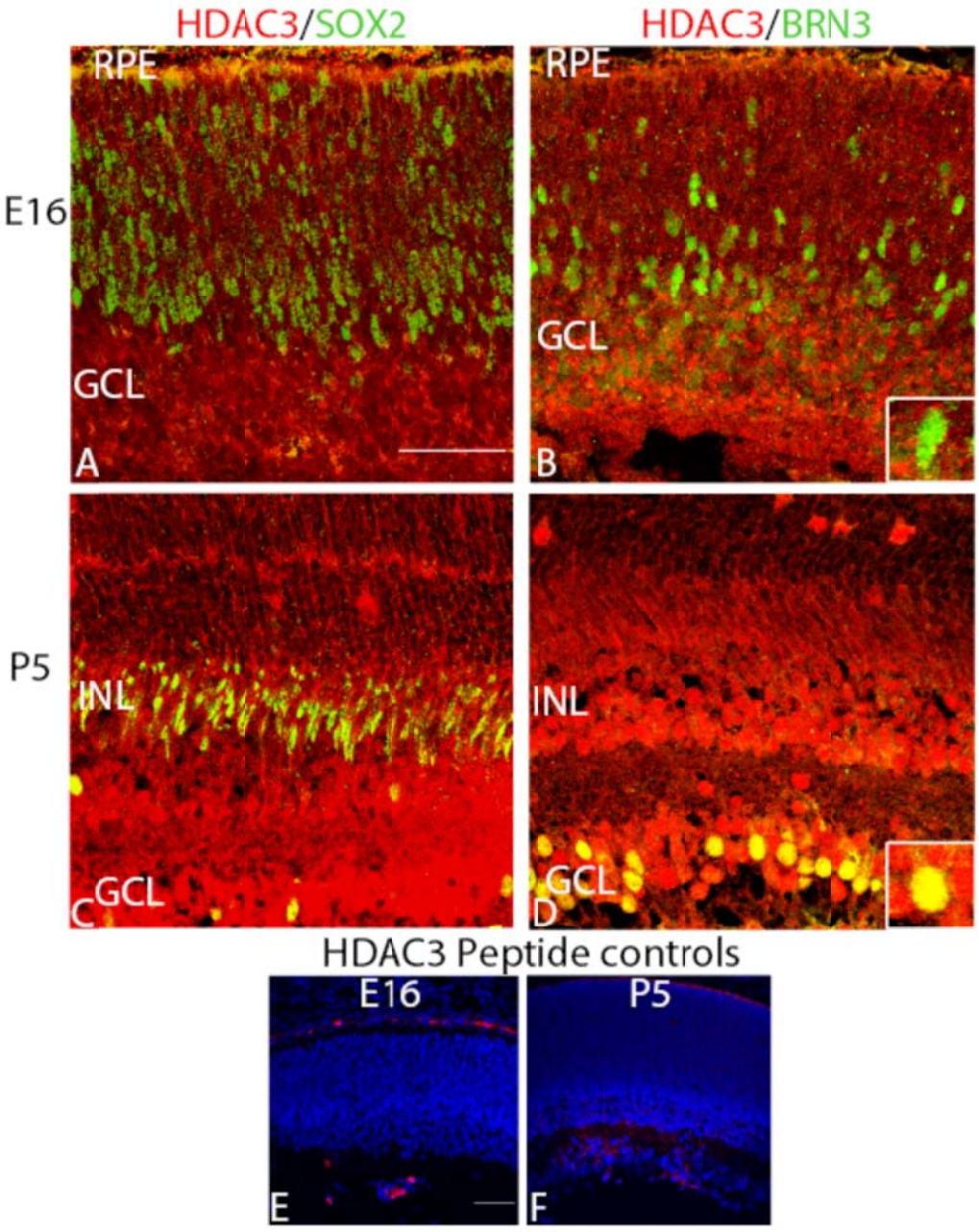

Figure 34 HDAC3 localization in the developing murine retina. E16 (A-B) and P5 (C-D) retinal sections labeled with HDAC3 showed a nuclear and cytoplasmic pattern of localization. No co-localization of HDAC3 was noted in the SOX2 labeled retinal progenitors at E16(A), but substatntial co-localization was noted in Müller glial cells, cholinergic amacrine cells and retinal astrocytes at P5 (C).

HDAC3 and BRN3C at E16 (B) and BRN3A at P5 (D) showed co-localization. Insets show magnified view of labeled ganglion cells (B, D). Peptide controls for HDAC3 were performed on E16 (E) and P5 (F) retinal sections to test the specificity of the antibody used. Scale bar of 50μm shown in A representative for images A-D. 50μm scale bar shown in E representative of E-F.

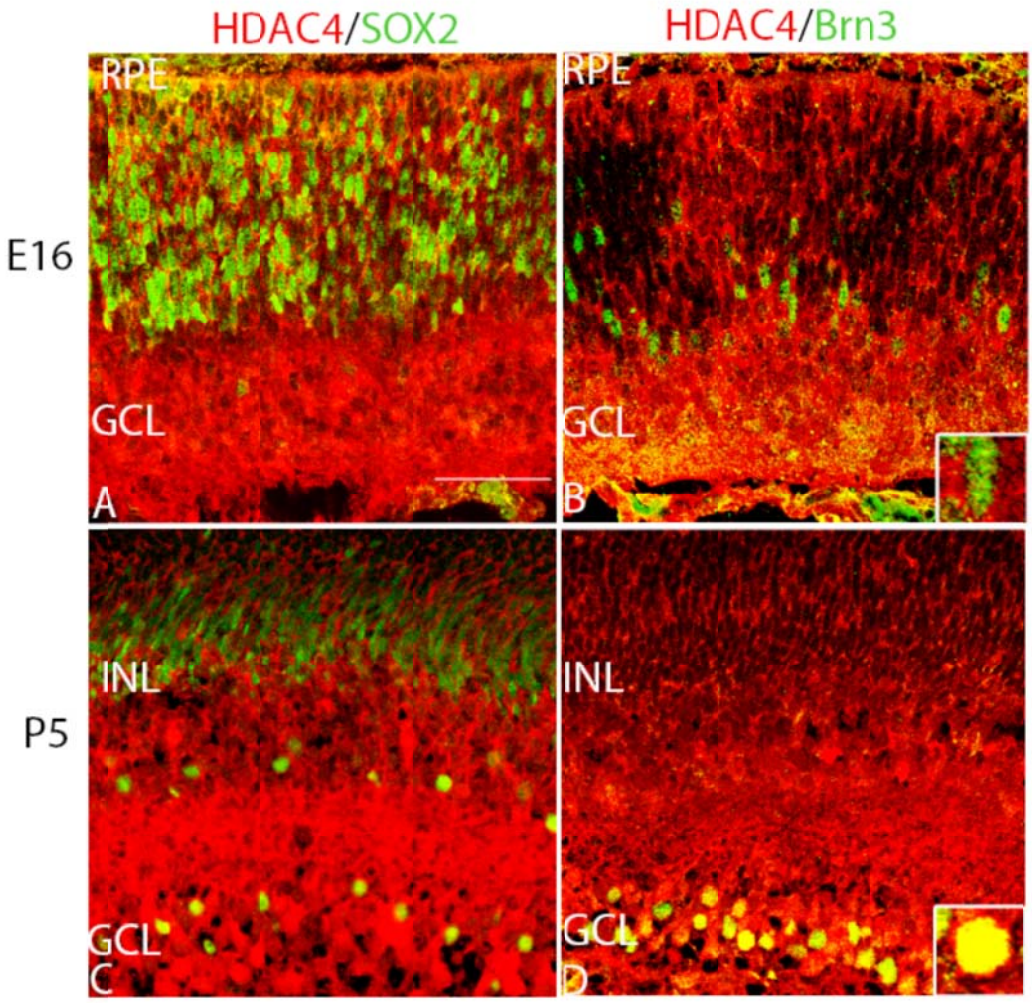

Figure 35 HDAC4 localization in the developing murine retina. Localization patterns of HDAC4 in the developing murine retina were found to be nuclear and cytoplasmic in pattern. SOX2 and HDAC4 were co-localized at E16 (A), but HDAC4 was co-localized only to the nucleus of cholinergic amacrine cells and retinal astrocytes at P5 (C). No nuclear localization appeared to be present in Müller glia at P5(C). BRN3C labeled ganglion cell nuclei were co-labeled with HDAC4 at E16 and BRN3A labeled cells co-labeled at P5 (D). Insets show magnified view of labeled ganglion cells (B, D). Scale bar of 50μm shown in A representative for images A-D.

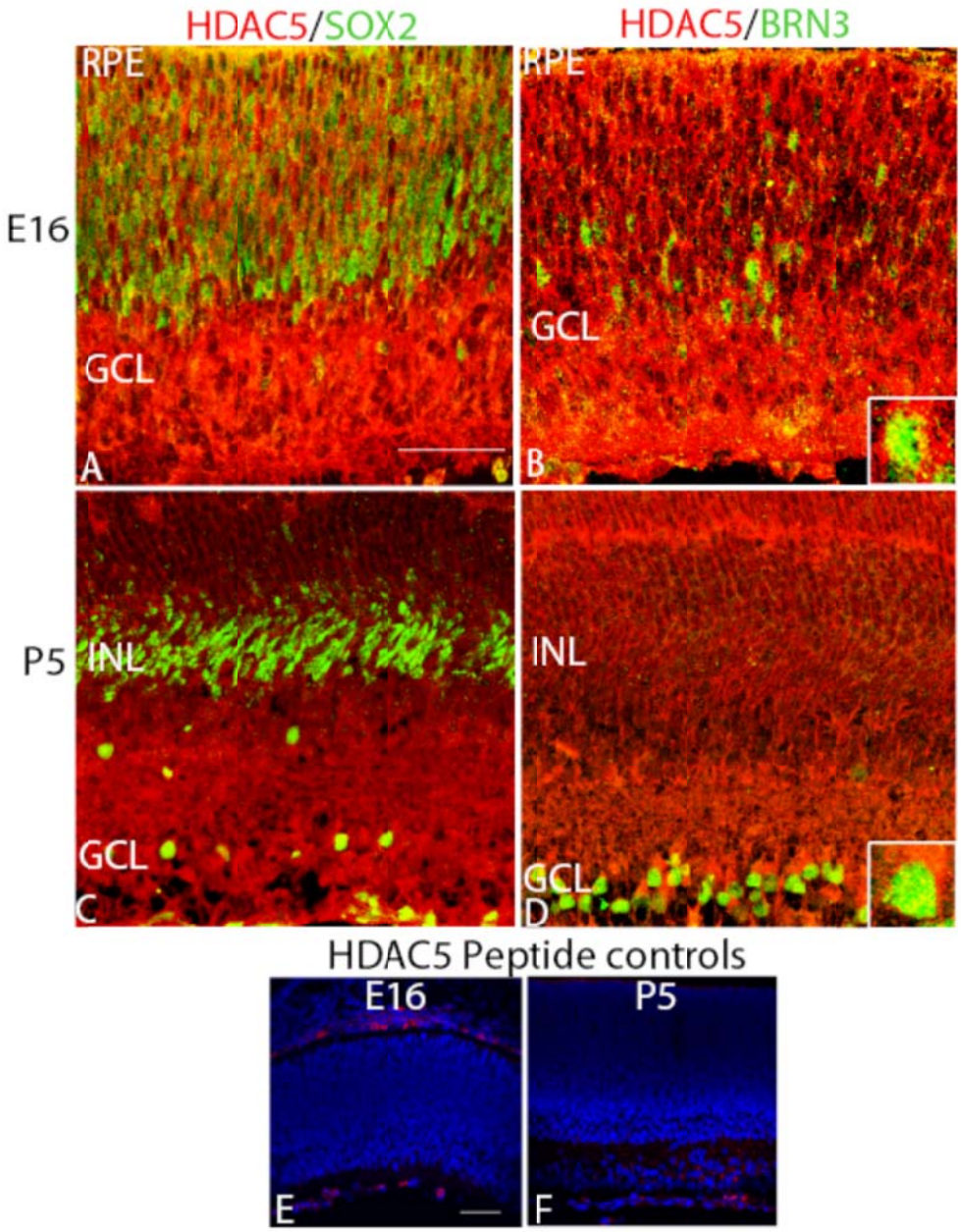

Figure 36 Localization of HDAC5 in the developing murine retina. SOX2(+) progenitors at E16 (A) and cholinergic amacrine cells and retinal astrocytes at P5 (C) were co-labeled with HDAC5. Müller glial nuclei were not co-labeled with HDAC5 (C). BRN3C and BRN3A labeled cells were also positive for HDAC5 (B, D). Insets show magnified view of labeled ganglion cells (B, D). Peptide controls

for HDAC5 were performed on E16 (E) and P5 (F) retinal sections to test the specificity of the antibody used. Scale bar of 50μm shown in A representative for images A-D. 50μm scale bar shown in E representative of E-F.

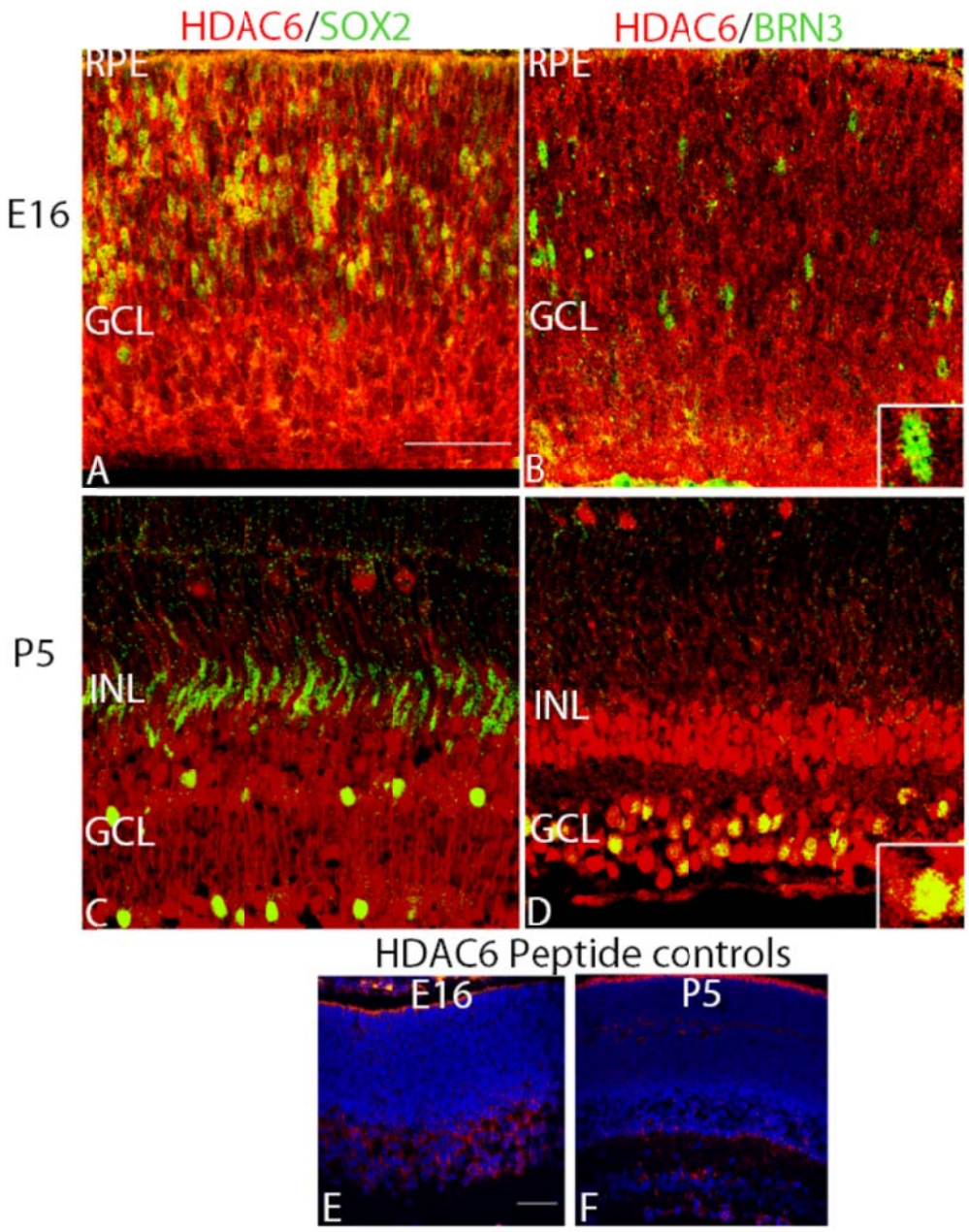

Figure 37 Localization of HDAC6 in the developing murine retina. HDAC6 was co-localized with SOX2 (+) retinal progenitors at E16 (A), and cholinergic amacrine and retinal astrocytes at P5 (C). No co-label was detected in the nucleus of Müller glial cells at E5. Weak nuclear localization was detected in BRN3C(+) cells at E16(B), but substantial co-localization of HDAC6 was noted in

the BRN3A(+) cells at P5 (D). Insets show magnified view of labeled ganglion cells (B, D). Peptide controls for HDAC6 were performed on E16 (E) and P5 (F) retinal sections to test the specificity of the antibody used. Scale bar of 50μm shown in A representative for images A-D. 50μm scale bar shown in E representative of E-F.

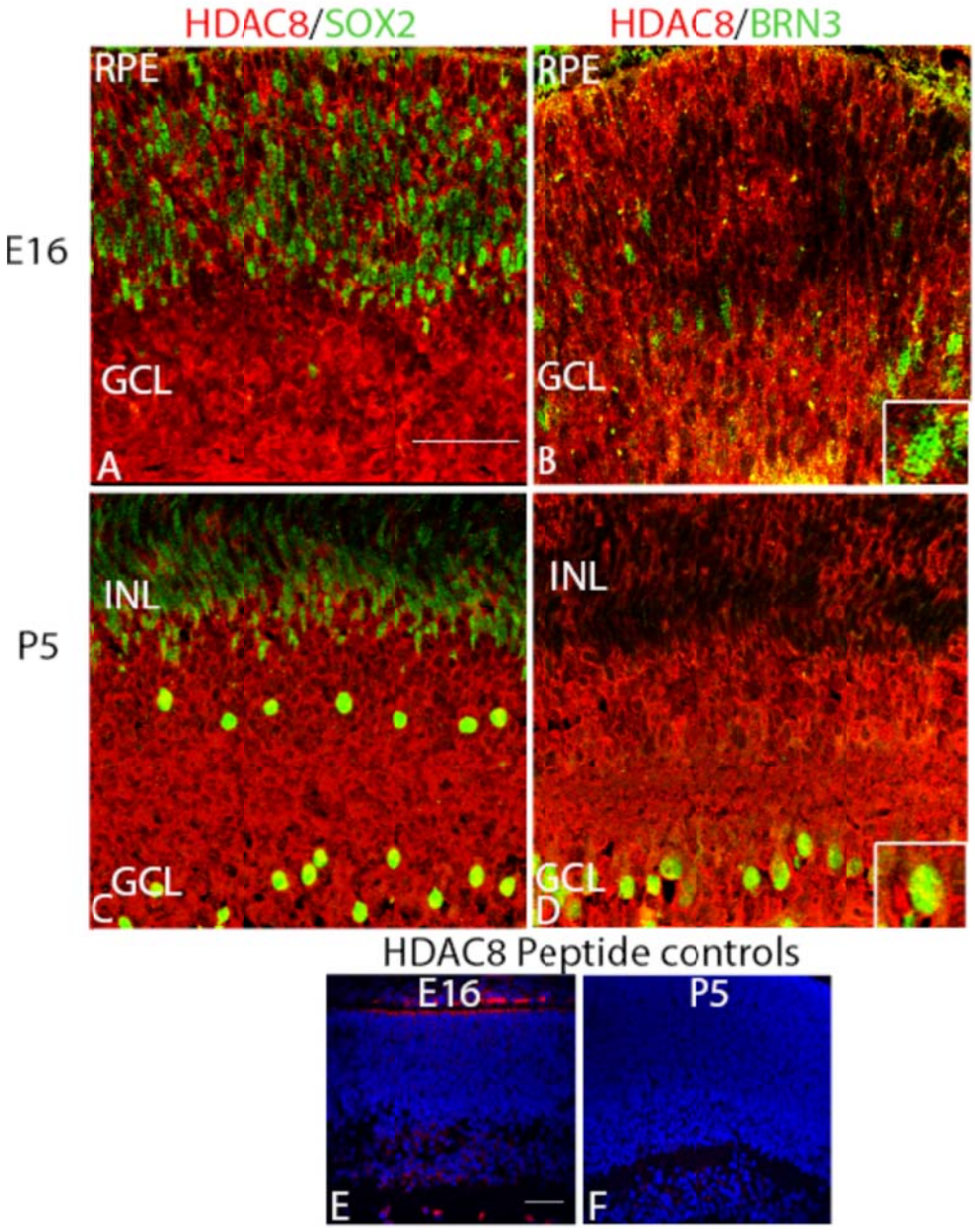

Figure 38 Localization of HDAC8 in the developing murine retina. SOX2 labeled progenitors and Müller glia showed no nuclear localization of HDAC8. Cholinergic amacrine cells and retinal astrocytes labeled by SOX2 at P5 showed co-localization of HDAC8 at P5(C). Ganglion cells showed weaker nuclear with ganglion cell markers BRN3C at E16 (B), but increased co-localization with

BRN3A at P5 (D). Insets show magnified view of labeled ganglion cells (B, D). Peptide controls for HDAC8 were performed on E16 (E) and P5 (F) retinal sections to test the specificity of the antibody used. Scale bar of 50μm shown in A representative for images A-D. 50μm scale bar shown in E representative of E-F.

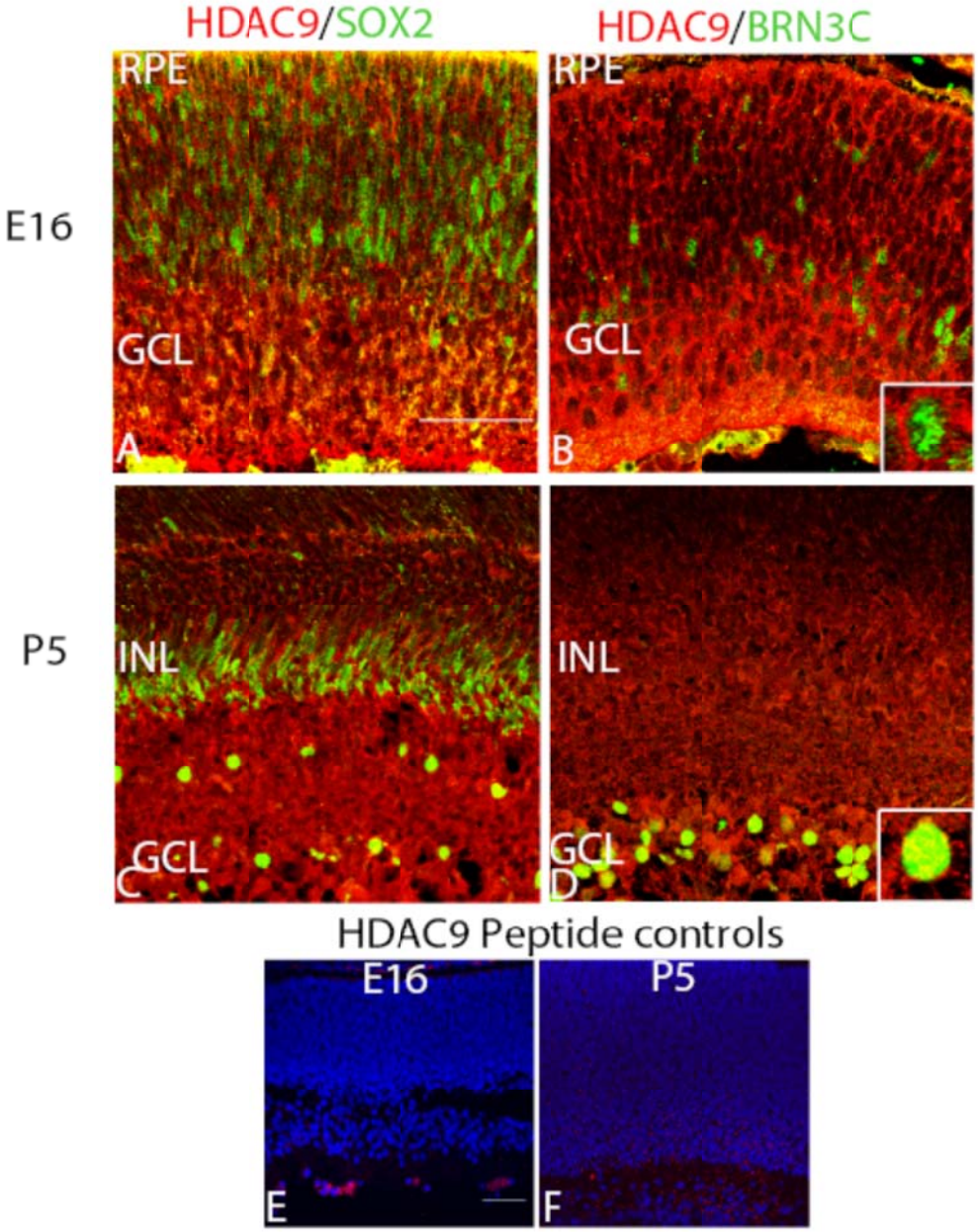

Figure 39 Localization of HDAC9 in the developing murine retina. SOX2 labeled progenitors at E16 (A) and Müller glial cells at P5 showed no co-localization with HDAC9. Nuclei of cholinergic amacrine cells and retinal astrocytes were co-labeled with HDAC9. HDAC9 did not appear to label BRN3C labeled ganglion cells at E16 but could be detected in the nucleus of BRN3C cells at P5 (D).

Peptide controls for HDAC9 were performed on E16 (E) and P5 (F) retinal sections to test the specificity of the antibody used. Scale bar of 50μm shown in A representative for images A-D. 50μm scale bar shown in E representative of E-F.

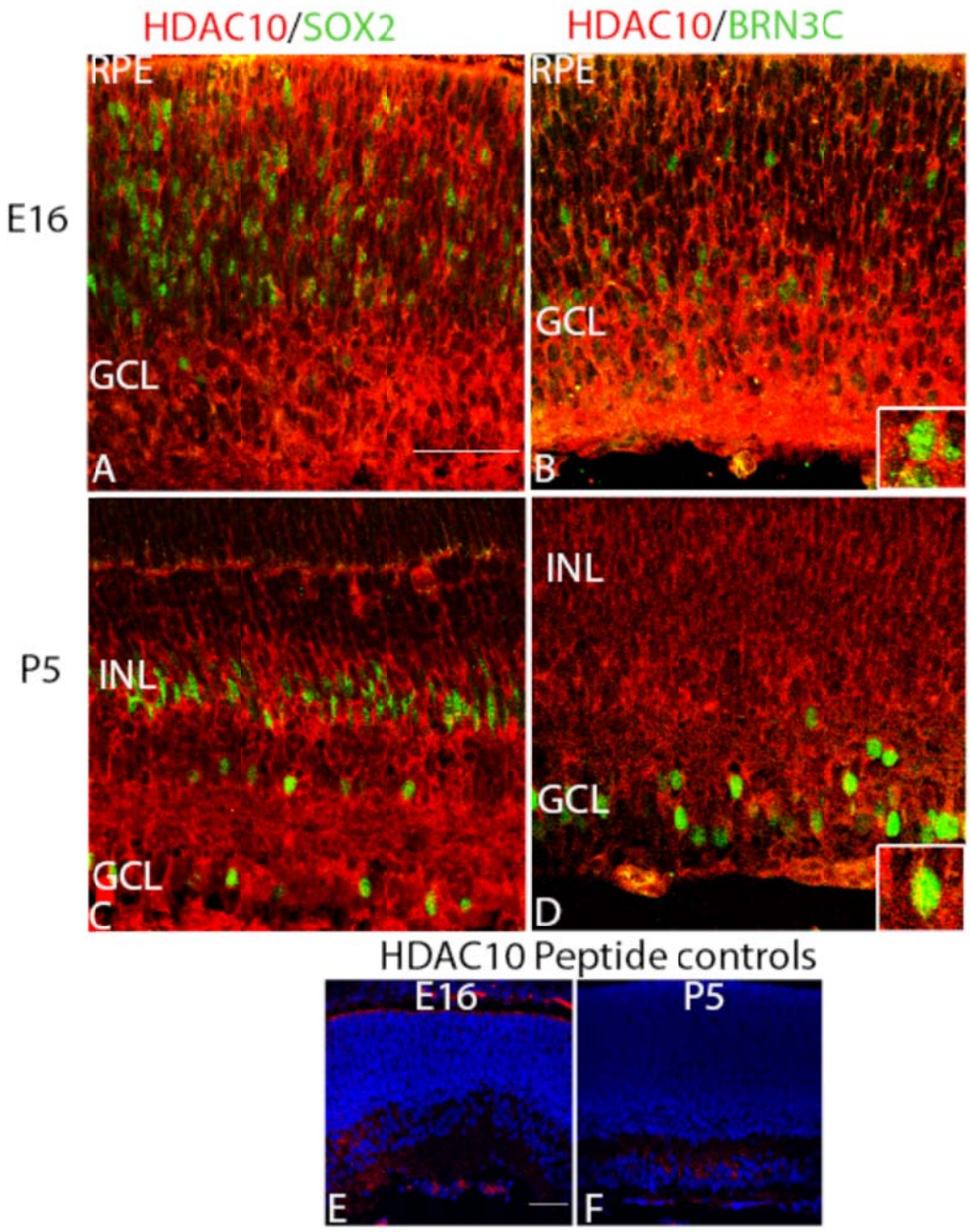

Figure 40 Localization of HDAC10 in the developing murine retina. HDAC10 was found to have a nuclear and cytoplasmic pattern of localization in the developing murine retina. No co-localization of HDAC10 with SOX2 labeled progenitors at E16(A) or Müller glia at P5 (C) was noted. Nuclear localization of HDAC10 was apparent in cholinergic amacrine cells, retinal astrocytes (C) and ganglion cells

(B, D). Peptide controls for HDAC10 were performed on E16 (E) and P5 (F) retinal sections to test the specificity of the antibody used. Scale bar of 50μm shown in A representative for images A-D. 50μm scale bar shown in E representative of E-F.

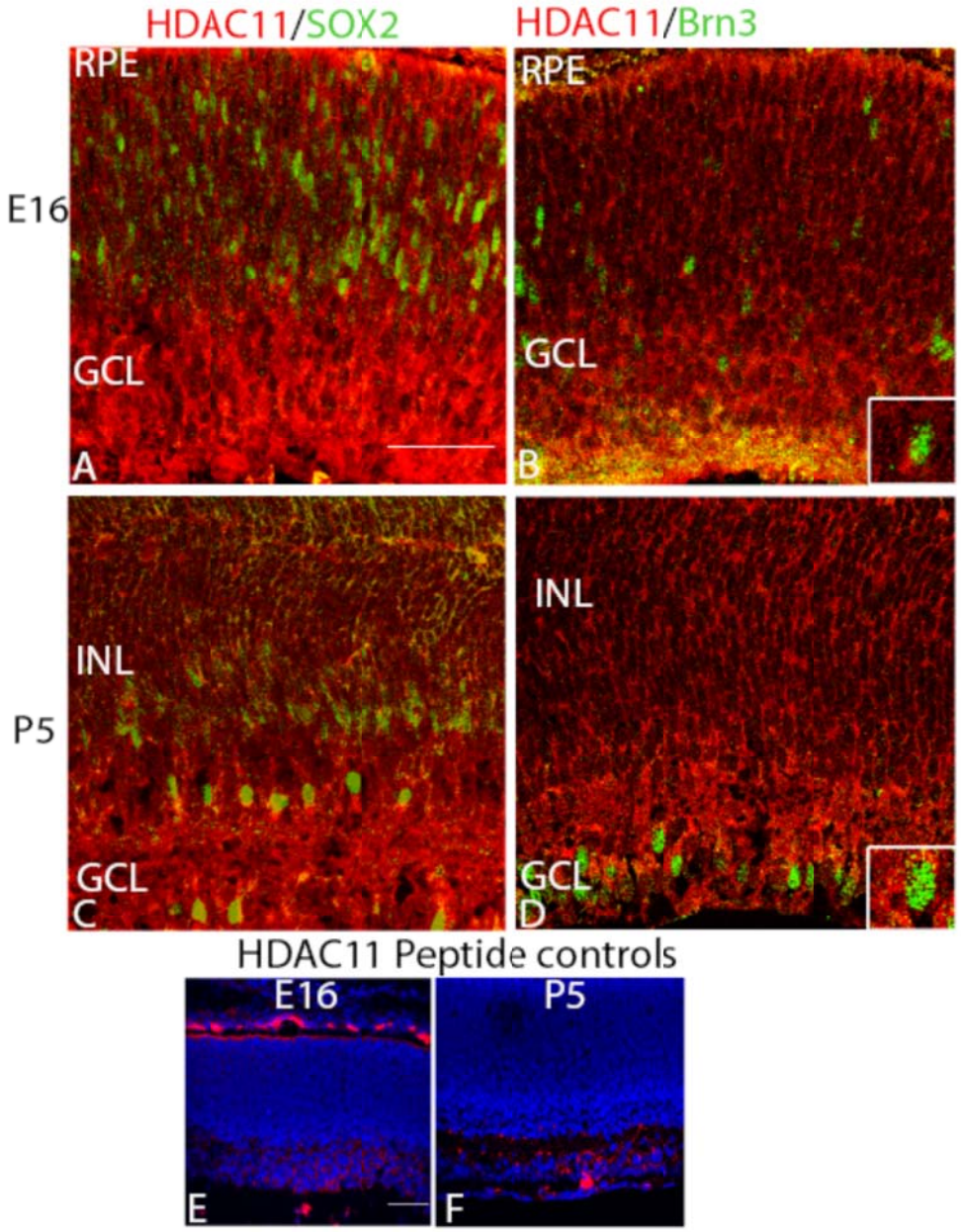

Figure 41 Localization of HDAC11 in the developing murine retina. HDAC11 localization in the developing murine retina was nuclear and cytoplasmic in pattern. HDAC11 showed no nuclear co-localization in retinal proigenitors at E16 Müller glia, but nuclear localization was apparent in cholinergic amacrine and retinal astrocytes at P5 (C). No nuclear localization of HDAC11 was observed in

BRN3C labeled ganglion cells at E16 (B) or in the BRN3A labeled cells at P5 (D). Peptide controls for HDAC11 were performed on E16 (E) and P5 (F) retinal sections to test the specificity of the antibody used. Scale bar of 50μm shown in A representative for images A-D. 50μm scale bar shown in E representative of E-F.